EMPIRICAL KINETIC MODELING OF OXYGEN DELIGNIFICATION PRETREATMENT OF WHEAT STRAW

by

SAM KING HO LI

B.A.Sc., The University of British Columbia, 2010

A THESIS SUBMITTED IN PARTIAL FULFILLMENT OF

THE REQUIREMENTS FOR THE DEGREE OF

MASTER OF APPLIED SCIENCE

in

THE FACULTY OF GRADUATE STUDIES

(Chemical and Biological Engineering)

THE UNIVERSITY OF BRITISH COLUMBIA

(Vancouver)

August 2013

Abstract

With diminishing supplies of oil reserves and surging oil prices, research on renewable and sustainable energy has significantly increased. Biofuels have shown their potential in replacing traditional fossil fuels, such as gasoline. Second generation biofuels that use nonfood lignocellulosic biomass to produce bioethanol have been identified as one of these renewable sources.

Oxygen delignification has been identified as an effective pretreatment method for agricultural waste, such as wheat straw, to increase the enzymatic hydrolysis yield. The purpose of this study was to develop a kinetic model for the delignification of wheat straw.

An experimental design was planned to enable the development of an empirical model of the reaction kinetics for oxygen delignification of wheat straw. This was accomplished by studying the effects of substrate loading (2-4% w/w), reaction temperature (90-130°C) and caustic loading (5-15% w/w). From the experiments, an empirical model that can predict the lignin content of wheat straw after oxygen delignification pretreatment based on reaction temperature, caustic loading and lignin content was developed:

$$\frac{d[L]}{dt} = -k_L[L]^{a_1}(k'([L] - [L_0]) + [OH_0^-])^{a_2}$$

Where:

k_L = kinetic constant of lignin

k' = constant for the relationship between kinetic constant of lignin and hydroxide ion

L = concentration of lignin in substrate

L_0 = concentration of initial lignin substrate

OH_0^- = concentration of hydroxide ion

a_1 = reaction order for lignin

a_2 = reaction order for hydroxide ion

The pretreated substrate was analyzed and showed increased sugar concentration and sugar yield when subjected to enzymatic hydrolysis at 20 FPU/g glucan. It was also found that caustic loading would become saturated when it was above 10-12% w/w. Out of all the operating parameters, caustic loading had the greatest effect on lignin solubilization, carbohydrate recovery and sugar yield.

An economic analysis on the oxygen delignification pretreatment process was performed with Aspen Plus and Aspen Economic Analyzer. Using sugar produced as a basis, it was found that the pretreatment cost was 26.20 ¢/lb sugar. A sensitivity analysis was also performed on the cost of biomass, caustic (NaOH), and enzyme. It was concluded that the cost of enzyme had the most significant effect on the cost of pretreatment.

Preface

The adaptions of Tables and Figures in this thesis are used with permission and referenced to applicable sources. The procedure for dissolved lignin determination outlined in 3.7 and 3.8 were developed by Dr. Duff, Dr. Posarac and I. The ODE solver, EASY-FIT$^{\text{Model Design}}$, was used with permission from Professor Klaus Schittkowski, University of Bayreuth, Germany. All laboratory experiments, kinetic model development, ODE model solving, Aspen Plus simulation work and data analyses were original work and performed by me.

Table of Contents

List of Tables

List of Figures

Nomenclature

A	Pre-exponential factor ((1/min * (g/l)$^{(1-a1-a2-a3)}$)
a_1	Reaction order with respect to lignin
a_2	Reaction order with respect to hydroxide ion
a_3	Reaction order with respect to oxygen
a_4	Reaction order with respect to carbohydrate
C_x	Cellulose, hemicellulose or total carbohydrate sugar equivalent (g)
Ea	Activation energy (J/mol or kJ/mol)
k'	k_{OH}/k_L
k_{90}	Lignin kinetic constant at 90°C (1/min * (g/l)$^{(1-a1-a2)}$) for single ODE
k_{110}	Lignin kinetic constant at 110°C (1/min * (g/l)$^{(1-a1-a2)}$) for single ODE
k_{130}	Lignin kinetic constant at 130°C (1/min * (g/l)$^{(1-a1-a2)}$) for single ODE
k_{carbo90}	Carbohydrate kinetic constant at 90°C
$k_{carbo110}$	Carbohydrate kinetic constant at 110°C
$k_{carbo130}$	Carbohydrate kinetic constant at 130°C
k_L	Lignin kinetic constant (1/min * (g/l)$^{(1-a1-a2)}$)
k_{L90}	Lignin kinetic constant at 90°C (1/min * (g/l)$^{(1-a1-a2)}$) for system of ODEs
k_{L110}	Lignin kinetic constant at 110°C (1/min * (g/l)$^{(1-a1-a2)}$) for system of ODEs
k_{L130}	Lignin kinetic constant at 130°C (1/min * (g/l)$^{(1-a1-a2)}$) for system of ODEs
k_{OH}	Hydroxide ion kinetic constant (1/min * (g/l)$^{(1-a1-a2)}$) for system of ODEs
k_{OH90}	Hydroxide ion kinetic constant at 90°C (1/min * (g/l)$^{(1-a1-a2)}$) for system of ODEs
k_{OH110}	Hydroxide ion kinetic constant at 110°C (1/min * (g/l)$^{(1-a1-a2)}$) for system of ODEs
k_{OH130}	Hydroxide ion kinetic constant at 130°C (1/min * (g/l)$^{(1-a1-a2)}$) for system of ODEs
kwh	Kilowatt-hour
L	Residual lignin concentration (solid) (g/l)
L_0	Initial lignin concentration (solid) (g/l)

$L_{dissolved}$	Dissolved lignin (g/l)
lb	pound
MJ	Mega joule
O_2	Oxygen gas (g/l)
OH^-	Hydroxide ion (g/l)
OH_0^-	Initial hydroxide ion concentration (g/l)
R	Universal gas constant (8.314 J/mol k)
r_L	Rate of delignification (g/L min)
r_{OH^-}	Rate of hydroxide ion consumption (g/L min)
T	Temperature (kelvin or °C)
t	Time (minutes or second)
S_x	Cellulosic, hemicellulosic or total sugar (g)
ΔL	Change in lignin concentration (solid) (g/l)
Δt	Change in time (min)
$	U.S. dollar
¢	U.S. cent

List of Abbreviations

AFEX	Ammonia fiber explosion
CBU	Cellobiose unit
CO_2	Carbon dioxide
CO_{2eq}	Carbon dioxide equivalent
FPU	Filter paper unit
GHG	Green-house gas
h	hour
HPLC	High Performance Liquid Chromatography
min	minutes
NREL	National renewable energy laboratory
ODE	Ordinary differential equation
ODW	Oven dry weight
PTFE	Polytetraflurorethylene
SHF	Separate hydrolysis & fermentation
SSF	Simultaneous scarification & fermentation
USDA	United States Department of Agriculture
UV	Ultra violet
w/w	weight to weight

Acknowledgements

I would like to thank the National Science Engineering Research Council (NSERC) for providing the necessary funding for this research.

I would also like to thank both of my supervisors Dr. Sheldon Duff and Dr. Dusko Posarac for their valuable support, patience, guidance and mentorship throughout my years as a graduate student. You two have helped me to become a better researcher and engineer, for that I am truly thankful. Special thanks to Dr. Heather Trajano for her suggestions in our weekly meetings and to Professor Klaus Schittkowski for the EASY-FIT$^{\text{Model Design}}$ program. I would also thank my lab mates, Oscar Rosales Calderon, Derek Pope, Tong Wu, and David Kuan for their help and making my graduate studies an enjoyable experience.

Finally, I would like thank my family, friends and my girlfriend Michele Szeto for their ongoing support for the last two years.

1 Introduction

1.1 Biomass to fuel

For decades, humanity has relied on burning fossil fuels such as petroleum, coal and natural gas as the primary energy sources to sustain the ever-increasing demand for consumer goods [**1**]. The continuous consumption of fossil fuel poses economic volatility as well as sustainability and environmental challenges [**2**]. Presently, there is an estimated 1.2 trillion barrels of oil in reserve and it is being consumed at an alarming rate of 85 million barrels of oil per day globally [**3**,**4**]. Fossil fuel is a finite resource and the reserves in the world are likely to be exhausted within the next century if this trend continues [**5**]. Major green-house gas (GHG) contributors such as carbon dioxide (CO_2) are generated as a by-product of fossil fuel combustion. It is widely accepted that GHG contributes to global warming, increasing temperature on a global scale [**6**]. Moreover, it is inevitable for the price of oil to increase due to its finite volume on this planet. The crude oil price is closely linked to global events (Figure 1) especially to those affecting major oil exporting countries in the Middle East [**3**,**7**]. The unstable relationship between Middle Eastern countries and Western nations, such as the U.S., compounds the volatile nature of oil prices in recent years. This economic dependence on Middle Eastern countries ultimately poses an energy security problem to the Western nations [**8**]. Due to these reasons, the interest in research and development of sustainable energies has been growing for the past decades.

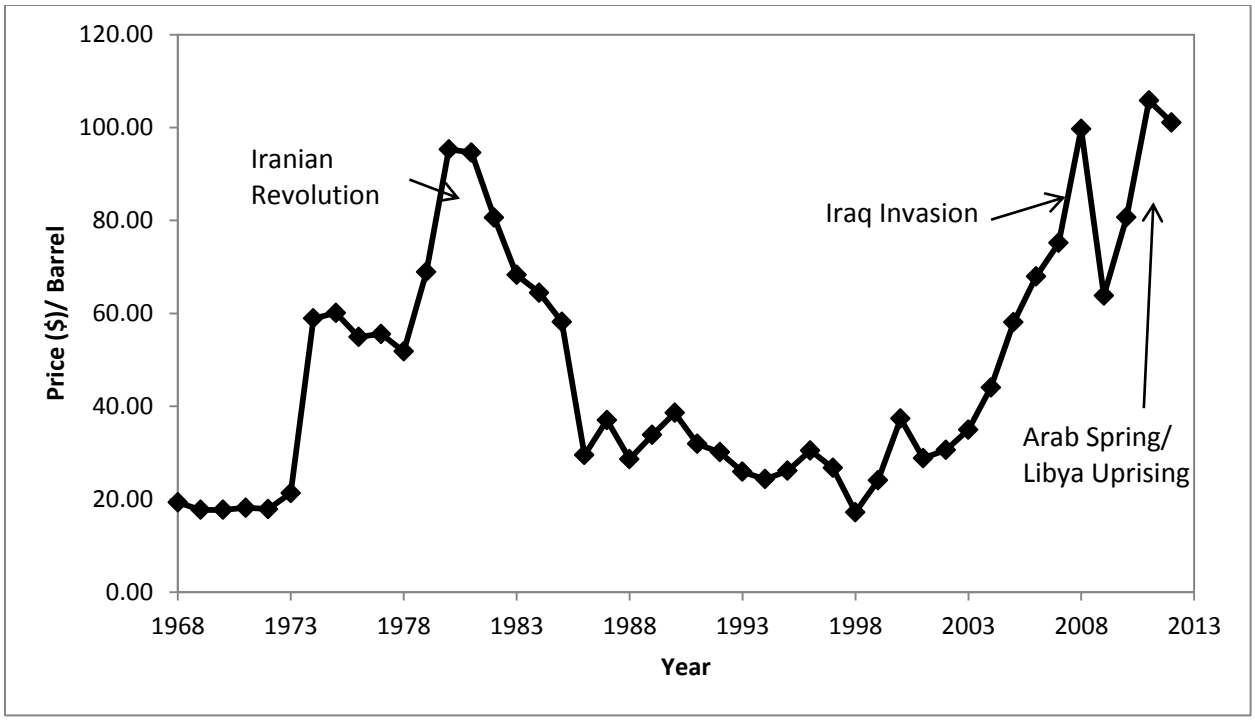

Figure 1: Crude oil price history $/barrel, data adapted from the U.S. Energy Information Administration [7]

The transportation sector has been identified as the biggest GHG emitter in developed countries [**9**]. In 2005, the U.S.'s transportation sector emitted approximately 34% of the total CO_2 released into the atmosphere [**9**]. Similarly, Vancouver, Canada reported that 36% of the city CO_2 emission originated from the transportation sector [**10**]. It is necessary for us to establish energy dependency on alternative sustainable energy sources to reduce GHG emissions. Different types of alternative energy sources (biomass, solar, wind, geothermal, and nuclear) have been under research and biofuels from biomass have received significant attention due its versatility in producing different alternative fuels including bioethanol [**9**,**11**]. Figure 2 provides an example of potential biomass conversion technology pathways and their associated products [**1**].

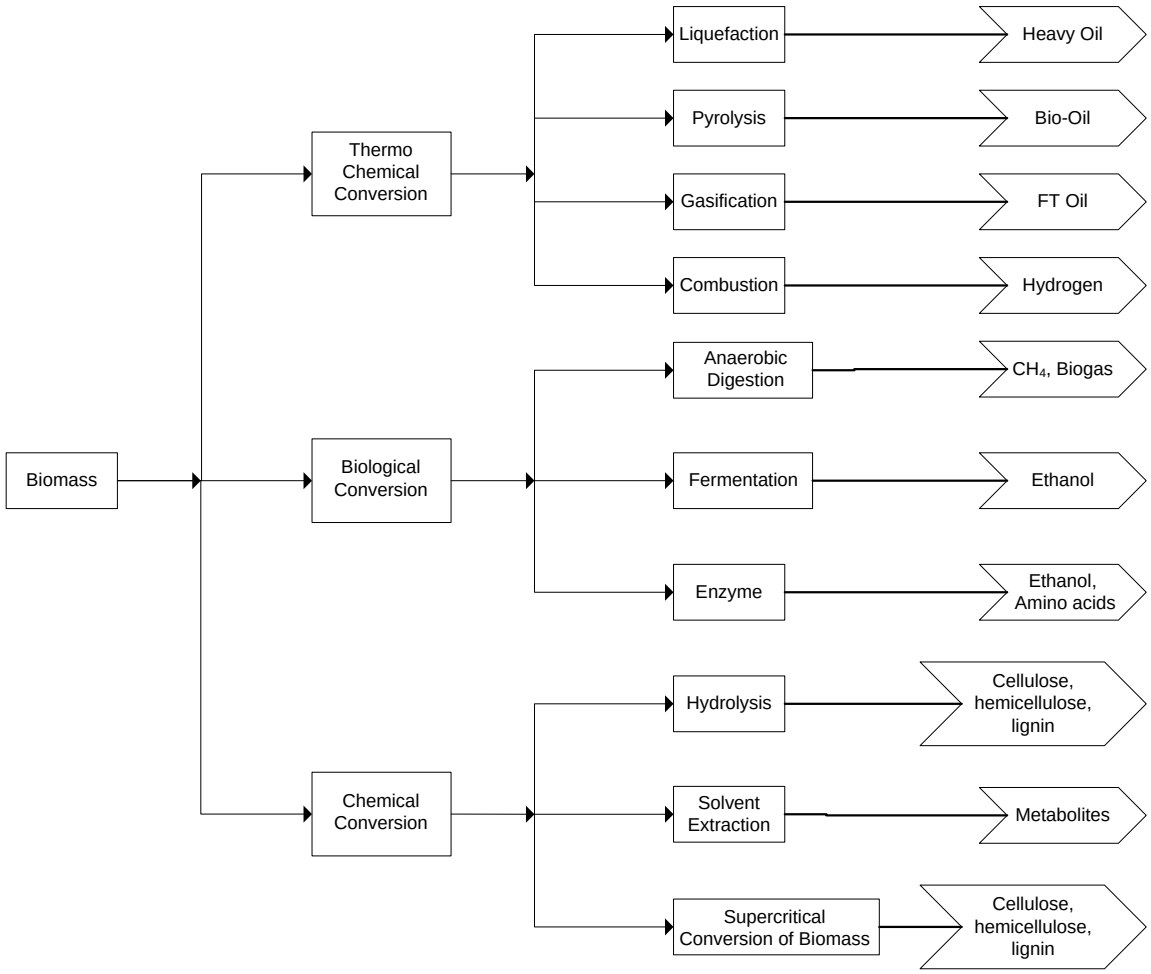

Figure 2: Conversion technologies and products pathways from biomass adapted from Naik et al. (2010) [1**]**

The three main objectives to be achieved by the development of biofuel are [**12**,**13**]:

- Energy independence
- Fuel supply security
- Carbon neutrality

In order to achieve energy independence and fuel supply security, a large supply of biomass must be available for biofuel production. The agriculture and forestry industry are two of the biggest industries in Canada and produce a combined 72.9 million tonnes of biomass residue annually [**14**]. It has been estimated that 1.1 million tonnes of these lignocellulosic waste material could yield 250-350 million litres of fuel grade ethanol [**15**]. Emission of CO_2 can be

reduced or even eliminated if petroleum-based fuels were replaced by biomass-derived fuels [**5**,**16**].

The ideal CO_2 life-cycle in production of biofuel begins with fixation of CO_2 through photosynthesis in energy crops. These crops can be harvested and converted into biofuels. CO_2 is released into the atmosphere during the biofuel production process and the end use of the fuel. Lastly, crops reabsorb the CO_2 from the atmosphere during their growth phase again from the atmosphere to reinitiate the carbon cycle. This ideal CO_2 life-cycle of a biofuel production is qualitatively shown in Figure 3. Since some energy input (fossil fuel) is always needed in different stages of the CO_2 life cycle (eg. plant harvest and biofuel production phase), therefore this ideal cycle can never be reached.

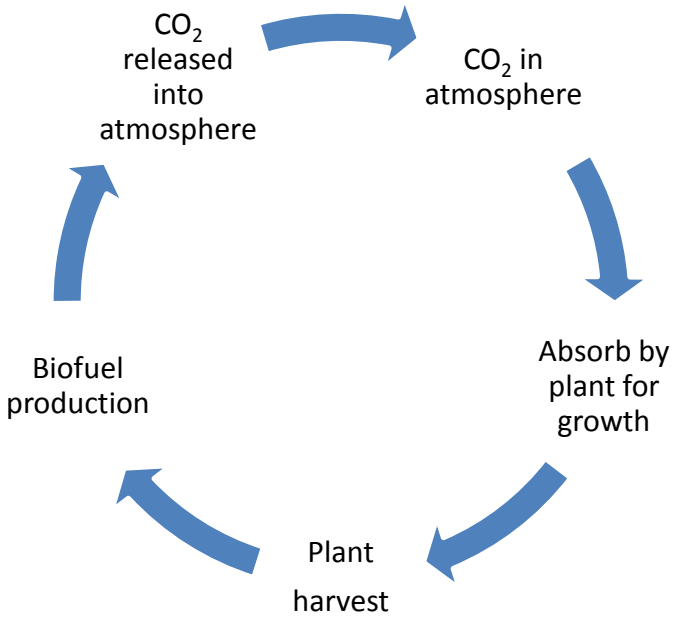

Figure 3: An ideal CO_2 life-cycle of biofuel production

Life-cycle analysis of biofuel production from lignocellulosic biomass have shown that up to 80% of CO_2 can be displaced if biofuel produced from lignocellulosic biomass is to replace fossil fuels; leading to a net CO_2 emission reduction.

1.2 Bioethanol

As previously mentioned, the transportation sector is one of the largest contributors of CO_2 to the atmosphere. In order to be easily integrated into existing fuel networks, biofuels should be compatible with current distribution infrastructure and engine technology. Given these criteria, ethanol has been identified as a good candidate for biofuel for the transportation sector. Despite the lower energy content of ethanol, a specially-tuned engine can operate on pure ethanol more efficiently than traditional engine [**17**]. Currently, ethanol is added into gasoline, delivered as a blend for vehicle use and it has been proven that burning ethanol can help reduce smog formation [**13**,**17**,**18**].

Bioethanol refers to ethanol produced from renewable feedstocks such as starch crops, agricultural and forest residues. The leading countries for bioethanol production are the U.S. and Brazil, utilizing corn and sugarcane, respectively, as feedstock to produce ethanol [**11**,**19**]. The demand for bioethanol is also on the rise. For example, in 1999 it has been reported that the U.S. has been consuming up to 1.2 billion gallons per year of ethanol solely for transportation use [**20**]. The future of bioethanol is promising, with an estimated production of approximately 10 billion litres by next year [**12**,**21**].

The foundation of current and future bioethanol production is the continual advancement in biotechnology [**17**]. Unlike fossil fuel, the production of bioethanol is a green technology because it uses renewable feedstocks and biocatalysts such as enzymes and yeast to produce sustainable and renewable fuel. There are two types of bioethanol, first and second generation. First generation bioethanol is a mature technology and has already been commercialized; however it faces sustainability challenges from life-cycle analysis of GHG emissions. Second generation biofuels have the potential to produce ethanol in a more sustainable way [**11**]. However the processes in producing second generation fuels face technical and economic barriers and are the subject to intense research and development [**13**,**22**,**23**].

1.3 First Generation Biofuel and Bioethanol

First generation biofuels utilize food crops as the biomass feedstock. Through the use of transesterification and esterification technology, biodiesel can be produced by using vegetable

oil or animal fat as feedstocks. Bioethanol can be produced through the application of enzyme (amylase) hydrolysis and fermentation technology by using high sugar food crops such as corn and sugarcane [**12**].

Even though first generation biofuel technology is well understood, it is plagued with sustainability problems such as land and water use, ethical issues of using food crop as feedstock and inflation of overall food crop prices [**1**,**12**,**24**,**25**]. Also, with the exception of sugarcane [**12**,**26**], recent life-cycle analysis have shown that improvements in the carbon balance of first generation biofuel is miniscule [**1**], therefore an alternative approach in producing biofuel is needed [**12**]. Table 1 shows a direct comparison of CO_{2eq} emission saved between different biofuel generations and feedstocks. The CO_{2eq} emission was calculated based on assumed reference petrol vehicle that consumes 2.5 MJ/km and produces 230 g CO_{2eq}/km [**27**].

Table 1: The CO_2 equivalent saving of different feedstock to produce biofuel adapted from Tan et al. (2008) [11**]**

First generation biofuel feedstocks	$CO_{2eq.}$ emission saved (g/km)	$CO_{2eq.}$ emission saved (tonne /100 l)
Sugar Crops	90	1.2
Starch Crops	30	0.4
Brazilian Sugarcane	212	2.9
Second generation biofuel feedstocks		
Lignocellulosic crops	183	2.5
Lignocellulosic residues	191	2.6

1.4 Second Generation Biofuels and Bioethanol

Given the issues with the first generation biofuels, it is more logical to use non-food lignocellulosic biomass such as corn stover, wheat straw, bagasse or any agricultural for production of second generation biofuels [**1**,**12**]. Compared to first generation, the most noticeable difference in the process in production of second generation bioethanol is an extra pretreatment process. Due to presence of components such as lignin, protein and lipid [**28**] in the cell wall of lignocellulosic biomass, a pretreatment process is needed in order to improve the conversion of carbohydrates (cellulose and hemicellulose) in the cell wall into fermentable sugar.

Lignocellulosic biomass, especially low value residues from the agricultural and forest industries, is ideal for bioethanol production due to their reasonably high sugar content in the cell wall and because these materials are typically categorized as waste. In terms of GHG emissions, lignocellulosic biomass have a saving of 191 g CO_{2eq}/km and 2.6 tonne CO_{2eq}/1000L (Table 1) [**11**,**27**]. Studies have estimated that 75-85% reduction in GHG emissions could be achieved if the second generation bioethanol were to fully replace gasoline [**12**,**29**]. Traditional use of these lignocellulosic materials is to generate heat and electricity through incineration. However due to the high sugar content found in the plant cell wall [**30**], interest has grown in the potential of utilizing these sugar-rich lignocellulosic biomass to produce liquid fuel such as bioethanol [**1**]. As a feedstock, lignocellulosic materials include plants and crops that contain mainly lignin, sugar-rich cellulose and hemicellulose. A summary of different lignocellulosic materials composition distribution is shown in Table 2 [**13**,**31**].

Table 2: Lignocellulosic feedstock composition data adapted from Stamatelatou et al. (2012) and Sun & Cheng (2002) [13,31**]**

Lignocellulosic Materials	Cellulose (%)	Hemicellulose (%)	Lignin (%)
Hardwood stems	40-55	24-40	18-25
Softwood stems	45-50	25-35	25-35
Nut shells	25-30	25-30	30-40
Corn cobs	45	35	13
Grasses	25-40	35-50	10-30
Paper	85-99	0	0-15
Wheat straw	30	50	15
Sorted refuse	60	20	20
Leaves	15-20	80-85	0
Cotton seed hairs	80-95	5-20	0
Newspaper	40-55	25-40	18-30
Waste papers from chemical pulps	60-70	10-20	5-10
Primary wastewater solids	8-15	N/A	24-29
Swine waste	6.0	28	N/A
Solid cattle manure	1.6-4.7	1.4-3.3	2.7-5.7
Coastal Bermuda grass	25	35.7	6.4
Switch grass	45	31.4	12.0

The general process for second generation bioethanol is to convert biomass into ethanol by [**25**,**32**,**33**]:

- pretreatment to enhance sugar digestibility of the biomass
- enzymatic hydrolysis to convert the polymeric sugar into monomeric sugar
- yeast fermentation to ferment monomeric sugar into ethanol
- distillation and dehydration (molecular sieve) to concentrate the ethanol stream from fermentation into fuel grade ethanol

Digestibility is expressed as a ratio between the sugar produced per gram of pretreated dry mass. The more digestible the substrate is, the more sugar it can produce and the more concentrated the sugar will be in the hydrolysate. A simplified process flow diagram of the second generation bioethanol production is shown in Figure 4.

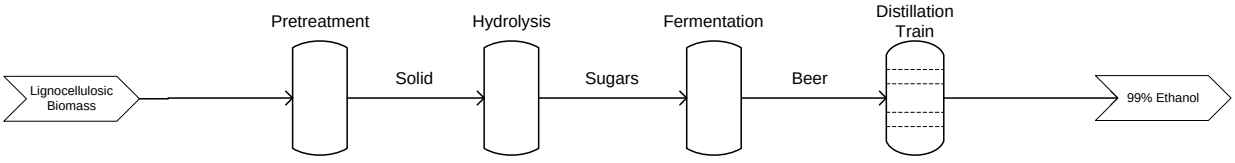

Figure 4: Second generation ethanol production pathways

Even though second generation bioethanol has the potential of providing the world a solution to sustainable transportation fuel, there are issues that must be addressed prior to commercialization. Cost is one of the major challenges for the production of lignocellulosic bioethanol. Despite the large quantity and relatively cheap price of lignocellulosic biomass, pretreatment and enzymatic hydrolysis remain comparatively expensive, reducing the economic competitiveness of second generation bioethanol relative to conventional gasoline and first generation bioethanol [**12**,**34**,**35**,**36**]. Most lignocellulosic wastes are harvested seasonally, thus a well thought out collection and delivery system must be in place to ensure continuous feedstock supplies [**12**]. Lastly, the tradeoff for burning higher octane ethanol is 33% lower heating value when compared to gasoline (Table 3). This means, a vehicle needs 33% larger volume of ethanol to achieve the same energy output as gasoline [**34**]. This poses a challenge as consumers will not be inclined to pay more to switch from gasoline to ethanol.

Table 3: Ethanol and gasoline comparison [34**]**

Fuel Parameter	Ethanol	Gasoline
Net Heat of Combustion, Btu/gal	75,700-76,000	109,000-119,000
Octane Number, (R+M)/2	96-113	85-96

1.5 Wheat Straw Feedstock for Second Generation Biofuels

Agricultural residues such as wheat straw are produced abundantly in Canada mainly in the prairie provinces (Alberta, Saskatchewan and Manitoba). It had been reported that the availability of wheat straw in Canada fluctuates between 15.5 to 33.3 Mt with an average of 25.0 Mt throughout 1994-2003. Wheat straw as a feed stock for biofuel production is attractive not only because it is a residue, but also its relatively low lignin and high lignin content Table 4.

Table 4: Wheat straw composition from literature [37**]**

Reference	Extractive (%)	Ash (%)	Lignin (%)	Cellulose (%)	Hemicellulose (%)
Satheesh Kumar (2009) [**38**]	-	-	16-21	-	-
Ali et al. (1991) [**39**]	5.8	7.5-8.5	16-17	33.7	25.0
Aronovsky (1948) [**40**]	4.5	8.1	20.1	34.8	27.6
Mohan (1988) [**41**]	4.7	9.99	23.0	-	28.9
Utne & Hegbrom (1992) [**42**]	-	4-9	16-20	29-35	26-32
Misra (1987) [**43**]	3.7	6.6	16.7	39.9	28.2
Misra (1987) [**43**]	2.9	3.7	20.5	41.6	31.3
Petersen (2009) [**44**]	-	6.5	15.6	35.0	22.3

Bioenergy companies had shown the commercialization potential through demonstration and pilot plants by using wheat straw as feedstock. In Canada, the company Iogen is currently involved in a demonstration plant located in Ottawa which has the capacity to process 20-30 tonnes of wheat straw to produce 5,000-6,000 litres of ethanol on a daily basis [**45**]. Back in 2011, Abengoa Bioenergy had announced a 25 Mgal (100 Ml) ethanol facility in Kanas, US, that utilizes local agricultural waste (wheat straw and switch grass) as feedstock [**46**]. Clariant, a Swiss company, has a pilot plant in Germany that has the capacity to produce 1,000 tonnes of ethanol using 4,500 tonnes of wheat straw [**47**]. Lastly, in Denmark, Dong Energy (Inbicon), has a 80 million USD demonstration plant that can utilizes 3,3000 tons of straw to produce 5.4

million litres of ethanol annually [**48**]. What is unique about this bio-refinery plant is that it also co-generated 1,4300 tons of lignin pellets for the plant's heating utilities and 1,2210 tons of molasses for animal feed [**48**]. Commercial companies have shown their commitment and involvement towards wheat straw, showing its potential as feedstock for ethanol production. This reinforces the reason why wheat straw is the substrate of interest in this study.

1.6 Chemistry of Lignocellulosic Biomass

The cell walls of lignocellulosic materials are composed of many structural molecules such as cellulose, pectin, hemicellulose, proteins, glycoprotein, lignin, cutin, suberin and waxes with lignin and carbohydrates (cellulose and hemicellulose) present in the highest quantity [**49**]. It is suggested that the lignin carbohydrate complexes are formed by hydrogen bonds and covalent bonds [**49**,**50**]. In order to increase the sugar yield, it is crucial to disturb these chemical bonds and expose the cellulose structure. Factors that affect hydrolysis include cellulose crystallinity, surface area, lignin, cellulose and hemicellulose content [**13**,**28**,**51**,**52**,**53**].

1.6.1 Cellulose

Cellulose is a major polysaccharide in cell walls of lignocellulosic materials. It is a chemically stable and extremely insoluble molecule that interacts with the rest of the cell wall matrix mainly through hydrogen bonding with hemicellulose [**49**]. Cellulose is composed of unbranched repeating units glucose molecules linked through a β-1,4 linkage [**49**]. It is the inter- and intra-molecular hydrogen bonds between the β-1,4 linked glucose chains that give the cellulose its linear structure [**53**,**54**]. Through these interactions, cellulose can be assembled into a highly organized crystalline structure and a less organized amorphous region [**55**]. The chemical structure of cellulose is shown in Figure 5. It is the crystalline regions that are more resistant to enzymatic attacks compared to their amorphous counterparts.

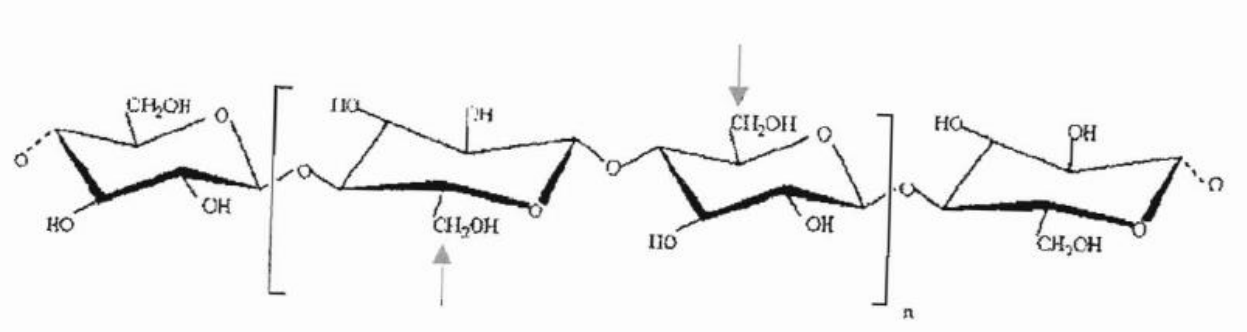

Figure 5: Chemical structure of cellulose and its repeating units adapted from Brown et al. (2004) [55**] used with permission from John Wiley and Sons**

1.6.2 Hemicellulose

Hemicellulose is a complex carbohydrate polymer that consists of large amount of pentose (arabinose, xylose) and trace amount of hexose (galactose, glucose, and mannose) sugars [**56**,**57**]. Unlike cellulose, hemicellulose is a highly branched, non-crystalline structure which results in higher solubilization during pretreatment processes. Of the pentose sugars, xylose is found to be most abundant in hemicellulose [**58**,**59**,**60**] and, along with lignin, it shields the cellulose from enzymatic attacks [**61**]. Hemicellulose recovery has not received as much attention because yeast (*S. cerevisiae*) typically utilizes glucose and other hexose sugars to produce ethanol. However, in recent years, xylose-fermenting yeasts have been identified which utilize xylose under aerobic conditions [**62**]. Moreover, with the technological advances in genetic engineering, recombinant yeast and bacteria can also be engineered to ferment xylose into ethanol [**62**]. Due to these reasons, it has become more attractive to recover both cellulose and hemicellulose to further improve the hydrolysis yield, ethanol yield and economics of the bioethanol production process. Figure 6 is a representation of hemicellulose and its branched constituents [**63**].

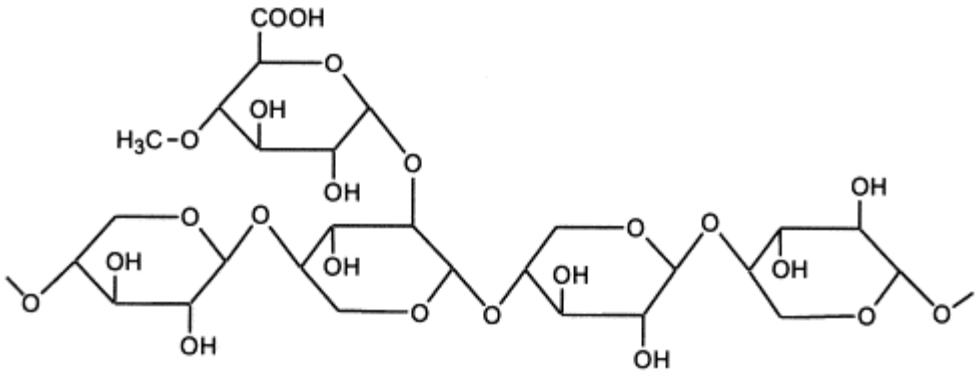

Figure 6: Structure of hemicellulose showing branches with reaping xylan backbone Tanczos et al. (2002) [63**] used with permission from Elsevier**

1.6.3 Lignin

Lignin is an amorphous, aromatic and complex macromolecule that is found naturally in cell walls of lignocellulosic materials. A proposed wheat straw lignin chemical structure by Sun et al. (1997) is shown in Figure 7 [**64**]. Lignin, cellulose and hemicellulose are bonded in a cross-linked matrix, forming a lignin-carbohydrate complex [**65**]. The lignin matrix is a sturdy and durable layer which has a shielding effect that protects the carbohydrate from enzymatic hydrolysis [**66**].

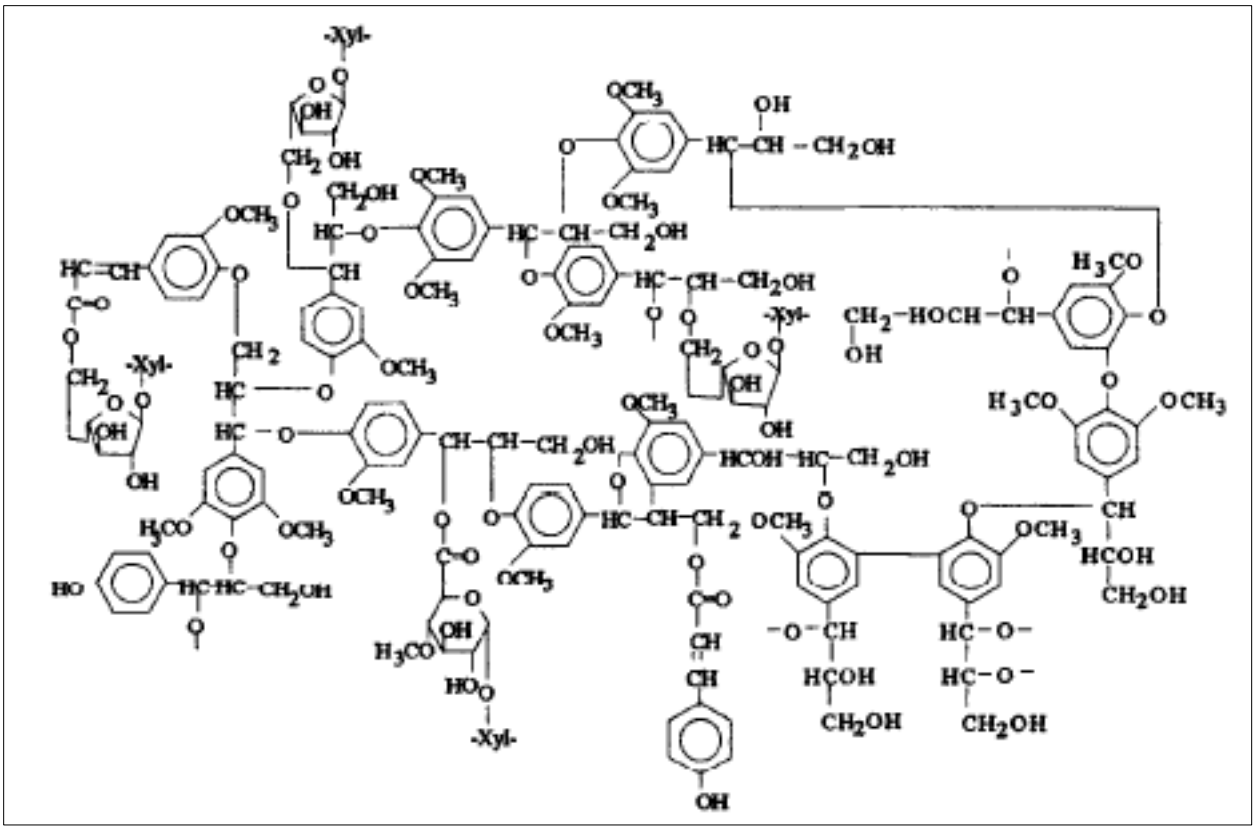

Figure 7: A tentative chemical structure of wheat straw lignin adapted from Sun et al. (1997) [64] used with permission from Elsevier

Lignin as a by-product in the bioethanol production process has its own value in terms of process operation and application. Solubilized lignin in alkali pretreatment can be recovered via precipitation from the pretreatment liquor by the addition of acid [**67**]. The retrieved lignin has a relatively high heating value (25.4 MJ/kg) [**28**] compared to the heating value lignocellulosic biomass (17.4 MJ/kg) [**68**]. As a result, lignin wastes can be combusted to generate heat and electricity for the process. Degradation of lignin and sugar could arise from different pretreatment conditions and these degradation compounds are generally inhibitory to the fermentation process. As a standalone application, retrieved lignin can be processed to produce polymer products such as biocomposites and epoxy resins [**69**].

1.7 Pretreatment of Lignocellulosic Materials Prior to Enzymatic Hydrolysis

1.7.1 The Need for Pretreatment

In the conversion of lignocellulosic biomass into ethanol, pretreatment is necessary in order for the overall process to have a higher hydrolysis yield and to be cost effective [**66**,**70**]. Pretreating lignocellulosic biomass results in an enhancement in cellulose digestibility and subsequent increase in ethanol production [**13**,**71**,**72**]. This is done by disturbing the lignin-carbohydrate complex/cellulose crystallinity, removing lignin/hemicellulose and increasing the porosity/surface area of the lignocellulosic biomass [**13**,**51**,**52**,**53**,**73**].

Depending on the feedstock, the correct pretreatment has a substantial impact on the process upstream (size reduction and storage), downstream (neutralization and inhibitory compound removal), overall process schematic [**70**], and extent and rate of delignification [**66**,**74**]. It has been estimated that the cost of the pretreatment is 18-19% of the total process cost [**34**,**70**,**75**,**76**], therefore the pretreatment method has to be chosen carefully to optimize the process. Generally, there are three types of pretreatment methods: physical, chemical and physicochemical.

1.7.2 Criteria for Ideal Pretreatment

After evaluating the technical aspects of different pretreatment methodologies, researchers have generated a list of criteria of what an ideal pretreatment would be for the production of bioethanol from lignocellulosic biomass. Criteria of an ideal pretreatment method includes [**13**,**28**,**66**,**74**,**77**,**78**]:

- Simple equipment and procedure for pretreatment
- Suitable for variety of substrates (lignocellulosic materials)
- Lignin separation from lignocellulosic materials to enhance enzyme hydrolysis yield
- Preserve both cellulose and hemicellulose for enzymatic hydrolysis and subsequent ethanol fermentation
- Reduce and disturb cellulose crystallinity to increase rate and yield of enzymatic hydrolysis

- Minimize capital, maintenance, equipment, energy and chemical cost
- Minimize production of inhibitory compounds that could affect the hydrolysis or the fermentation process
- Generate valuable co-products to enhance process economy

1.7.3 Physical Pretreatment

One of the major physical pretreatment processes is size reduction of the feedstock. Size reduction includes mechanical chipping, grinding and milling which reduce feedstock particle size thereby increasing the surface area [**13**]. One drawback of physical pretreatment is that the chemical composition remains the same, thus the shielding effect from lignin and hemicellulose is still present. Moreover, physical pretreatment is time consuming and energy demanding, making this an unattractive standalone pretreatment method. Due to these reasons, mechanical size reduction is usually used in combination with other pretreatment methods.

1.7.4 Physicochemical Pretreatment

Steam explosion is a physicochemical pretreatment method that uses high pressure saturated steam in the range of 180-270°C to rapidly heat up the feedstock for a given period of time (from seconds up to a few minutes) followed by a rapid cool down and depressurization to end the pretreatment [**79**,**80**]. During the heat up, organic acids from the feedstock hydrolyze a portion of the hemicellulose and alter the structure of lignin [**72**]. The sudden drop in pressure at the end of the reaction causes the biomass particles to swell up and expand, increasing the surface area of biomass at the molecular level. Lignocellulosic material pretreated by steam explosion has shown increased sugar conversion during enzymatic hydrolysis, however the loss of hemicellulose sugar and evolution of inhibitory products from carbohydrate degradation are considered undesirable for the downstream process of ethanol production [**72**].

Ammonia fiber explosion (AFEX) is a physicochemical pretreatment and is similar to steam explosion where instead of saturated steam, liquid ammonia is used as catalyst to improve downstream enzymatic hydrolysis. The process parameters for this pretreatment method are pressure (100-400 psig or 790-2859 kPa), temperature (70-200°C), reaction time (up to 30 min),

water to biomass ratio (up to 10:1 w/w) and liquid ammonia to biomass ratio (up to 2:1 w/w) [**71**,**72**,**81**]. The combined effects of ammonia and depressurization solubilize hemicellulose, remove lignin, de-crystalize cellulose and expand the cell wall of the treated biomass; these factors allow for a higher rate and extent of the enzymatic hydrolysis [**32**,**71**]. AFEX pretreatment is promising due to its advantages of ammonia recovery after pretreatment, limited washing requirements after pretreatment, relatively low generation of degradation product and absence of neutralization before enzymatic hydrolysis [**82**].

1.7.5 Chemical Pretreatment

Similar to steam explosion, catalyzed steam explosion pretreatment uses acids such as SO_2, H_2SO_4 or CO_2 to impregnate the lignocellulosic material to catalyze the pretreatment process [**72**]. Due to the presence of acids, hemicellulose is more readily removed, thus increasing the cellulosic digestibility of the substrate. Compared to other acids, SO_2 received the most attention due to overall lower inhibitory production, lower equipment requirement and higher sugar yield [**72**,**83**]. Catalyzed steam explosion suffers the same drawbacks mentioned in steam explosion; in addition, SO_2 is considered a toxic gas that poses potential hazards towards the health and safety of operators and the environment.

Dilute acid, especially sulfuric acid, is a chemical pretreatment process which is effective in hydrolyzing hemicellulose in the lignocellulosic biomass. The reaction temperature range is from 140-200°C, the acid concentration is usually lower than 4% (w/w) and the reaction time with the biomass is from minutes up to one hour [**51**]. The digestibility of the lignocellulosic material increases after dilute acid pretreatment with up to 90% of hemicellulose solubilized [**84**]. Major disadvantages of this pretreatment method include equipment corrosion problems and the generation of unwanted degradation products, which have inhibitory effects on the subsequent enzyme hydrolysis and fermentation processes [**72**]. The co-production of gypsum due to the required neutralization with lime in the downstream process is another unwanted by-product of dilute acid pretreatment [**70**].

Alkaline pretreatment is a chemical pretreatment method that uses lime, potassium hydroxide (KOH), sodium hydroxide (NaOH), ammonia or hydrogen peroxide (H_2O_2) as the caustic reagent

to pretreat the biomass [**75**]. Alkaline pretreatment has been performed on a wide range of lignocellulosic materials such as poplar wood, newspaper, grass stover, switch grass, corn stover and wheat straw [**73**,**85**,**86**,**87**]. Biomass after alkaline pretreatment has higher enzyme digestibility due to increase in internal surface area, lignin depolymerization and hemicellulose solubilization [**31**]. Of the five caustic reagents mentioned, NaOH has been reported to give the best results in maximizing the solubilization of hemicellulose and lignin, minimizing solubilization of cellulose and having the shortest reaction time [**31**,**75**]. Delignification as high as 90% and significant hemicellulose solubilization has been reported on wheat straw using alkaline pretreatment making it an attractive pretreatment method [**74**,**88**]. The operation parameters for alkaline pretreatment include moderate temperature at 55-160°C, and a wide range of residence times from 1 hour to 8 weeks [**89**]. A summary of different pretreatment costs is shown in Table 5.

Table 5: Cost evaluation of different pretreatment method adapted from Banerjee et al. (2010) [28**]**

Pretreatment	Equipment cost	Neutralization	Chemicals	Detoxification	Chemical Recovery	By-products	Energy
Mechanical	Low	NS	NS	NS	NS	NS	High
Dilute acid	Medium	Medium	Medium	Medium	Low	Low	Low
Alkaline	NS	Medium	Medium	Medium	Low	Medium	Low
Steam Explosion	High	High	Medium	NS	Medium	Low	Medium
AFEX	Medium	Low	High	NS	Medium	Low	Medium
Oxygen Delignification	High	Low	NS	NS	NS	Low	Low

NS – Not significant

1.8 Oxygen Delignification

Oxygen delignification is a pretreatment technique that is performed in a caustic environment and uses oxygen as an oxidizing agent to oxidize both organic and inorganic components [**52**]. It is a proven technology that has been used in the pulp and paper industry in order to reduce the lignin content of pulp [**90**].

Oxygen delignification was selected as the pretreatment method for this research of on wheat straw. Previous studies have shown that oxygen delignification can effectively remove lignin from lignocellulosic substrate and thereby enhance enzyme hydrolysis. These substrates include: pulp [**15**,**91**], sugarcane bagasse [**92**], corn stover [**93**] and wheat [**94**,**95**]. The delignification mechanism of oxygen delignification is through swelling, increasing biomass surface area, solubilizing lignin, partially solubilizing hemicellulose and de-crystallizing the cellulose structure [**87**,**96**]. During the oxygen delignification pretreatment process, little cellulose reacts as lignin and hemicellulose are solubilized [**87**,**97**,**98**,**94**,**99**]. This selective removal of lignin and hemicellulose is very desirable as it increases the digestibility of cellulose and minimum cellulose loss. The key process parameters are oxygen pressure (20-100 psig or 239-790 kPa), reaction time (up to 60 min), temperature (55-320°C) and caustic loading (0.5-10% w/w) [**28**,**86**,**94**,**100**]. Multiple studies have been conducted on lignocellulosic biomass using oxygen delignification as pretreatment at different operating conditions and the general conclusions were [**28**,**87**,**97**,**98**,**94**,**95**]:

- Fast lignin solubilization in the first 10-15 minutes and up to 40-65% lignin solubilized at the end of reaction
- Cellulose content in the solid fraction increased up to 70% per weight basis
- Hemicellulose solubilization produced a pentose-rich liquor that could potentially be used for pentose fermentation
- Few fermentation inhibitors were produced due to limited degradation of cellulose, hemicellulose and lignin

1.9 Oxygen Delignification Pretreatment for Bioethanol

In oxygen delignification, the lignocellulosic biomass first goes through size reduction such as milling to increase surface area and to have a uniform size distribution for subsequent processes. The next stage is the oxygen delignification where the biomass is reacted and fractionated into a cellulose-rich solid and lignin/hemicellulose-rich liquor. The cellulose rich solid will be converted into fermentable sugar through enzymatic hydrolysis and used to produce ethanol through fermentation. A beer stream (up to 10% ethanol) from the fermentation process is formed and will go through distillation and dehydration (molecular sieve) and finally into fuel grade ethanol. As a by-product from the pretreatment, lignin can be precipitated out by pH reduction. This can be done by bubbling CO_2 gas generated in the fermentation step. The precipitated lignin solution can then be separated and the hemicellulose can be hydrolyzed into pentose sugar for pentose fermentation. The solid lignin can be dried and used as a feedstock to produced lignin-based polymer products or combusted to generate heat and electricity for the plant. A process flow diagram for a bioethanol production plant using oxygen delignification is shown in Figure 8.

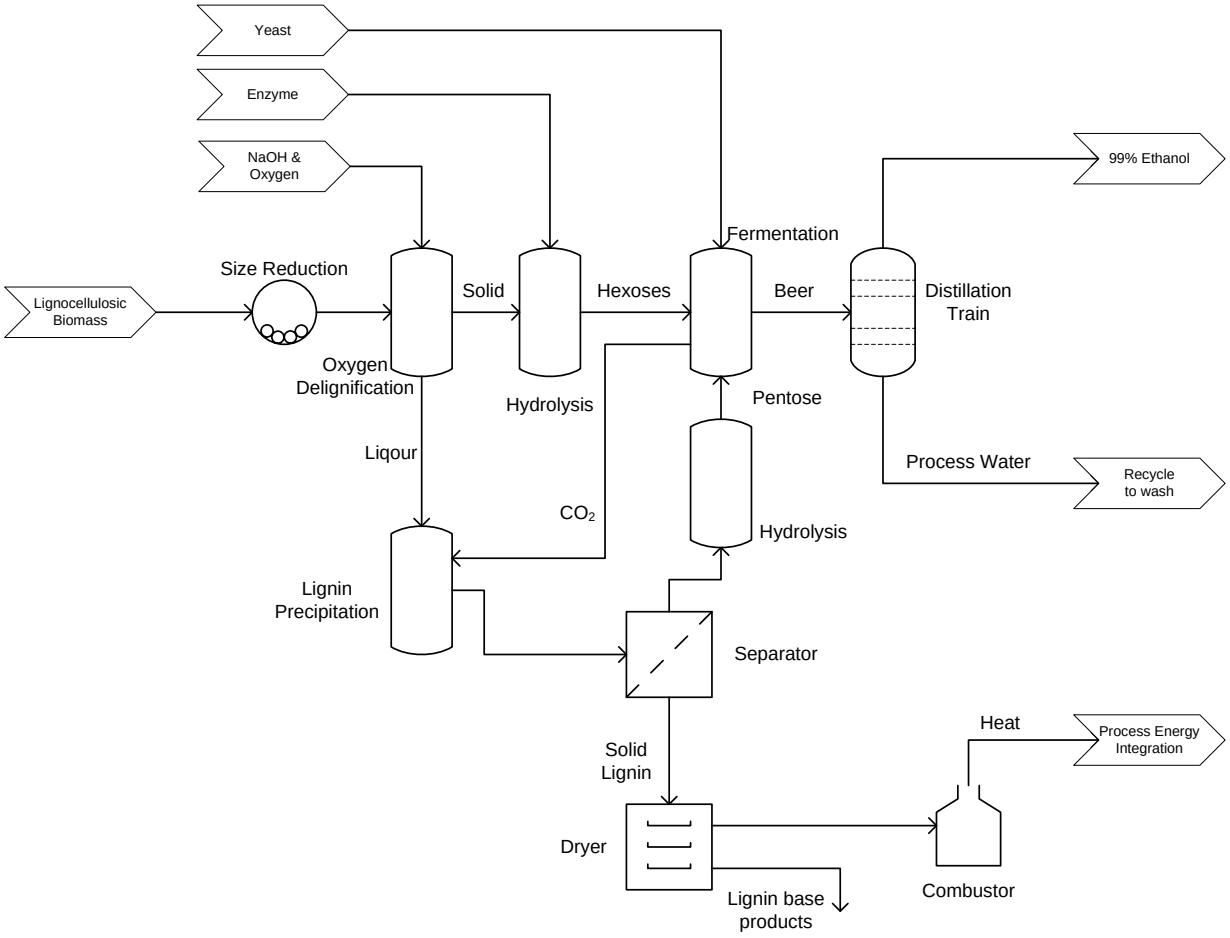

Figure 8: Process flow diagram for ethanol production from lignocellulosic biomass

1.10 Hydrolysis of Pretreated Lignocellulosic Material

Hydrolysis is the chemical reaction that cleaves long chain polysaccharide such as cellulose and hemicellulose into their respective oligosaccharides, disaccharides and monosaccharides. There are two predominate hydrolysis technologies: acid hydrolysis and enzymatic hydrolysis.

1.10.1 Acid Hydrolysis

Acid hydrolysis is a well understood technology that that has been used since the 1940s and the dominant chemical used in acid hydrolysis is H_2SO_4 [**101**]. Concentrated and dilute acid hydrolysis are the two types of acid hydrolysis in use. Typically, concentrated acid hydrolysis is performed in a one stage process where high sugar yield is achieved through the hydrolysis of cellulose. Dilute acid hydrolysis is performed in two stages where hemicellulose is hydrolyzed

in the first stage and cellulose is hydrolyzed in the second stage. A brief comparison of both hydrolysis modes is listed in Table 6.

Table 6: Concentrated acid and dilute acid hydrolysis adapted from Taherzadeh et al. (2007) and Karimi et al. (2006) [101,102**]**

Criteria	Concentration Acid Hydrolysis	Dilute Acid Hydrolysis
Sugar yield	Higher	Lower
Operating temperature	Lower	Higher
Acid loading	Higher	Lower
Corrosiveness	Higher	Lower
Reaction time	Shorter	Longer
Equipment and maintenance cost	Higher	Lower
Gypsum production due to neutralization	Higher	Lower
Energy cost	Higher	Lower
Sugar degradation	Higher	Lower
Inhibitor formation	Higher	Lower

1.10.2 Enzymatic Hydrolysis

Compared to acid hydrolysis, the major advantage of enzyme hydrolysis is that it does not require large volume of hazardous chemicals. Enzyme hydrolysis uses hydrolytic enzymes, mostly produced by fungi, to convert cellulose and hemicellulose into fermentable sugar. Based on techno-economical analysis, the enzyme cost range between 0.10-0.40 $/gal (0.03-0.11 $/l) ethanol produced [**103**,**104**,**105**]. In the biotechnology industry, Novozymes, a commercial enzyme producer, was able to produce enzyme at 0.50 $/gal (0.13 $/l) ethanol produced and it is expected to be reduced further with enzyme production technological advances in the future [**106**]. Nevertheless, the biofuel production will only become more economically attractive if the enzyme production costs are lowered [**107**].

Cellulase is the enzyme that is responsible for cellulose depolymerization. It is an enzyme complex that consists of different components and it differs in composition depending on the source microorganism, substrate and culture [**61**]. Cellulase consists of endoglucanases, exoglucanases and β-glucosidases [**108**]. Hydrolysis is initiated by absorption of endoglucanases and exoglucanases when absorbed into the amorphous region of the cellulose

surface [**61**]. The function of endoglucanase is to randomly cleave the β-1,4-glycosidic bonds in the straight chain cellulose molecule into smaller oligosaccharides [**108**,**109**] while the function of exoglucanase is to bind to the ends of the oligosaccharide chains and progressively cleave the chain into cellobiose units [**109**]. Finally, the β-glucosidase hydrolyzes the cellobiose into glucose [**108**]. The production of cellobiose has an inhibitory effect towards the enzymatic hydrolysis as it binds to endo- and exoglucanase, therefore it is important to have excess β-glucosidase in order to minimize this inhibitory effect [**108**,**110**,**111**,**112**].

Hemicellulase is required for the depolymerization of hemicellulose. The depolymerization of hemicellulose is similar to that of cellulose where coordination of endo- and exo- acting enzymes is required to cleave the carbohydrate into smaller units. The hydrolysis of hemicellulose is more complicated because of its highly branched structure. Due to the specific nature of enzymes, different types of enzymes have to be used in order to break all the specific branched linkages possessed by hemicellulose [**56**]. This might seem impractical, because of the numerous types of enzymes needed, however cellulase and the necessary hemicellulase are produced together by fungi [**108**]. Furthermore, commercial cellulase "cocktails" usually have activity towards both cellulose and hemicellulose [**56**], therefore this helps reduce the potential cost of producing these two enzymes separately. It has also been shown that, for biomass pretreated with steam explosion, replacing cellulase with xylanase helps increase the rate and the extent of the enzymatic hydrolysis [**113**].

1.11 Cellulose-to-Ethanol Process Configuration

There are multiple process configurations for the conversion of cellulose to ethanol. Although, several studies have examined the economic and technical aspects of such process configurations, the results are highly dependent on the feedstock and type of pretreatment. The configuration of enzymatic hydrolysis and fermentation is also a key processing decision, the hydrolysis and fermentation can be done separately (SHF) or simultaneously (SSF), shown in Figure 9 [**114**,**115**]. SHF was used in this research due to its applicability in laboratory.

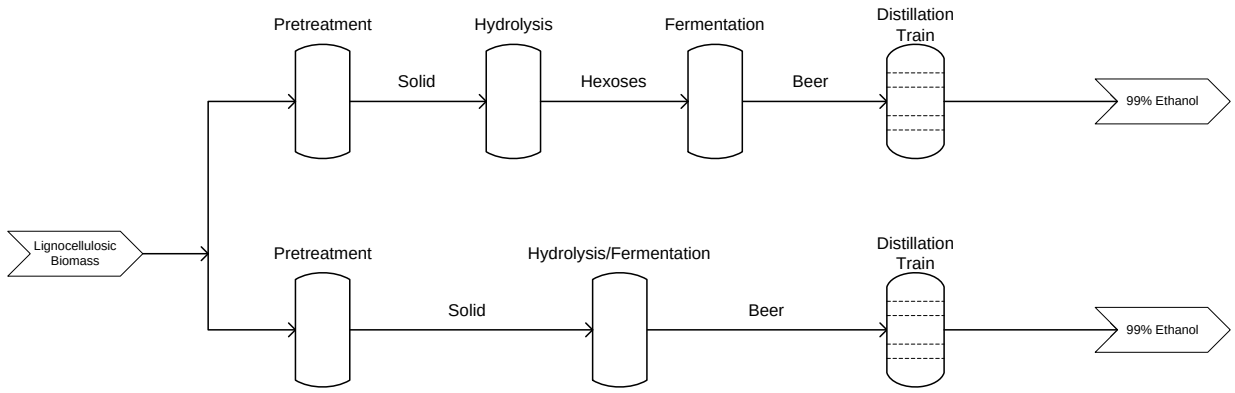

Figure 9: Simplified SHF and SSF process diagram [28**,**61**]**

During SHF, the cellulose enriched pretreated solids are enzymatically hydrolyzed by enzymes at 45-50°C to monosaccharides [**61**]. The sugar-rich hydrolysate is then used to ferment ethanol at 30°C [**61**]. The advantage of SHF is the ability to control and optimize each process unit individually in order to produce the highest sugar and ethanol yield. However, inhibitory effects of sugars to cellulase and β-glucosidase during enzymatic hydrolysis cause the rate of enzymatic hydrolysis to decrease, thereby longer operation time is needed to achieve complete hydrolysis [**108**,**110**,**111**,**112**].

The SSF configuration combines enzymatic hydrolysis and fermentation into a single process step. The cellulose-rich pretreated solids are hydrolyzed and fermented to ethanol at 37-38°C simultaneously in a single vessel. This configuration results in sugar being consumed by the fermenting organism rapidly, thus, reducing the sugar's inhibitory effect on cellulase and β-glucosidase and leads to an increase in the effective enzyme loading. The capital and operating costs are also reduced due to lesser equipment demand. Since the two process steps are combined into one, the operating condition is a compromise of the SHF individual process unit, lowering the efficiency of enzymatic hydrolysis and fermentation [**61**]. To overcome these challenges, genetically engineered organisms with higher optimum growth temperature can be used so that the process can be operated closer to the optimum temperature of the cellulase enzyme.

1.12 Oxygen Delignification Chemistry

A considerable amount of research has been performed on the oxygen delignification process, however, due to the complexity of the three phase reaction system, the chemical reaction fundamentals are not well understood [**90**,**116**].

According to Lucia et al. (2001), due to the alkali environment, the first step of the oxygen delignification reaction is thought to be initiated by deprotonation of the guaiacyl unit, a lignin polymer subunit, which a phenolate ion is produced [**90**,**116**]. Oxygen, acting as free radical, reacts with the phenolate ion to form a reactive intermediate called hydroperoxide and superoxide anion [**90**]. From that point, the hydroperoxide intermediate undergo oxidative cleavage by either oxygen or the superoxide anion into smaller radicals. These radicals ultimately break the lignin down into smaller molecules [**90**,**116**]. Figure 10 shows this oxidative cleavage mechanism of lignin [**116**].

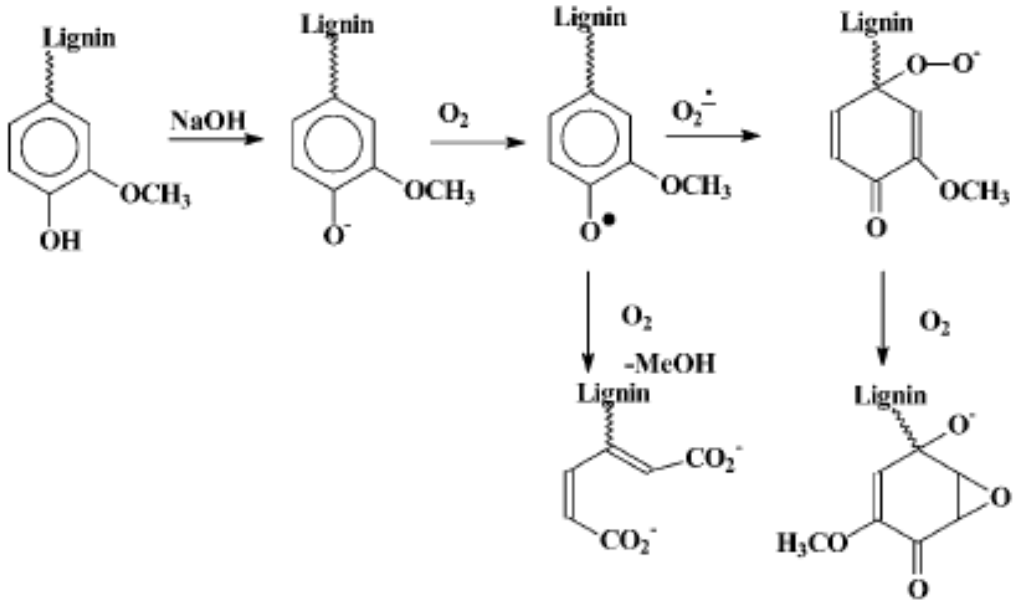

Figure 10: Mechanism of oxidative cleavage of lignin proposed by Lucia et al. (2001) [116**] used with permission from IUPAC**

This chain of radical reactions is possible due to the evolution of the superoxide anion. Gierer et al. (2001) proposed a reaction mechanism during the oxygen delignification process (Figure 11) [**117**]. The dissolved oxygen gas is ultimately reduced to hydrogen peroxide then to water

and a hydroxyl radical through a series of electron transfers. Each one of the four electron transfer step is described in detail by Gierer et al. (2001) [**118**]. The formation of hydrogen peroxide in Figure 11 is desirable as it can deprotonate into hydroxyl radical which promotes further delignification [**90**,**116**].

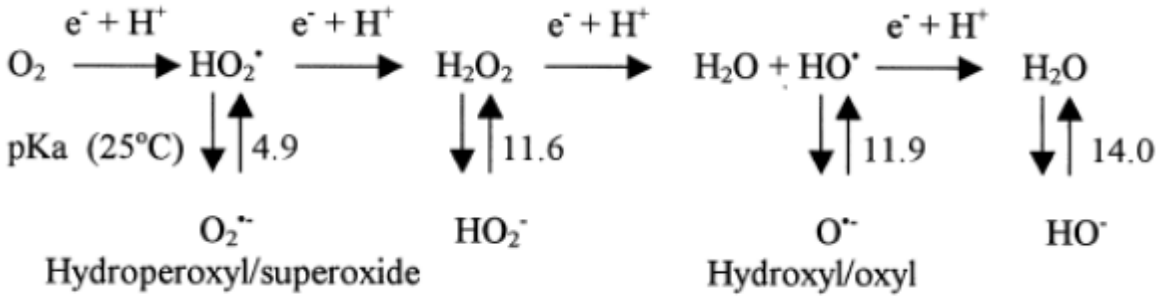

Figure 11: Fenton type reaction of oxygen to hydroxyl radical proposed by Gierer et al. (2001) [117**] used with permission from Taylor & Francis Online**

McDonough (1996) has suggested that along with lignin, carbohydrate in lignocellulosic biomass is also subject to oxidation during the oxygen delignification process [**90**]. The carbohydrate chains can be cleaved randomly by free radical reactions. The carbohydrate degradation reaction can be thought of as a "peeling" reaction with oxygen where the carbonyl group of the monomeric sugar unit at the end of the carbohydrate chain acts as an initiation identifier for this reaction. Once the sugar unit is utilized, the next monomeric sugar unit with the carbonyl group is exposed and the reaction continues as long as the carbonyl group is exposed. It is hypothesized that parallel competing reactions and modification of the carbonyl group would slow and stop this "peeling" reaction [**90**].

1.13 Effect of Oxygen Delignification Operating Parameters on Performance

As mentioned before, oxygen delignification has been widely used in the pulp and paper industry to remove lignin in the substrate. In order for the process to be effective, a pressurized alkaline environment at an elevated temperature is required. The oxygen delignification process, which separates lignin from the substrate, is governed by 5 main operating parameters: oxygen pressure, reaction time, temperature, caustic loading and substrate loading. The general effect of increasing these operating parameters is an increase in

delignification of lignin; however, carbohydrate will also have a higher degradation when operating conditions are more severe, therefore pretreatment conditions have to be optimized.

1.13.1 Effects of Oxygen Pressure

A higher rate of delignification can be achieved by increasing the oxygen partial pressure from 29-220 psig (301-1618 kPa) of oxygen, but the increase in delignification is not as significant when compared to the increase in temperature and caustic loading [**90**]. Charles et al. (2003) have shown limited improvement in delignification when oxygen pressure is increased from 70-100 psig (584-790 kPa) [**91**]. This effect of oxygen pressure is further demonstrated by Agrawal et al. (1999) (Figure 12) where the kappa number, is comparable between conditions at 60 and 100 psig (515-790 kPa) [**100**]. The kappa number is a measure of residual lignin and can be calculated by TAPPI standard procedure (T236 cm-85) using permanganate [**119**]:

$$kappa = \frac{p\ x\ f}{w} \qquad 1.1$$

where:

p = amount of 0.1N permanganate consumed, ml

f = factor correction to a 50% permanganate consumption

w = weight of moisture-free pulp, g

From these results, it is speculated that oxygen will be in excess and no significant change in delignification will result beyond 100 psi.

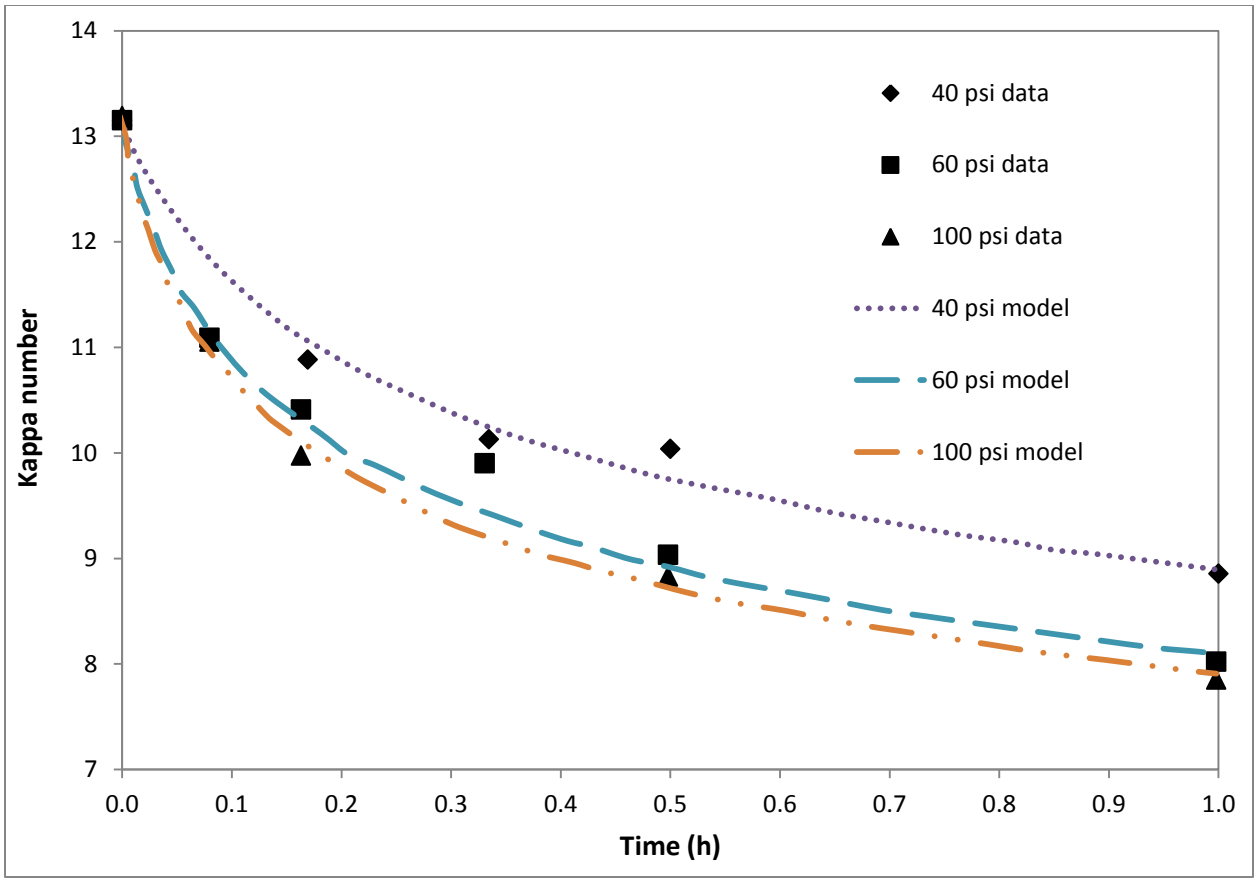

Figure 12: Effect of oxygen pressure on delignification of Southern hardwood pulp at 100°C and 2.5% (w/w) NaOH adapted from Agrawal et al. (1999) [100**]**

1.13.2 Effects of Reaction Temperature and Time

Increasing the temperature increases the rate and extent of delignification; however as Gierer et al. (2001) has demonstrated that the rate of carbohydrate degradation in cellulosic material is dependent on temperature [**117**]. Tao (2005) has also shown that the carbohydrate content of delignified softwood pulp decreases as the temperature increases from 100-140°C [**120**]. Kleppe et al. (1972) has suggested that there is minimal carbohydrate degradation at operating temperature range between 90-120°C [**121**].

Increasing the reaction time increases the extent of delignification of lignocellulosic material; however, carbohydrate degradation also increases if the reaction time is too long. This has been demonstrated by Schmidt et al. (1997), where the carbohydrate content (cellulose and hemicellulose) of wheat straw decreases with increasing reaction time. Furthermore, in a continuous production setting, shorter reaction time results in a smaller reactor. This translates

into lower capital cost, thereby benefiting the overall economy of the bioethanol production. Figure 13 shows how the residence time and temperature affect the delignification of Southern hardwood pulp [**100**].

It is obvious that the optimization of the desired rate and extent of delignification and carbohydrate degradation is possible if these two parameters are manipulated.

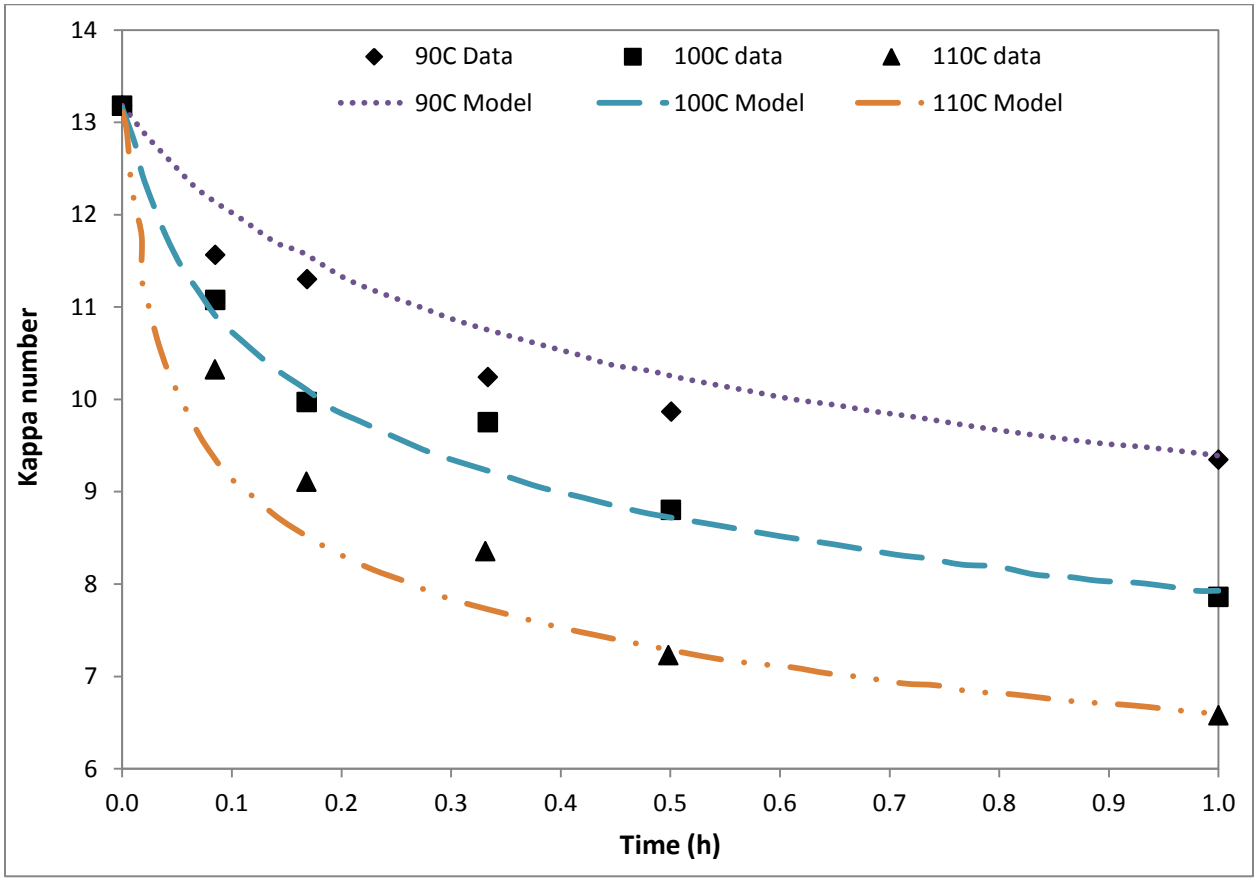

Figure 13: Effect of reaction temperature and time on delignification of Southern hardwood pulp at 100 psig oxygen and 2.5% (w/w) NaOH adapted from Agrawal et al. [100**]**

1.13.3 Effects of Caustic Loading on Oxygen Delignification Pretreatment

Increasing the caustic loading in oxygen delignification has a positive effect on delignification of lignocellulosic material [**87**,**90**,**91**]. This is shown in Figure 14, where increasing delignification was observed with increasing caustic loading over a range 1.5-3.5% w/w [**100**]. Higher caustic loading leads to higher concentration of hydroxide ions in the reaction medium, hence, the deprotonation rate of the lignin polymer increases. Due to production of organic acids from

carbohydrate and lignin degradation, hydroxide ions in the medium are consumed not only by ionizing lignin but also by neutralization of these acids. Caustic reagents are relatively expensive when compared to other pretreatment chemicals such as dilute sulfuric acid, ammonia etc.; therefore, the caustic loading has to be optimized in order for the pretreatment process to be economically viable. As lignin molecules are depolymerized through oxygen delignification, cellulose and hemicellulose become more vulnerable to oxidative attack by radicals; therefore increasing caustic loading also leads to higher carbohydrate loss [**87**]. This has been demonstrated by Varga et al. (2002), where up to 22.40% of carbohydrate was degraded when caustic loading increased from 1 to 10% w/w [**99**].

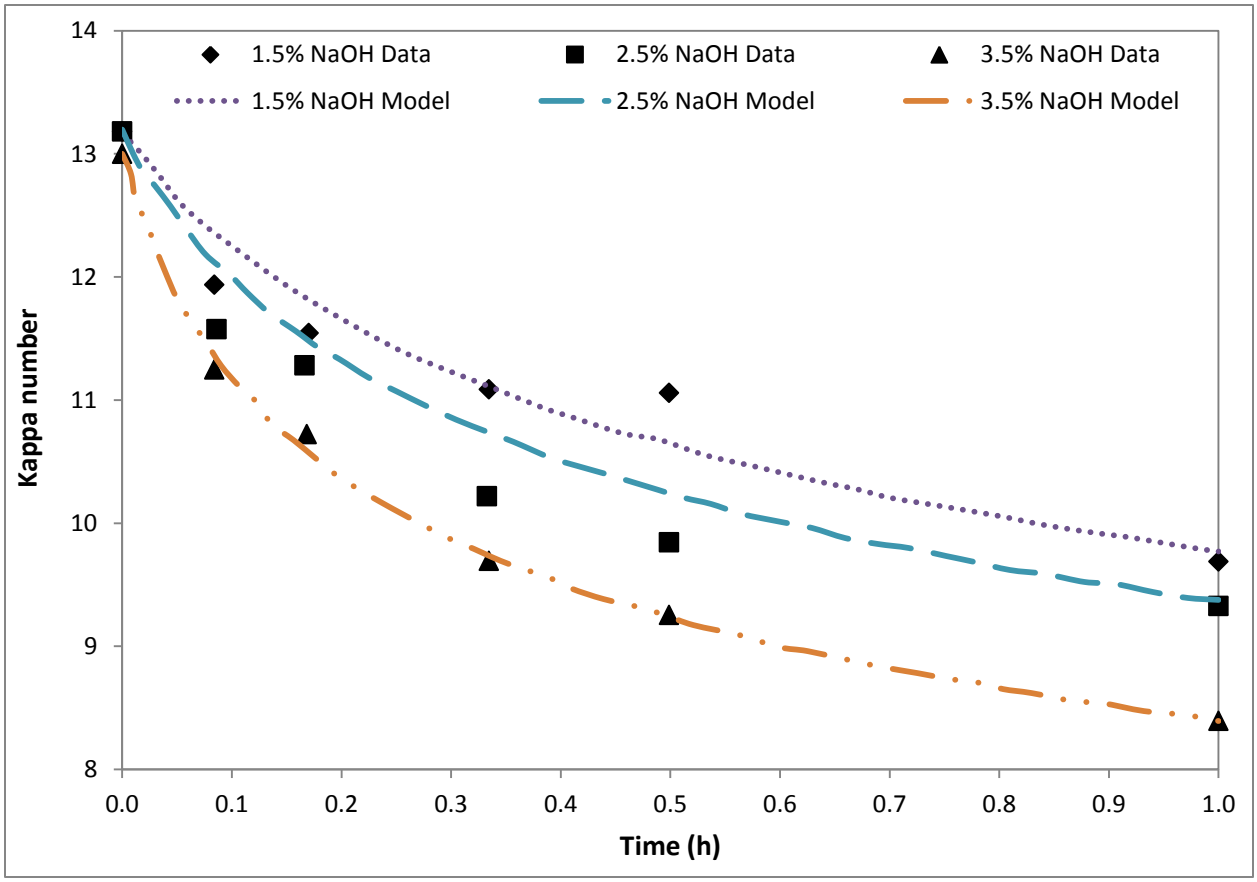

Figure 14: Effect of caustic loading on the delignification of Southern hardwood pulp at 100 psig oxygen and 100°C adapted from Agrawal et al. [100**]**

1.13.4 Effects of Initial Lignin Content

Substrates with higher initial lignin content have shown higher initial delignification rate [**100**]. Tao et al. (2005) have concluded that rate of oxygen delignification increases with increasing

initial lignin content [**120**]. Wood pulp lignin content as high as 14% w/w was tested by Tao and the delignification curves exhibit similar trend with respect to time (Figure 15). The difference in initial delignification rate is believed to be caused by the different amount of lignin moieties present in the lignocellulosic material [**100**,**122**].

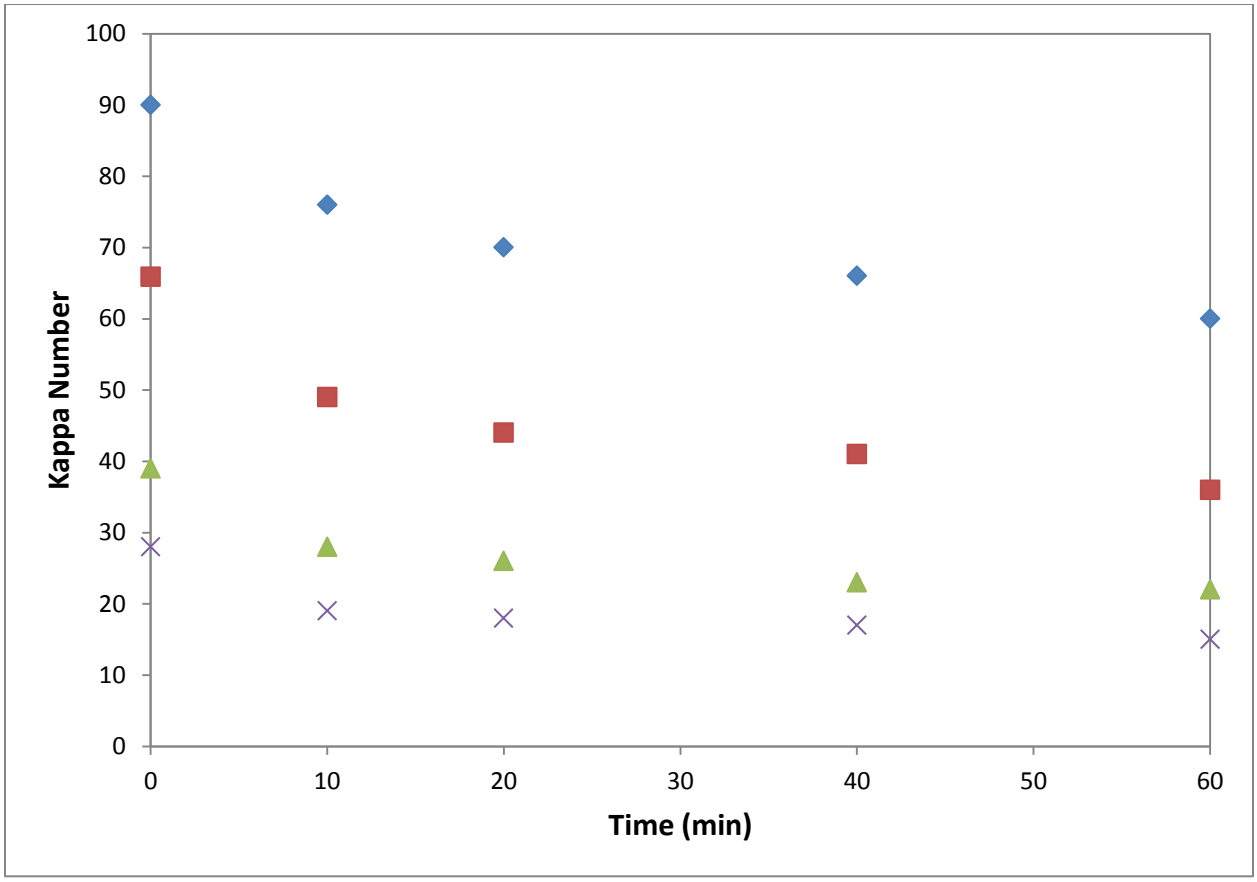

Figure 15: Effects of initial lignin content on oxygen delignification adapted from Tao et al. (2005) [120**]**

1.13.5 Effects of Operating Parameters on Selectivity of Delignification

In oxygen delignification, selectivity is defined as the ratio of the rate of delignification to the rate of carbohydrate degradation [**120**,**123**,**124**]. It is important for the pretreatment to be selective towards removing lignin and not the carbohydrates in order to maximize the carbohydrate recovery for hydrolysis. Even though it has been reported that oxygen delignification degrades lignin five to six times faster compared to carbohydrates, hydroxyl radicals are still able to cleave the carbohydrate chains indiscriminately [**120**,**123**]. The higher lignin content is thought to have a shielding effect that protects the carbohydrates from

degradation [**124**]. Sierra-Ramirez et al. (2011) observed that oxygen delignification is least selective with a 120 minutes reaction time, moderate temperature (160°C), moderate pressure (129 psig or 991 kPa) and high initial lignin content (29.12%) [**123**].

The general effects of initial lignin content, alkali concentration, temperature and pressure have on the selectivity of lignin in oxygen delignification has been studied by Tao et al. (2005) [**120**]. It was concluded that selectivity:

1. Increases as the initial lignin content in substrate increase from 3.68-13.26%.
2. Decreases as alkali concentration increase from 3-6% caustic (w/w)
3. Decreases as operating temperature increase (100 to 140°C)
4. Decreases as operating pressure increase from 45 to 105 psig (412 to 825 kPa)

In general, increasing operating parameters decrease selectivity and the caustic concentration has the greatest effect.

1.14 Delignification Kinetic Model Review

Multiple, predominantly empirical, kinetic models of oxygen delignification have been developed. The majority of these kinetic studies are performed on wood pulp and there is limited kinetic information on agricultural waste substrate. One of the most common approaches to modeling the kinetics of delignification is the assumption of first order reaction with respect to lignin. Schmidt et al. (1997) suggested that lignin, hemicellulose and cellulose removal follow pseudo first order kinetics in the oxygen delignification process when oxygen is in excess [**94**].

Yet, the most common approach for the kinetic study is an empirical model fitting of a power law equation. A variation to this approach is the two-region and multi region model proposed by Olm & Tedder (1979) and Kim & Holtzapple (2006) respectively [**125**,**126**]. A polymeric reaction model proposed by Schoon (1982) tried to characterize the delignification process with an infinite parallel reaction approach. Ji (2007) proposed that the reactor configuration could play a part in the kinetics of delignification and proposed a novel mechanistic model that

follows fundamental chemistry reactions in a Langmuir type isotherm [**125**]. Each of these modeling approaches will be discussed in the following sections.

1.14.1 Pseudo First Order Model

Schmidt et al. (1997) investigated the oxygen delignification kinetics of wheat straw. The derivation of the kinetic model starts from writing the delignification reaction (Equations 1.2-1.5) with assumption of the reaction being of elementary, second order, irreversible and each reacting component (hemicellulose, lignin and cellulose) reacting only with oxygen.

$$\mathrm{H} + \mathrm{O} \xrightarrow{k_1} \mathrm{P} \qquad 1.2$$

$$L + \mathrm{O} \xrightarrow{k_2} \mathrm{P} \qquad 1.3$$

$$\mathrm{C} + \mathrm{O} \xrightarrow{k_3} \mathrm{P} \qquad 1.4$$

Where:

H = hemicellulose

L = lignin

C = cellulose

P = products (including lignin and carbohydrate degradation products)

k_1, k_2, k_3 = kinetic constant for each reaction Equation 1.2 to 1.4

Using hemicellulose as an example, the second order kinetic expression can be written as:

$$-r_H = -\frac{d[C_H]}{dt} = -\frac{d[C_O]}{dt} = k_1[C_H][C_O] \qquad 1.5$$

Where:

C_H = concentration of hemicellulose

C_O = concentration of oxygen

With oxygen being in excess, Schmidt combined the oxygen term in Equation 1.5 with the kinetic constant k_1 and integrated it into a pseudo first order equation as:

$$-\ln\frac{[C_H]}{[C_{H_0}]} = k_1' t + c \qquad 1.6$$

Equation 1.6 was then fitted with data to solve for constant k'_1 and intercept *c*. High R^2 value (0.92-0.99) was achieved for all three components, showing high correlation between the pseudo first order kinetic model and the data. The solved kinetic model, however, only fit for the set of experiments Schmidt performed at 185°C and not at 200°C. The authors suggested that the solved pseudo first-order model does not fit well due to coating of cellulose at higher temperature. The pseudo first order model proposed by Schmidt et al. (1997) gives a general approach to characterizing the oxygen delignification, but only for specific pretreatment conditions [**94**]. The lack of the Arrhenius expression (which accounts for the temperature parameter) in Equation 1.6 might be the reason why Schmidt's model did not fit for higher temperature. Furthermore, due to the complexity of the delignification reactions, the assumption of first order elementary reaction with respect to lignin, cellulose and hemicellulose is questionable and a higher order reaction model has to be considered.

1.14.2 Power Law Model

A general power law can be used to model the rate of oxygen delignification as shown in Equation 1.7:

$$\frac{d[L]}{dt} = -k[L]^{a_1} \qquad 1.7$$

L = residual lignin in solid (g/l)

t = time (min)

k = kinetic constant (1/min *$(g/l)^{1-a1}$)

a_1 = reaction order

The kinetic constant in Equation 1.7 is a lumped constant which combines the effects of temperature, oxygen pressure (dissolved oxygen) and hydroxide ion into a single parameter.

For kinetic studies with varying temperature, oxygen pressure and caustic concentration, Equation 1.7 has to be rewritten in order to take into account the effects of these parameters (Equation 1.8).

$$\frac{d[L]}{dt} = -A\exp(-\frac{E_a}{RT})[L]^{a_1}[OH^-]^{a_2}[O_2]^{a_3} \qquad 1.8$$

t = time (min)

A = pre-exponential factor (min^{-1} $(g/l)^{1-a1-a2-a3}$)

E_a = activation energy (J/mol)

R = universal gas constant (8.314 J/mol K)

T = temperature (K)

L = residual lignin in solid (g/l)

OH^- = hydroxide ion concentration (g/l)

O_2 = dissolved oxygen concentration (g/l)

a_1 = reaction order with respect to lignin

a_2 = reaction order with respect to hydroxide ion

a_3 = reaction order with respect to dissolved oxygen

A typical delignification curve for oxygen delignification of lignocellulosic biomass (wood pulp) is shown in Figure 16. The delignification curve has a distinct initial and secondary reacting phase. In the initial phase, the lignin is removed faster compared to the slower secondary reacting phase [**91**]. Johansson et al. (1994) suggested that the different type of linkages present in the lignin polymer is what causes the transition from the fast to the slow secondary reacting phase [**122**].

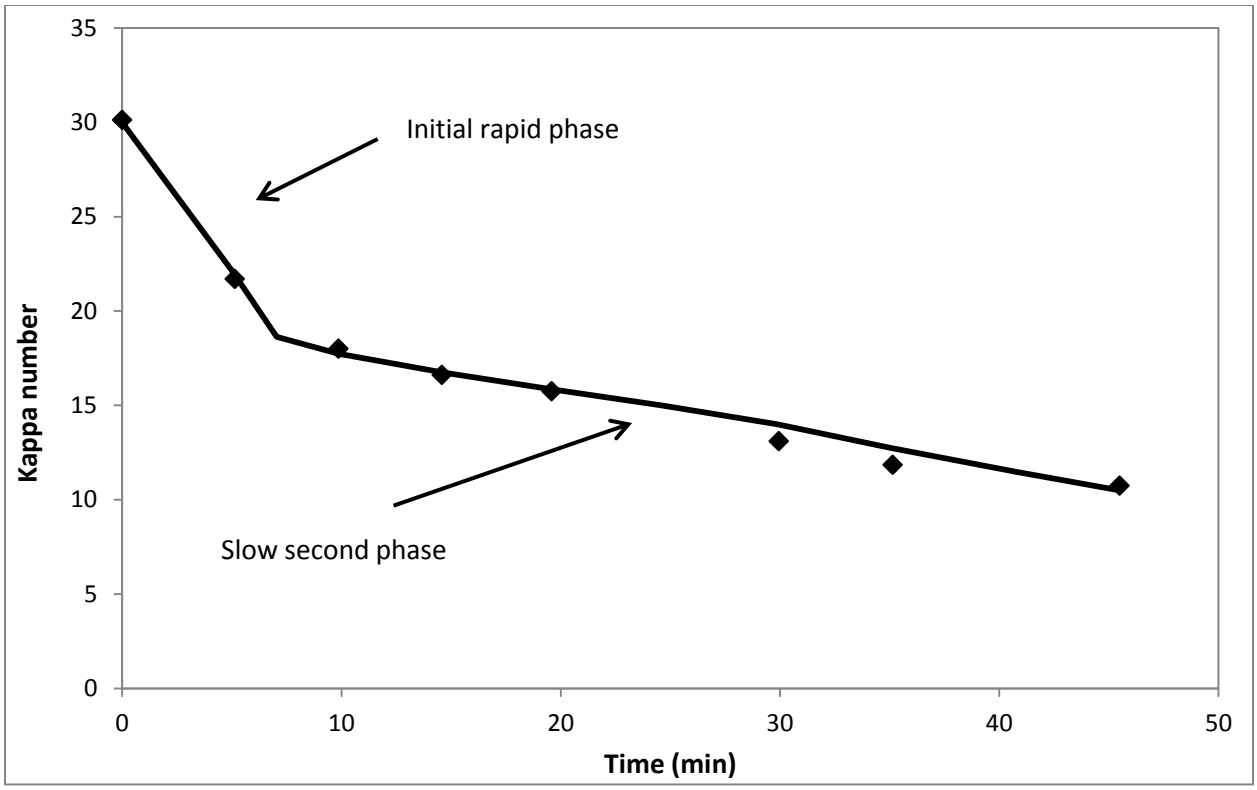

Figure 16: A typical oxygen delignification curve of wood pulp adapted from Olm & Tedder (1979) [35**]**

In order to model the fast and slow reacting phases, Olm & Tedder (1979) proposed that the overall oxygen delignification reaction is a summation of fast and slow reacting lignin and can be represented by a two-region kinetic model (Equations 1.9 and 1.10) [**35**]:

$$\frac{d[L]_{fast}}{dt} = -k_{fast}[L]^{a_{f1}}[OH^-]^{a_{f2}}[O_2]^{a_{f3}} \quad 1.9$$

$$\frac{d[L]_{slow}}{dt} = -k_{slow}[L]^{a_{s1}}[OH^-]^{a_{s2}}[O_2]^{a_{s3}} \quad 1.10$$

The constants *k* are temperature dependent and are given by the Arrhenius equation. The exponents, a_{f2}, a_{f3}, a_{s2} and a_{s3} are determined empirically whereas the constants a_{f1} and a_{s1} are usually assumed to be 1 [**127**]. Reported values of these parameters are shown in Table 7.

Table 7: Literature reported solved parameters of the two-region model [127**]**

Author	Substrate	Phase	Lignin exponent a_1	Hydroxide ion exponent a_2	Oxygen exponent a_3	EA (kJ/mol)	Pre-exponential factor
Iribarne & Schroeder (1997) [**128**]	Softwood pulp (Pine)	Fast	1	1.2	1.3	67	$3.6x10^{12}$
		Slow	1	0.3	0.2	40	$6.0x10^{4}$
Vincent et al. (1994) [**129**]	Hardwood Pulp	Fast	1	0	0.4	24.2	27.5
		Slow	1	0.39	0.38	46.3	7667
Olm & Tedder (1979) [**35**]	Softwood pulp	Fast	1	0.1	0.1	10	-
		Slow	1	0.3	0.3	45	-

Kim et al. (2006) modified the two-region model further into a three-region model and obtained an overall 0.88 reaction order with respect to lignin for corn stover [**126**]. Even though the two-region kinetic model offers a good prediction for the experimental data, there are no systematic ways to decide where the transition point between the fast and slow reacting lignin should be. The transition point, where fast reacting phase changes to slow reacting phase, depends on the experimental setup and substrate type. This results in an arbitrary assignment of the transition point that depends on the researcher's best judgment.

The two-region kinetic model can be simplified into a single power law model (one-region model) that is represented by Equation 1.7. Agrawal et al. (1995) have shown that a single-region power law model was able to capture the trend of the delignification of Southern hardwood pulp with sufficient precision (Figure 12-14) [**100**]. One major difference between the single-region and the two-region model is that there is less ambiguity on where the fast and slow reacting lignin transition point should be. Another difference is the reaction order with respect to lignin. Most two-region models have an assumed reaction order of 1, whereas the single-region model that Agrawal et al. (1995) presented has a reaction order of 7.7 [**100**]. The single-region model has a higher lignin reaction order because there is only one equation to account for the highly curved transition point between the fast and slow reacting phase.

The downfall of using empirical kinetic models is that they do not offer any information on the reaction mechanism. Due to the nature of empirical models, the single and two-region kinetic models can only model the delignification curve for the specific substrate type and pretreatment condition. The simplicity of the power law model approach allows researchers to solve for the reaction orders and kinetic constants through series of experiments; however it is time consuming to perform all the necessary experiments. Different operating parameters such as oxygen pressure, temperature and caustic loading etc. must be varied individually in order to solve the parameters in the power law model. Moreover, substrate samples must be collected at different reaction times for kinetic analysis. The compounding effect of varying operating parameters and sample collection time leads to an increase in experimental error.

1.14.3 Schoon's Model for Oxygen Delignification

Schoon (1982) provided an explanation of the higher order reaction seen in the oxygen delignification process. He assumed that there are infinite parallel reactions during the oxygen delignification with different rate constants corresponding to different regions in the oxygen delignification curve. This theory assumes the reactions are elementary, first order, with equal activation energies, but with unique reaction rate constants. The difference in rate constants can be rationalized because the reaction involves different moieties of the lignin polymer each with different reactivities. In deriving the model expression, Schoon started with the use of the power law model and integrated into:

$$-\int_{L_0}^{L} \frac{d[L]}{[L]^{a_1}} = k \int_{t=0}^{t} dt \qquad 1.11$$

Where *L* is the reacting lignin concentration, a_1 is the lignin reaction order and *k* is the lumped reaction constant incorporating the temperature, oxygen pressure and caustic loading. This is only possible when the operating parameters are assumed to be constant throughout the reaction and Equation 1.11 can be solved to give Equation 1.12:

$$\left(\frac{1}{[L]^{a_1-1}}\right) - \left(\frac{1}{[L_0]^{a_1-1}}\right) = k(a_1 - 1)t \;\; for\; a_1 \neq 1 \qquad 1.12$$

Equation 1.12 can be rearranged to predict the lignin content as function of reaction time (Equation 1.13):

$$[L] = \left[\left(\frac{1}{[L_0]^{a_1-1}}\right) + k(a_1 - 1)t\right]^{-\left(\frac{1}{a_1-1}\right)} for\ a_1 \neq 1 \qquad 1.13$$

With the special scenario where a_1 is 1:

$$\ln\left(\frac{[L]}{[L_0]}\right) = -kt\ \ for\ a_1 = 1 \qquad 1.14$$

Schoon's model gives the relationship between the lignin order, concentration and residence time. Using this model, Argawal et al. (1999) have demonstrated that the reaction order increases with decreasing initial lignin content in wood pulp [**100**].

1.14.4 Mechanistic Adsorption/Desorption Model

A mechanistic model for oxygen delignification was proposed by Ji et al. (2007). This model is based on proposed elementary reactions through the adsorption/desorption mechanism [**125**]. In this model, it was assumed that delignification is initiated by the deprotonation of lignin. The rate determining step is when the dissolved oxygen adsorbs and reacts with the deprotonated lignin adsorption sites (Equation 1.15). Ji's model additionally assumes that the total number of adsorption sites is constant and the adsorbed oxygen follows Langmuir-type adsorption isotherm.

$$-\frac{d[L_c]}{dt} = k[L^{*-}] \cdot [O_{2ads}] \qquad 1.15$$

Where:

L_c = residual lignin concentration

K = kinetic constant

L^{*-} = lignin active sites

O_{2ads} = concentration of oxygen adsorbed onto lignin active sites

After a series of derivations and substitutions, Equation 1.15 can be rewritten as Equation 1.16 and 1.17.

$$-\frac{d[L_c]}{dt} = C_1\left(\frac{[OH^-]}{K_{water} + k_{HL^*}[OH^-]}\right)\left(\frac{[P_{O_2}]}{1 + K_e[P_{O_2}])}\right)[L_c] \qquad 1.16$$

$$C_1 = k \cdot K_{HL^*}C \cdot K_e C_t \qquad 1.17$$

Where:

k = kinetic constant

k_{HL*} = equilibrium constant for deprotonation of lignin

K_{water} = equilibrium constant for water

C = proportionality constant of active lignin sites

C_t = total lignin active sites

K_e = equilibrium constant of oxygen adsorption and desorption

P_{O_2} = partial pressure of oxygen (psia)

The partial pressure of oxygen in alkaline solution was determined by using Tromans model equation for oxygen solubility in inorganic solutions [**130**]. Ji et al. (2007) solved Equations 1.16 and 1.17 by holding either the caustic concentration or the oxygen pressure constant, while varying the other parameter. Equation 1.18 is the final form of this mechanistic derivation when the delignification process was performed at 90°C.

$$-\frac{d[L_c]}{dt} = 1.18 \times 10^{-3}\left(\frac{[OH^-]}{0.111 + [OH^-]}\right)\left(\frac{[P_{O_2}]}{1 + 2.26 \times 10^{-2}[P_{O_2}]}\right)[L_c] \qquad 1.18$$

Through adsorption theory, Ji's model is the first to provide a mechanistic approach to oxygen delignification. A drawback of this model is the data treatment whereby the rapid change of delignification before the 10 minute mark was neglected. Consequently, the delignification data after the 10 minute mark fall into the linear region of what Olm & Tedder (1979) proposed in the two-region model [**35**]. This allows Ji to solve the unknown parameters as a first order reaction with respect to lignin. Due to this reason, it is highly possible that Ji's model might not be able to predict the oxygen delignification data in the rapid changing initial phase of the reaction.

2 Thesis Objective

Numerous oxygen delignification kinetic models have been proposed for lignocellulosic biomass such as wood pulp, however limited research was performed on agricultural waste such as wheat straw [**100**,**131**].

The primary objective of this research was to study the reaction kinetics of oxygen delignification of wheat straw. The independent operating parameters that were studied are reaction temperature (90-130°C), caustic loading (5-15% w/w) and substrate loading (2-4% w/w). Samples were taken at different time intervals in order to measure the change in solid lignin content and hydroxide ions. An empirical model was developed to predict the lignin content of the pretreated substrate as a function of the operating parameters.

In order to evaluate the effectiveness of the oxygen delignification process, a secondary objective was to explore the effects of different oxygen delignification conditions on the pretreated substrate. This was accomplished by compositional analysis at different experimental conditions and by enzymatic hydrolysis of the pretreated substrate.

A third objective was to perform a techno-economical analysis of the oxygen delignification pretreatment. This was accomplished by developing a simulation of the oxygen delignification pretreatment process in Aspen Plus. The developed kinetic reaction model was implemented into the simulation. Using the economic analysis tool in Aspen Plus, the capital and operating cost of the pretreatment reactor were evaluated. The effects of different operating parameters on the costs of pretreatment were examined. Finally sensitivity analysis was performed on the cost of biomass, NaOH and enzyme to quantify their effects on the pretreatment cost.

3 Materials and Methods

3.1 Procedure for Substrate Preparation Pretreatment

The substrate studied in this research was wheat straw provided by Viterra. A hammer mill was used and wheat straw was passed through a 1 mm screen [**132**]. The milled substrate was stored in a Ziploc plastic bag and refrigerated at 4°C until use. The oven dry weight (ODW) of the milled substrate was determined by drying the substrate in a pre-weighed aluminum weigh boat at 105°C.

3.2 Procedure for Extractive Determination

NREL's TP-510-42619 procedure for determining extractives in biomass was adapted to determine the extractive content of the substrate [**133**]. The water extractives step was not performed due to observed delignification in the hot water bath, which could influence the subsequent delignification studies. The Soxhlet method was used to perform the extraction. The ODW of a flat bottom rounded receiving flask and a magnetic stirrer was first determined by drying them in an oven at 105°C for a minimum of 12 hours and cooling to room temperature in a desiccator. Approximately 5.0 g of substrate was placed in an extraction thimble and into the Soxhlet apparatus. The weight of the substrate and the thimble was recorded. Approximately 250 ml of 100% ethanol was placed in the receiving flask along with the magnetic stirrer. The heating mantle was adjusted to ensure that a minimum of 6-10 siphon cycles per hour was achieved. The apparatus was refluxed for at least 24 hours. After extraction was completed, the ethanol solvent was removed by heating to approximately 30-40°C under vacuum until all solvent was evaporated. The extract in the receiving flask, including the magnetic stirrer was stored in a desiccator overnight, after which the weight was recorded. The extractive content was determined by the weight difference of the receiving flask and magnetic stirrer before and after the extraction.

3.3 Procedure for Ash Determination

NREL's TP-510-42622 procedure of "Determination of Ash in Biomass" was used to determine the ash content [**134**]. A ceramic crucible was first fired in a Thermo Scientific Thermolyne bench-top furnace at 575°C. The crucible was cooled to room temperature in a desiccator and

the weight was recorded. Approximately 2.0 g of the milled substrate was transferred into the crucible and was ignited by heating over a Bunsen burner. The burnt substrate was then placed in the furnace at 575°C for at least 24 hours. The weight of the crucible and ash was recorded together after 1 hour of cooling in a desiccator.

Figure 17: Thermo Scientific Thermolyne bench-top furnace (photo credit: Pope [93])

3.4 Procedure for Carbohydrates and Lignin Determination

The composition of wheat straw was determined in order to quantify the contents of carbohydrates and lignin before and after pretreatment.

As adapted from NREL's TP-510-42620 procedure of "Preparation of Samples for Compositional Analysis", all substrate samples were dried at 35-40°C (< 10% moisture) before compositional analysis [**135**].

A slightly modified version of the NREL's TP-510-42618 procedure, "Determination of Structural Carbohydrate" was used to determine the carbohydrates and lignin content of wheat straw [**136**]. The goal of this procedure was to hydrolyze the carbohydrates in the substrate with concentrated sulfuric acid and leave the residual solids as acid insoluble lignin. Serum bottles (100 ml) were used in place of pressure glass tubes. To begin the procedure, 3.0 ml of 72%

(w/w) sulfuric acid was added to 300 mg of dry substrate. The solid/liquid solution mixture was mixed with a Polytetrafluoroethylene (PTFE) stir rod. The serum bottles were then transferred into a 30°C water bath and were stirred with PTFE stir rod every 10 minutes. After 60 minutes of reaction time, 84.0 ml of distilled water was added into each serum bottle in order to dilute the acid to a 4% w/w concentration, bringing the total volume (along with the sulfuric acid) to 86.73 ml. Calculation of the filtrate volume can be found in

Appendix A. The serum bottles were sealed with butyl rubber septum, crimped aluminum seals and autoclaved at 121°C for one hour in a Midmark M11 UltraClave.

After the autoclave cycle was completed, the serum bottles were cooled to room temperature before harvesting the solid contents through crucible filtration. A vacuum system was used to separate the solids from the acid hydrolyzed liquor. A pre-weighed crucible was used to retain the solid fraction and a plastic sampling tube was used to collect approximately 30 ml of acid hydrolyzed liquor for analysis of carbohydrates and dissolved lignin.

The solids in the crucible were first dried overnight at 105°C and the weight was recorded. Next, the crucible was placed in the bench-top muffle furnace at 575°C for at least 4 hours, cooled in a desiccator for 1 hour and the weight was recorded in order to determine the ash content. The acid insoluble lignin was calculated by the difference between the weight of the crucible and the weight of the crucible plus the solid dried at 105°C minus the weight of the ash.

The amount of lignin dissolved during the acid hydrolysis need to be determined in order to calculate the total lignin content of the substrate. The acid soluble lignin was quantified by using a UV-Visible spectroscopy method on the collected liquor. The selected wavelength was 320 nm and the absorptivity was 30 l/g cm [**136**]. As recommended by NREL, this wavelength was selected in order to minimize interference from carbohydrate degradation products. Distilled water was used as blank and the acid hydrolyzed liquor was diluted with distilled water into the absorbance range of 0.7-1.0 before recording the absorbance value. Each sample was analyzed within 6 hours of hydrolysis with ± 0.005 absorbance units.

The amount of acid soluble lignin was calculated by the following equation:

$$\text{Acid soluble lignin } \% = \frac{Abs * Vf * Df}{\varepsilon * ODW * cell} * 100 \qquad 3.1$$

Where:

Abs = absorbance value at 320 nm

Vf = volume of filtrate liquor, 86.73 ml

Df = dilution factor

ε = absorptivity, 30 l/g cm

ODW = Oven dry weight of sample (g)

cell = cell path length, 1 cm

Approximately 5 ml of the collected acid hydrolyzed liquor was used for carbohydrate analysis. Calcium carbonate was used to neutralize the acid hydrolyzed liquor into the pH 5-6 range and the resultant solids were allowed to settle. The supernatants were collected and passed through a 0.22 µm filter before the HPLC analysis for carbohydrates.

3.5 Procedure for Oxygen Delignification Pretreatment

Based on the experimental design listed in Table 8, the desired amount of either 10.0 or 20.0 grams (2 or 4 % substrate loading) of wheat straw was placed in a tarred PARR 4520 vessel and the vessel was sealed by fastening the split rings and safety drop ring. Additional experiments were performed at 90°C, 2% substrate loading and caustic loading at 7.5% (for model validation), 12 and 13% (for caustic saturation point estimation) and 17.5% (for caustic saturation confirmation). The parameter values listed in Table 8 were used due to several reasons. The temperature was chosen at the range of 90-130°C in order to avoid major carbohydrate loss as reported by Kleppe et al. (1972) (90-120°C). The effect of oxygen delignification at 2% substrate loading had been demonstrated in previous work by Pope et al. (2011). A doubled substrate loading (4% w/w) was used in order to observe the effects of the substrate parameter had on the pretreatment. Oxygen delignification pretreatment using caustic loading between 1 to 10% w/w had been reported in the literature, however there are limited data on caustic loading beyond 10%, therefore 15% was chosen as part of the experimental parameter. The oxygen pressure was chosen at 100 pisg due to results reported by Charles et al. (2003) and Agrawal et al. (1999) had demonstrated that oxygen pressure beyond 100 psig had limited improvement on delignification. The reaction time of the pretreatment was 60 minutes with sampling time at 2.5, 5, 10, 30 and 60 minutes in order to observe the pretreatment effects on carbohydrate and lignin content of the substrate.

The sealed reactor was placed onto a reactor mount and sparged with nitrogen gas at 60 psig (515 kPa) for 5 minutes to remove air and to avoid possible substrate auto ignition during heat up. An electrical heating jacket was used to heat the PARR 4520 reactor to the desired temperature.

Table 8: Experimental design and parameter values

Parameter	Value
Temperature (°C)	90, 110, 130
Substrate loading (% w/w)	2, 4
NaOH loading (% w/w of substrate weight)	5, 10, 15
Oxygen pressure (psig)	100 (790 kPa)
Reaction time (min)	60

A stainless steel cylindrical vessel was used to heat the caustic solution separately to ensure there was no delignification during heat up. The desired caustic concentration was prepared by diluting 50% w/w NaOH with distilled water. A ¼ in. (0.635 cm) diameter, 24 in. (60.96 cm) length convoluted stainless steel tube was used to connect the cylindrical vessel and the PARR 4520 vessel. The caustic solution was loaded into the cylindrical vessel and sparged with pure oxygen gas at 100 psig (790 kPa) continuously to promote mixing. An OMEGA heating tape was used for heating the cylindrical vessel to the desired reaction temperature. The oxygen delignification reactor setup is presented in Figure 18.

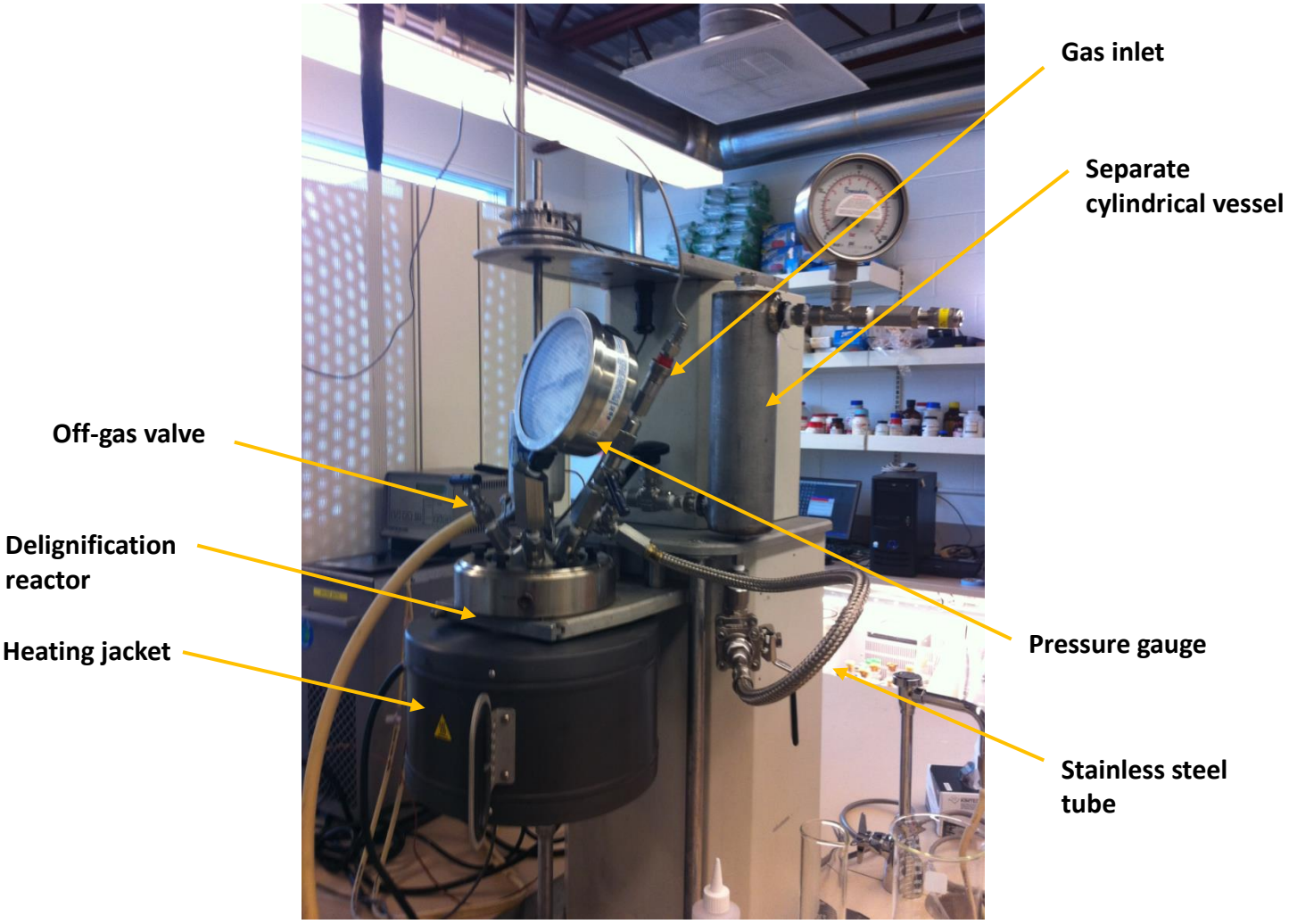

Figure 18: Oxygen delignification reactor setup

After the desired temperature was reached in both vessels, the caustic solution was charged from the cylindrical vessel into the PARR 4520 reactor to initiate the oxygen delignification reaction. During the reaction, pure oxygen was fed into the reactor continuously at 1 l/min. The samples were collected at 2.5, 5, 10, 30 and 60 minutes. Approximately 15-20 ml of sample was collected at each sampling time into a 100 ml graduated cylinder by opening the sampling port. The collected samples included both substrate (wheat straw) and liquor (liquid from reaction). When a sample was collected, it was stored in a glass test tube and quenched in an ice bath for at least 10 minutes to prevent further reaction. It was then centrifuged at 1533g for 5 minutes and filtered through a 0.22 µm filter before the dissolved lignin was determined. The solids that were removed during sampling were filtered, weighed and recorded as waste

for mass balance purposes. Some of the liquor was used to determine the dissolved lignin and carbohydrate concentration described in section 3.6, 3.7 and 3.8. After 60 minutes of pretreatment was completed, the pretreated substrate and liquor were filtered through a Büchner funnel under vacuum using a Whatman™ 541 filter paper. The filtered substrate was washed three times with a total of approximately 400 ml of distilled water. The moisture content of the washed substrate was approximately 80% and it was refrigerated at 4°C for carbohydrate determination and enzymatic hydrolysis.

3.6 Determination of Dissolved Carbohydrates after Pretreatment

NREL's TP-510-42623, procedure for "Determination of Sugars, Byproducts, and Degradation Products in Liquid Fraction Process Samples" was used to quantify the amount of carbohydrates released from wheat straw into the liquor during the oxygen delignification pretreatment [**137**].

Liquor samples (5.0 ml) were transferred into serum bottles and the pH of each sample was measured. Depending on the pH of the samples, the appropriate amount of 72% w/w sulfuric acid was added into the samples to bring the content to a final 4% w/w acid concentration. The solution was mixed by swirling the serum bottles. The serum bottles were sealed with butyl rubber septum, crimped aluminum seals and autoclaved at 121°C for one hour in a Midmark M11 UltraClave. After the autoclave cycle was completed, the serum bottles were cooled to room temperature before removing the aluminum seals and rubber septum. Calcium carbonate was used to neutralize the acid hydrolyzed liquor to the pH 5-6 range and the resultant solids were allowed to settle. The supernatants were collected and passed through a 0.22 µm filter before HPLC analysis.

3.7 Dissolved Lignin Determination after Pretreatment

It has been reported by other researchers that dissolved lignin from lignocellulosic biomass has an absorbance maximum at approximately 276 nm [**138**], 277.5 nm [**139**] and 280 nm [**125**,**132**,**140**,**141**]. In order to find the maximum absorbance of dissolved lignin of the wheat straw in this study, a spectrum scan between 190 to 600 nm was performed. A Shimadzu UV-1800 spectrophotometer along with the software UVProbe v.2.34 was used to identify the absorbance peak. Several diluted samples were scanned and, as seen in Figure 19, there is a

maximum absorbance at approximately 270 nm. The slight deviation compared to reported literature values by other researchers could potentially be caused by the method of lignin isolation or the type of substrate from which the lignin was isolated. Absorbance at 270 nm was chosen as the wavelength to be used in order to determine the concentration of the dissolved lignin in the liquor from pretreatment. The absorbance peak seen near the 205 nm is caused by NaOH in the sample [**125**]. This should not interfere with the absorbance reading at 270 nm.

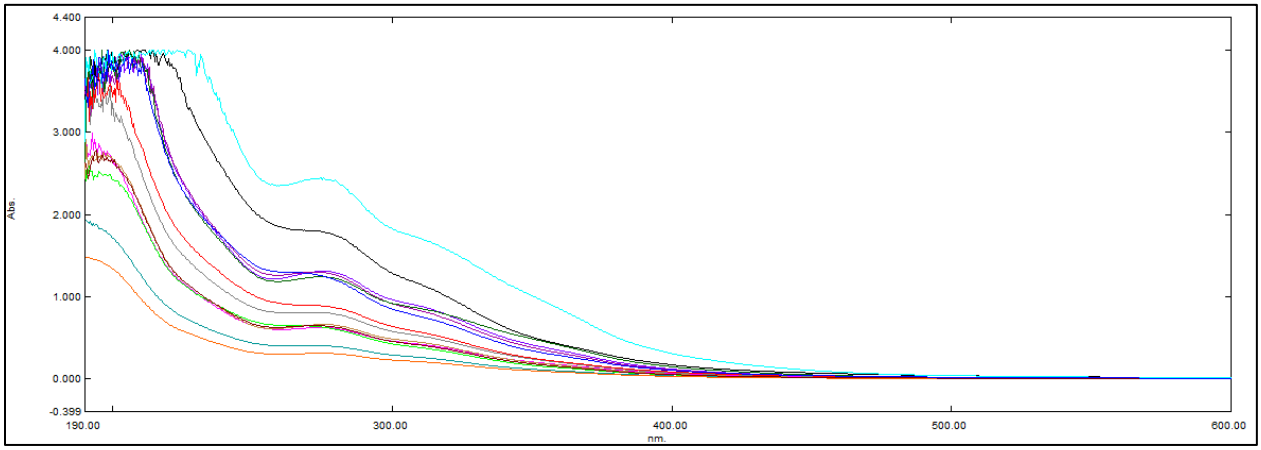

Figure 19: Lignin spectrum scan of liquor after different pretreatment conditions

3.8 Dissolved Lignin Absorbance Calibration

A calibration curve between the absorbance and the dissolved lignin concentration in the pretreated liquor was constructed at a 270 nm wavelength. Various solid and liquor samples at different temperature and caustic loading were collected during the oxygen delignification for this calibration. Once the samples were collected, approximately 5 ml of the pretreated liquor was transferred to a test tube, passed through a 0.22 µm filter and diluted with distilled water into the absorbance range of 0.2-1.0. In order to construct the calibration curve, the concentration has to be known for the corresponding absorbance reading; this was done by analyzing both the solid and liquid fraction of collected samples at different pretreatment times. The solids collected were first washed with distilled water thoroughly, passed through a Watman No. 4 filter and dried at 40°C. The residual lignin content present in the solids was determined by the acid hydrolysis procedure (section 3.4). The amount of lignin dissolved into

the liquor was determined through mass balance. A flow chart of this calibration is shown in Figure 20. The numeric values presented in Figure 20 are for reference only.

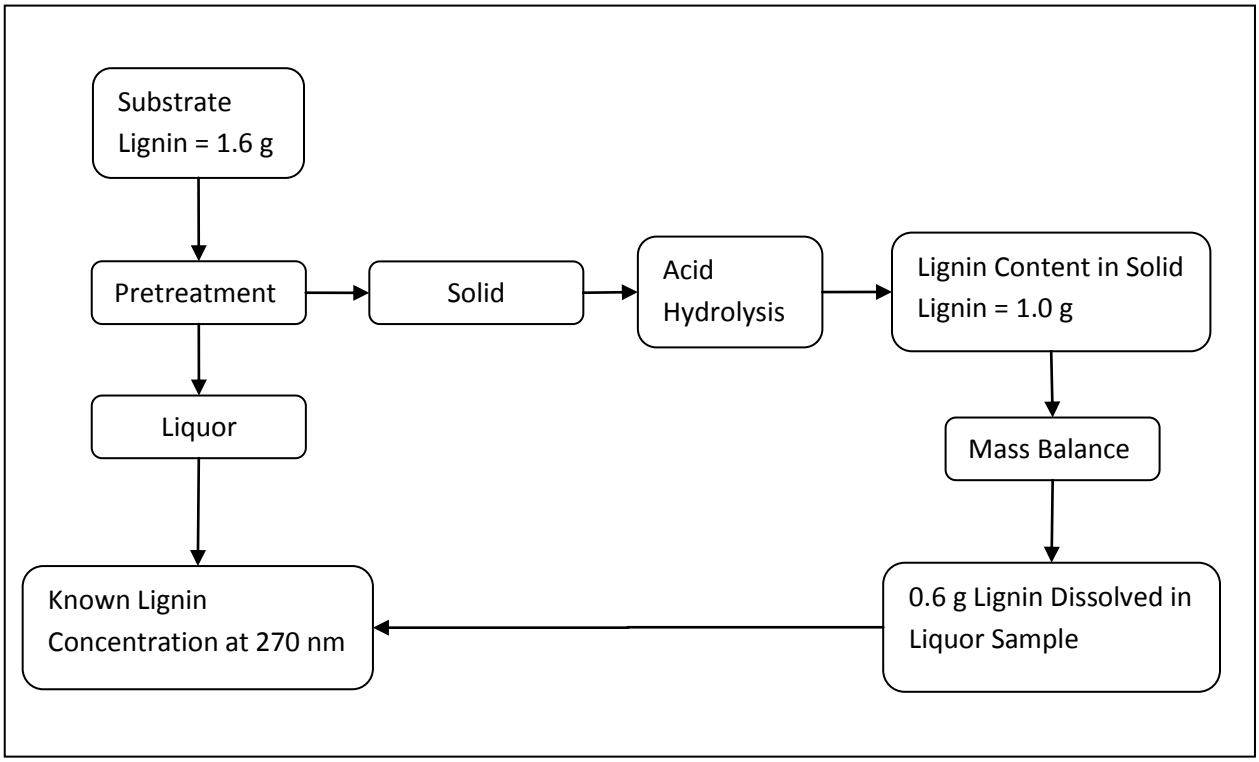

Figure 20: Example of the dissolved lignin calibration

The dissolved lignin calibration curve is shown in Figure 21. The correlation between absorbance at 270 nm and dissolved lignin concentration is high with a R^2 value of 0.97. Using Beer-Lambert Law where:

$$\text{Absorbance} = \frac{\text{Concentration}}{\text{k}} \qquad 3.2$$

Where 1/k is the extinction coefficient, its value is 29.5 l/g cm.

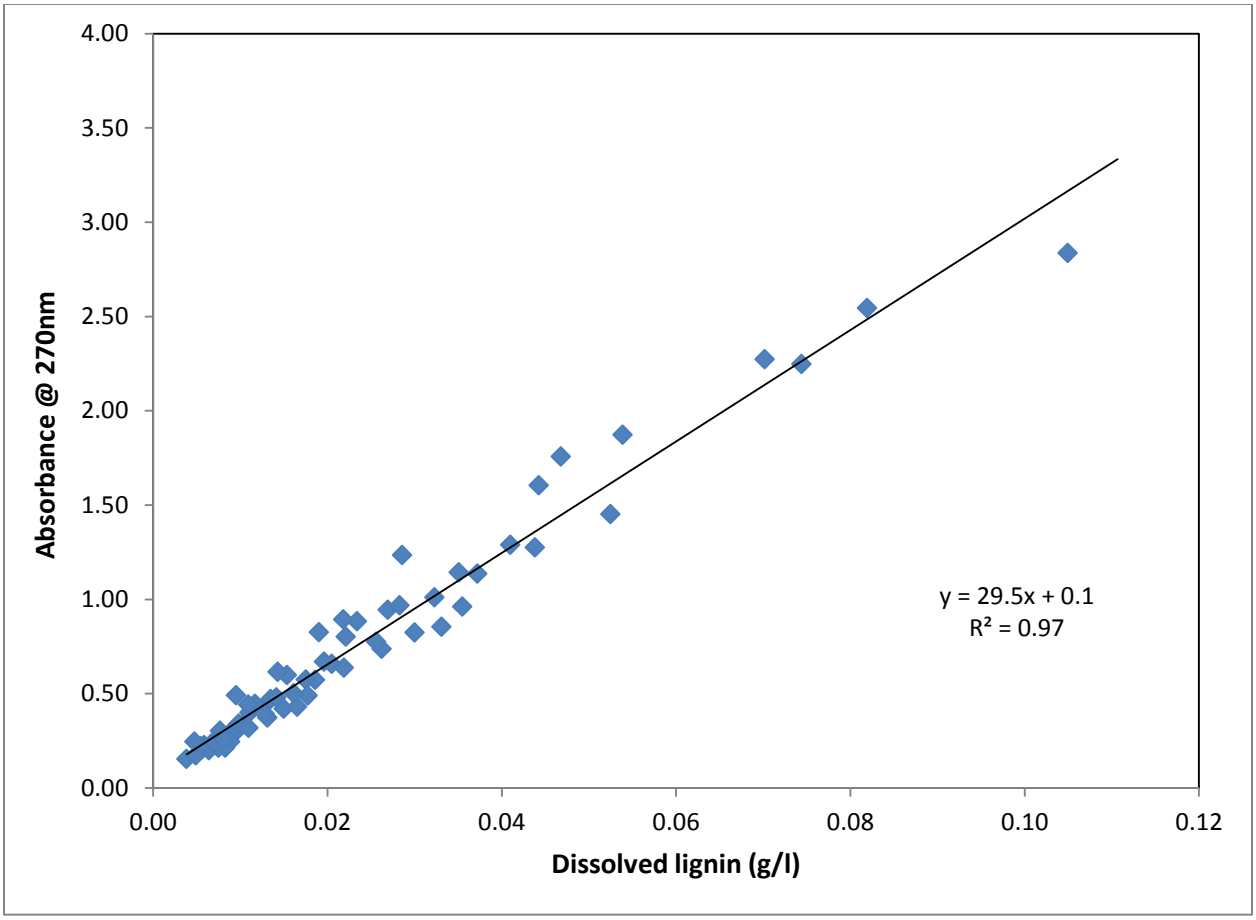

Figure 21: Dissolved lignin calibration curve

3.9 Procedure for Enzymatic Hydrolysis of Pretreated Wheat Straw

Novozyme Celluclast and Novozyme-50010 was used as the source of cellulase and β-glucosidase respectively, for the hydrolysis of cellulose and hemicellulose of the pretreated substrate. The activities of the enzymes were predetermined by colleague Oscar Calderon Rosales. The activity of the cellulase was 63.79 FPU/ml & 30.74 CBU/ml and the activity of β-glucosidase was 481.84 CBU/ml.

The enzymatic hydrolysis was carried out in a 250 ml Erlenmeyer flask. The substrate (1.25 g dry weight) was first loaded in the flask. The appropriate volume of 50 mM sodium acetate buffer (at pH 4.7) was added into the flask, which was based on the volume of cellulase, β-glucosidase and the moisture of the pretreated substrate. Novozyme Celluclast was added at 20 FPU per gram glucan in the substrate and Novozyme-50010 (481.84 CBU/ml) was added in

excess at ratio of 5 CBU to 1 FPU in order to prevent hydrolysis inhibition by cellobiose. The final volume of the enzymatic hydrolysis reaction mixture was 25 ml. The flasks were loaded into a New Brunswick Scientific I 24 incubator shaker, operated at 50°C and shook at 150 rpm. Samples (1 ml) were taken at 1, 4, 8, 12, 48, and 72 hours. The samples were centrifuged at 20817g for 5 minutes and the supernatants were collected and stored at -20°C for sugar analysis by the HPLC.

3.10 Procedure for Carbohydrate Analysis

The Dionex DX6000 HPLC system was used to quantify the concentration of carbohydrates in both the acid and enzymatic hydrolysate. A Dionex CarboPac PA1 column was used as stationary phase, nanopure water was used as the mobile phase and 0.248 M of NaOH was used both as the eluent and the detection enhancer. The flow rate of nanopure water and NaOH solution were 1.00 ml/min. Both solutions were first degassed with helium before each run. At the end of each analysis, nanopure water was used to wash the column before the next injection. A Dionex ED50 electrochemical detector was used to detect the carbohydrates. A Dionex AS50 auto sampler was used to inject samples into the column. The operating parameters of the HPLC tests are summarized in Table 9. The Chromeleon software was used to record and calculate the concentration of the carbohydrates by using the peak area data collected.

A three point sugar standard curve was generated using different concentrations (2.0, 0.5, 0.1 g/l) of arabinose, galactose, glucose, xylose, mannose and cellobiose (

Appendix C). Prior to analysis of sugars, frozen samples were thawed to room temperature and centrifuged at 20817g for 3 minutes. A volume of 0.400 ml of the hydrolysate samples were diluted to 4.90 ml with nanopure water. The internal standard was fucose (5 g/l) and 0.100 ml was added into all samples to increase the total volume to 5.00 ml.

Table 9: HPLC operating condition

HPLC Operating Condition	
Column Temperature	30°C
System Pressure	500-1300 psi
pH	10-13
Sample Injection Volume	25 µl
Total Retention Time	46 minutes

4 Oxygen Delignification Pretreatment Results and Analysis

4.1 Composition of Wheat Straw

A compositional analysis of the pretreated wheat straw performed and the results are summarized in Table 10. The three most abundant components were cellulose, hemicellulose, and lignin. The composition of wheat straw was found to be in the range of reported literature values (Appendix B). The total carbohydrate content was found to be 62.0% w/w. The majority of the carbohydrates were glucan (35.0% w/w) and xylan (22.1% w/w) (Table 11). The high content of cellulose and hemicellulose were desirable, making wheat straw an ideal feed for bioethanol production. The component "other" was calculated based on mass balance which included non-cell wall materials such as protein, uronic acid and other associated errors during the experiment, while the extractives component is includes non-structural sugars and waxes [**133**].

Table 10: Raw wheat straw composition analysis

Raw wheat straw composition % (g/g dry wheat straw)	
Extractives (%)	4.30±0.1
Ash (%)	6.74±0.2
Lignin (%)	16.1±0.2
Cellulose (%)	35.0±0.9
Hemicellulose (%)	27.0±1.8
Other (%)	10.8

Table 11: Average of raw wheat straw carbohydrate composition

	Hemicellulose				Cellulose	
	Arabinan	Galactan	Mannan	Xylan	Glucan	Total
	% (g/g dry wheat straw)					
Average	3.1	1.1	0.8	22.1	35.0	62.0

As mentioned before, lignin (16.1%) is an unwanted constituent that lowers the efficiency of enzymatic hydrolysis and sugar yield [**32**,**38**]. The purpose of the oxygen delignification pretreatment is to solubilize the lignin and as a result, enhance the enzymatic hydrolysis.

4.2 Wheat Straw Composition after Oxygen Delignification Pretreatment

After the oxygen delignification pretreatment, the wheat straw was separated into two phases: a cellulose-rich solid phase and a lignin-and hemicellulose-rich liquor phase. The extractives were assumed to be completely dissolved into the liquor phase. The term residual lignin refers to the lignin which remains in the recovered solid following the pretreatment. Figure 22 is a representation of the mass flow of the crucial components before and after the pretreatment.

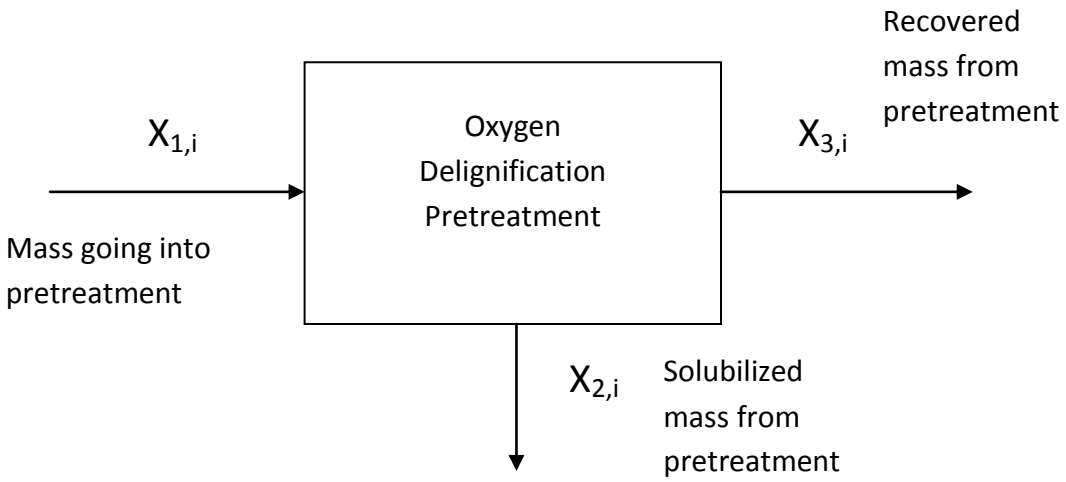

Figure 22: Mass flow diagram for oxygen delignification pretreatment

Where:

X = measured weight

i = substrate, cellulose, hemicellulose, lignin, carbohydrates

The recovery and solubilization of pretreatment of each component can be calculated by Equations 4.1 and 4.2:

$$\%\ \text{Recovery of i} = \left(\frac{X_{3,i}}{X_{1,i}}\right) \times\ 100\% \qquad 4.1$$

$$\%\ \text{Solubilization of i} = \left(\frac{X_{2,i}}{X_{1,i}}\right) \times 100\% \qquad 4.2$$

4.2.1 Effect of Oxygen Delignification Pretreatment on Wheat Straw Composition

A full factorial experiment was performed to explore the effects of a 60 minute pretreatment on wheat straw. A compositional analysis of the pretreated solids was performed on the pretreated substrate and the results are presented in % (g/g dry substrate) in Table 12. The recovery of carbohydrates and the pretreated substrate are also shown in Table 12. The "other" component was calculated to complete the mass balance. The mass balance discrepancy of the column "other" before and after pretreatment is probably due to missing analyses of the components in the pretreated liquor, extractives, uronic acid and other associated errors in the experiments.

Table 12: Recovered substrate composition and recoveries of pretreated wheat straw after 60 minutes of oxygen delignification

Temperature (°C)	Substrate loading (% w/w)	Caustic loading (%)	Cellulose (%)	Hemicellulose (%)	Lignin (%)	Ash (%)	Other (%)	Carbohydrate recovery (%)	Pretreated substrate recovery (%)
Raw wheat straw			35.0±0.9	27.0±1.8	16.1±0.2	6.7±0.2	10.8		
90	2	5	35.7±0.3	28.7±5.5	12.6±0.1	1.6±0.4	21.4	83.3±7.2	75.6±0.9
90	2	10	39.8±0.7	31.0±6.5	9.5±0.3	1.6±0.1	18.1	77.4±8.0	67.8±0.1
90	2	15	37.1±5.6	26.6±7.0	7.9±0.4	2.00±0.5	26.4	66.5±14.2	64.7±1.1
90	4	5	33.3±0.8	27.4±4.0	12.6±0.0	2.00±0.2	24.7	79.0±7.4	76.9±1.4
90	4	10	41.8±0.4	33.3±4.2	9.2±0.3	2.1±0.3	13.6	77.5±3.4	64.0±1.3
90	4	15	46.2	27.6	7.1	1.8	17.3	70.8	59.5
110	2	5	36.7±2.7	30.7±1.0	11.6±0.4	2.5±0.7	18.5	77.4±2.3	71.2±0.2
110	2	10	44.5	27.2	8.5	2.2	17.6	72.8	63.0
110	2	15	46.8±10.1	31.9±2.5	7.2±0.2	1.7±0.5	12.4	77.1±11.7	60.8±0.5
110	4	5	35.7	27.3	11.9	2.6	22.5	74.3	73.1
110	4	10	42.8±3.3	28.6±2.3	8.2±0.5	2.9±0.1	17.5	67.7±1.3	58.8±1.9
110	4	15	48.8±4.4	32.1±0.6	6.6±0.1	2.6±0.4	9.9	74.4±5.2	57.0±1.3
130	2	5	41.6	30.0	9.8	1.3	17.2	76.81	66.5
130	2	10	45.8±9.5	27.9±1.7	8.4±0.3	1.6±0.2	16.3	67.1±10.5	56.4±0.3
130	2	15	50.4±10.1	29.7±0.4	6.5±0.3	1.5±1.0	11.9	70.1±3.7	54.6±4.3
130	4	5	37.4±6.3	26.8±1.6	10.7±0.2	3.1±0.3	22.0	71.1±9.8	68.7±1.0
130	4	10	51.8	28.5	7.4	2.6	9.7	73.7	56.9
130	4	15	55.6±2.6	29.00±1.9	5.6±0.9	3.1±0.0	6.7	68.7±4.9	50.5±3.6

Varying the substrate loading from 2 to 4% did not show a strong effect on the composition of pretreated substrate after 60 minutes of reaction. Approximately 39.8 to 82.4% of lignin was solubilized over the full range of experimental conditions (

Appendix A). Both an increase in temperature and caustic loading had a positive effect on lignin solubilization. For constant caustic loading (5, 10 and 15%), increasing temperature from 90 to 130°C increased the lignin solubilization by a maximum of 18.7%. Compared to temperature, the caustic loading had a more pronounced effect on lignin solubilization. Comparison between untreated and pretreated substrate at condition 130°C, 5, 10 and 15% caustic loading is shown in Figure 23. For 2% substrate loading, when temperature was held constant at 90°C, a 19.2% increase in lignin solubilization was observed when caustic loading was increased from 5 to 10%. For temperature at 90°C, increasing the caustic loading from 10 to 15% increased the lignin solubilization by only a further 10.1%. This "diminishing" effect of lignin solubilization with increasing caustic loading was also observed with conditions at 110 and 130°C as well. A possible explanation to this observed "diminishing" effect is the saturation of caustic loading. In other words, maximum delignification could have been achieved when caustic loading was at 15%. This hypothesis is important to the interpretation of the delignification kinetic model discussed in section 5.3.

Figure 23: Raw wheat straw (left); pretreated wheat straw at condition 130°C, 15, 10 and 5% caustic loading (top to bottom)

The cellulose and hemicellulose content of wheat straw over the full range of the 60 minutes of pretreatment are summarized in Table 12. Overall, an increasing trend in carbohydrate content

with increasing temperature and caustic loading was observed which was in line with the literature [**87**,**98**].

Relative to the residual lignin, the cellulose and hemicellulose content of the pretreated substrate had larger variations (Table 12). The cellulose content of the pretreated substrate increased with the increasing temperature and caustic loading; this finding was supported by the literature [**87**,**94**]. The pretreatment condition that resulted in the highest cellulose content was 130°C, 4% substrate loading and 15% caustic loading. The "diminishing" effect of caustic loading was observed when caustic loading was increased from 5 to 15%.

The hemicellulose content of the pretreated substrate did not display specific patterns when the temperature or caustic loading increased while the others were held constant (Table 12). The pretreatment condition that produced the highest hemicellulose content was 110°C, 4% substrate loading and 15% caustic loading.

Overall, more severe pretreatment conditions led to higher lignin solubilization. Unfortunately, the oxygen delignification pretreatment attacks the lignin and carbohydrates molecules indiscriminately which led to carbohydrate solubilization. Thus, the recoveries of carbohydrates were examined.

4.2.2 Recoveries of Pretreated Substrate and Carbohydrates after Oxygen Delignification Pretreatment

The pretreated wheat straw was recovered, washed with distilled water and vacuum filtered. The dry weight of the pretreated substrate weighed less compared to the initial weight due to solubilization of lignin and carbohydrates. The solid and carbohydrate recoveries after 60 minutes of oxygen delignification pretreatment were determined using Equation 4.1 and were shown in Table 12.

The pretreated substrate and carbohydrate recoveries after oxygen delignification followed an overall decreasing trend with increasing temperature and caustic loading. The pretreated substrate recoveries also experienced the "diminishing" effect when the caustic loading increased from 5 to 15%. The carbohydrate recoveries in the pretreated solid ranged from 66.5-

83.3% across the full range of experimental conditions. The observed carbohydrate recoveries were lower as expected when compared to literature reported values (over 85% at higher operating temperature) [**98**,**94**]. The lower carbohydrate recovery was believed to be due to the longer reaction time (60 minutes in this study) compared to a shorter reaction time (10-15 minutes) reported in the literature [**98**,**94**]. This was confirmed by analyzing the carbohydrate content throughout the reaction, where it showed a decreasing trend with increasing reaction time (Figure 24). The substrate had a limited carbohydrate loss coupled with higher hydrolysis yield due to more delignified substrate (discussed in next section). Overall the recovery of carbohydrates showed a general decreasing trend with increasing temperature and caustic loading.

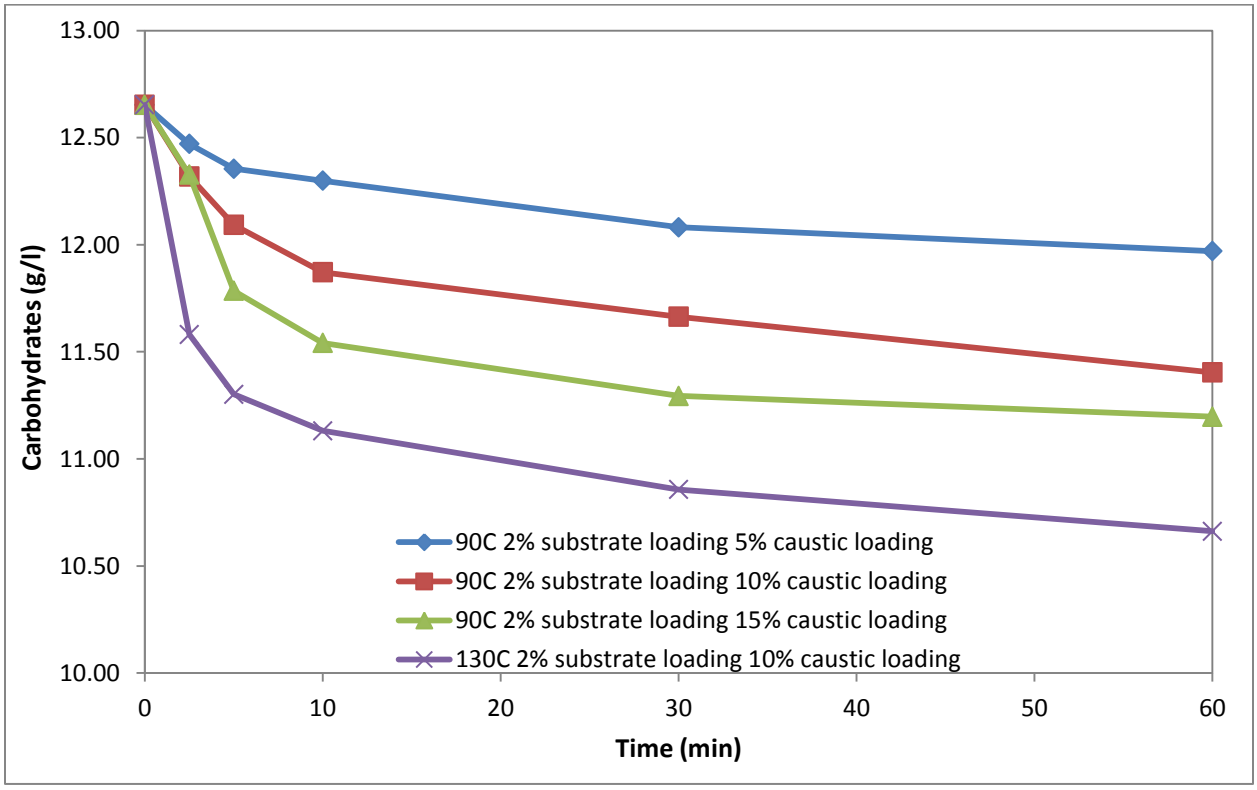

Figure 24: Carbohydrate profile of oxygen delignification pretreatment

4.3 Enzymatic Hydrolysis of Pretreated Wheat Straw

As discussed in earlier sections, increasing the temperature and caustic loading parameters aided the removal of lignin from the substrate. Increased sugar yield during enzymatic hydrolysis has been reported with decreasing lignin content in the pretreated substrate after pretreatment [**13**,**15**,**59**,**99**]. Enzymatic hydrolysis was performed on the pretreated substrate in order to hydrolyze the carbohydrates. The results of cellulosic, hemicellulosic and total sugar yield for 2 and 4% substrate loading after 72 hours of hydrolysis with 20 (FPU/g glucan) enzyme loading are summarized in Table 13 and 14 respectively.

The measured carbohydrates were converted into their sugar equivalents in order to calculate the sugar yields:

$$\text{Cellulosic Sugar (g)} = \text{Cellulose (g)} \times 1.11 \quad (4.3)$$

$$\text{Hemicellulosic Sugar (g)} = \text{Hemicellulose (g)} \times 1.14 \quad (4.4)$$

$$\text{Total Sugar (g)} = \text{Total (g)} \times 1.12 \quad (4.5)$$

The yield was calculated by using Equation 4.6:

$$\text{Hydrolysis Yield} = \frac{S_x \text{ (after hydrolysis)}}{C_x \text{ (before hydrolysis)}} \quad (4.6)$$

Where:

S_x = Cellulosic, hemicellulosic or total sugar (g)

C_x = Cellulose, hemicellulos or total carbohydrate sugar equivalent (g)

Table 13: Sugar yield for pretreatment conditions at 2% substrate loading after 72 hours of enzymatic hydrolysis

Pretreatment Condition		Hydrolyzed Sugar Yield (%)		
Temperature (°C)	Caustic (%)	Cellulosic Sugar (glucose)	Hemicellulosic Sugar	Total Sugar
Raw		24.9±2.1	11.4±0.9	18.7±1.1
90	5	46.7±2.1	31.7±4.8	39.1±1.9
90	10	75.5±6.9	66.6±8.4	71.0±0.4
90	15	86.7	69.7	78.8
110	5	61.9±16.6	44.7±8.7	53.5±12.4
110	10	66.3	72.8	68.8
110	15	90.4±13.1	78.9±7.4	85.0±4.0
130	5	58.3	52.4	55.6
130	10	77.3±15.1	67.1±2.0	72.8±9.7
130	15	79.9±13.8	68.8±3.1	74.9±7.1

Table 14: Sugar yield for pretreatment conditions at 4% substrate loading after 72 hours of enzymatic hydrolysis

Pretreatment Condition		Hydrolyzed Sugar Yield (%)		
Temperature (°C)	Caustic (%)	Cellulosic Sugar (glucose)	Hemicellulosic Sugar	Total Sugar
Raw		24.9±2.1	11.4±0.9	18.1±1.1
90	5	54.4±4.4	33.2±0.3	43.8±1.6
90	10	79.5±9.8	66.0±5.6	72.9±4.2
90	15	80.0±6.8	75.1±9.4	77.6±0.1
110	5	54.9	46.9	51.2
110	10	79.5±12.5	75.4±4.4	77.4±5.3
110	15	62.5	65.2	63.4
130	5	68.5±10.1	56.3±1.8	62.8±5.3
130	10	63.3	67.2	64.6
130	15	60.1±3.3	61.6±1.3	60.4±1.7

The sugar yield of the pretreated substrate reached a maximum at 110°C for both 2 and 4% substrate. The maximum cellulosic, hemicellulosic and total sugar yield for 2% substrate loading pretreatment condition were 90.4, 78.9 and 85.0% respectively at 110°C and 15% caustic loading. Increasing the caustic loading was more effective in increasing the hydrolyzed sugar yield than temperature.

Increasing temperature and caustic loading during the oxygen delignification pretreatment had a positive effect on the enzymatic hydrolysis which can be attributed to the increase in lignin solubilization during pretreatment [**59**,**97**]. The residual lignin in the substrate showed mild

correlation with the sugar yield as represented by a R^2 value of 0.70 (Figure 25). These results agree with Charles et al. (2003) and confirm the effect of lignin on enzymatic hydrolysis yield [**91**].

All in all, wheat straw after oxygen delignification pretreatment showed a significant increase in both hydrolyzed sugar concentration and sugar yield. This showed that oxygen delignification is an effective pretreatment for improving both the efficiency and the effectiveness of enzymatic hydrolysis.

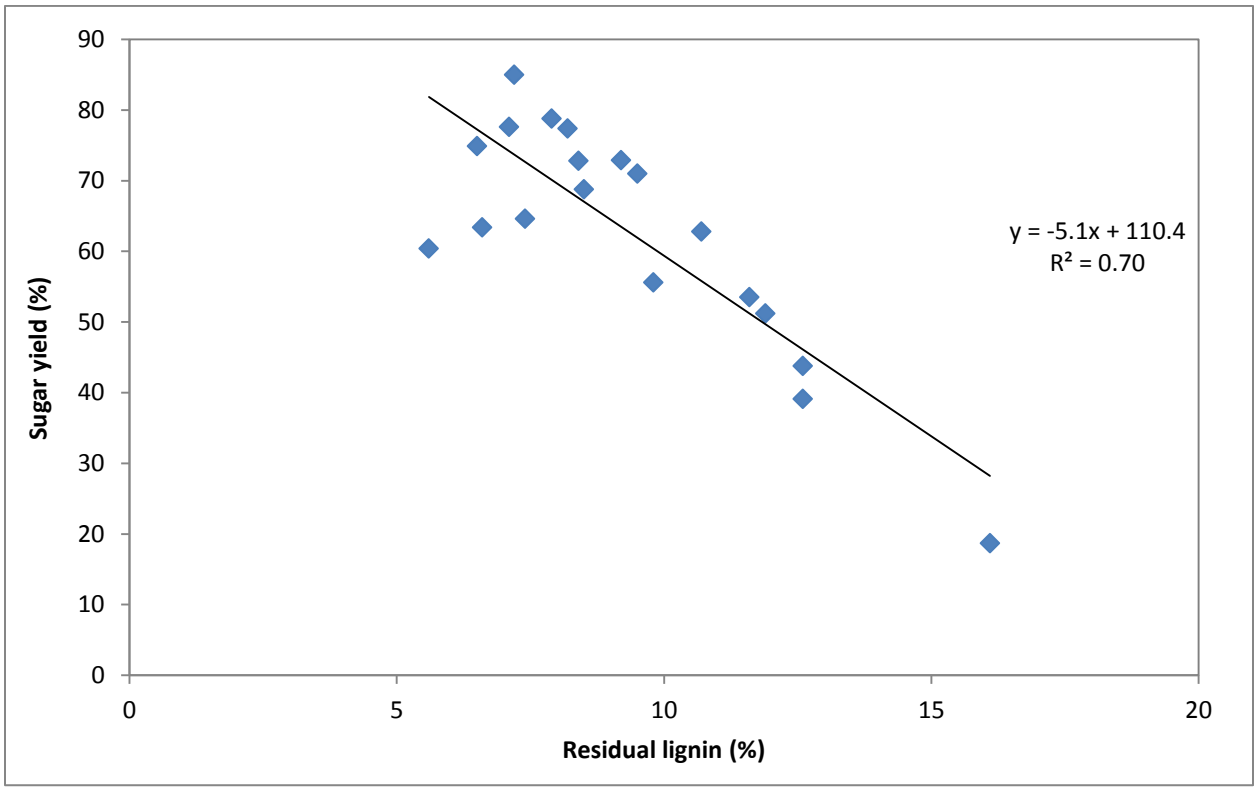

Figure 25: Effect of residual lignin on sugar yield during enzymatic hydrolysis of wheat straw for all pretreatment conditions

5 Analysis of Oxygen Delignification Kinetics

5.1 Effects of Temperature and Caustic Loading on Delignification Rate

The residual lignin profiles of the pretreated solid were analyzed with respect to time in order to develop a kinetic expression for the oxygen delignification process. The concentration of dissolved lignin in the pretreated liquor was measured at different sampling times (2.5, 5, 10, 30, 60 minutes) and the residual lignin was calculated based on method described in sections 3.7

and 3.8. The residual lignin profiles of all pretreatment conditions are shown through Figure 26-31.

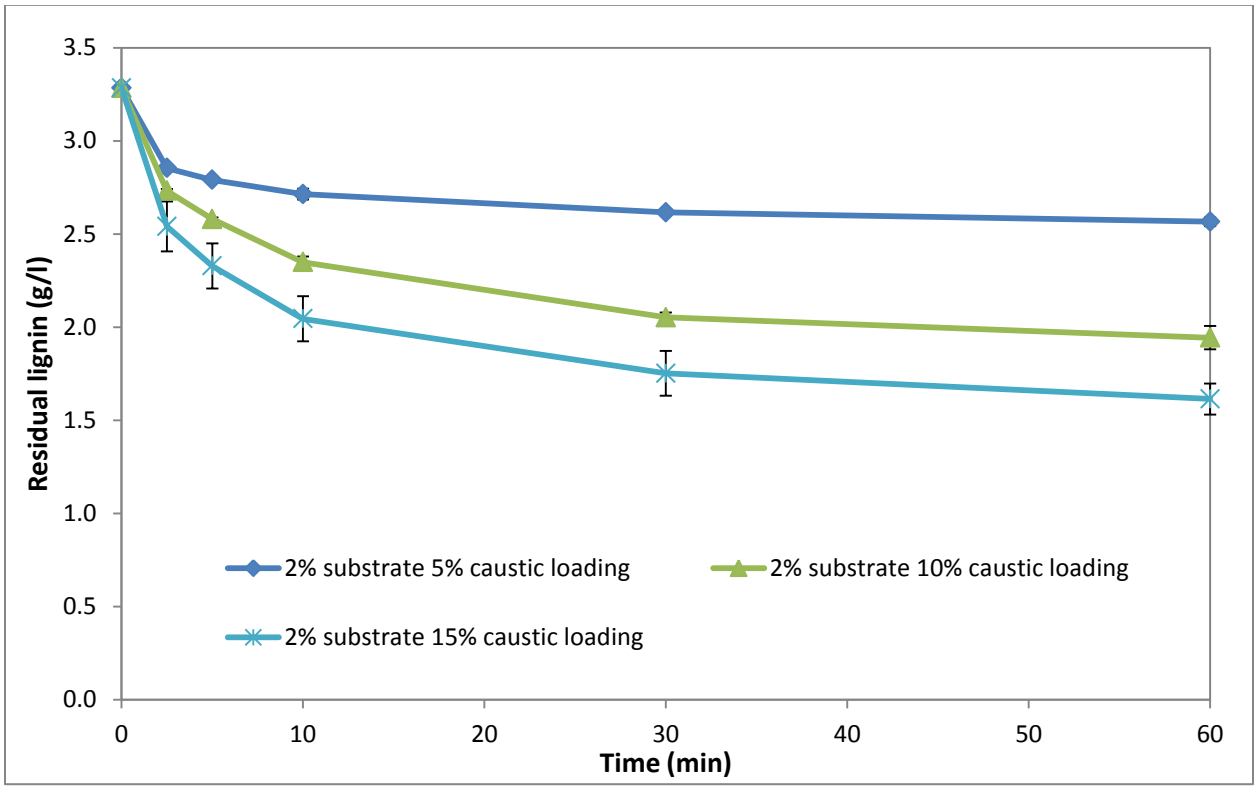

Figure 26: Delignification profile for 2% substrate loading and 90°C

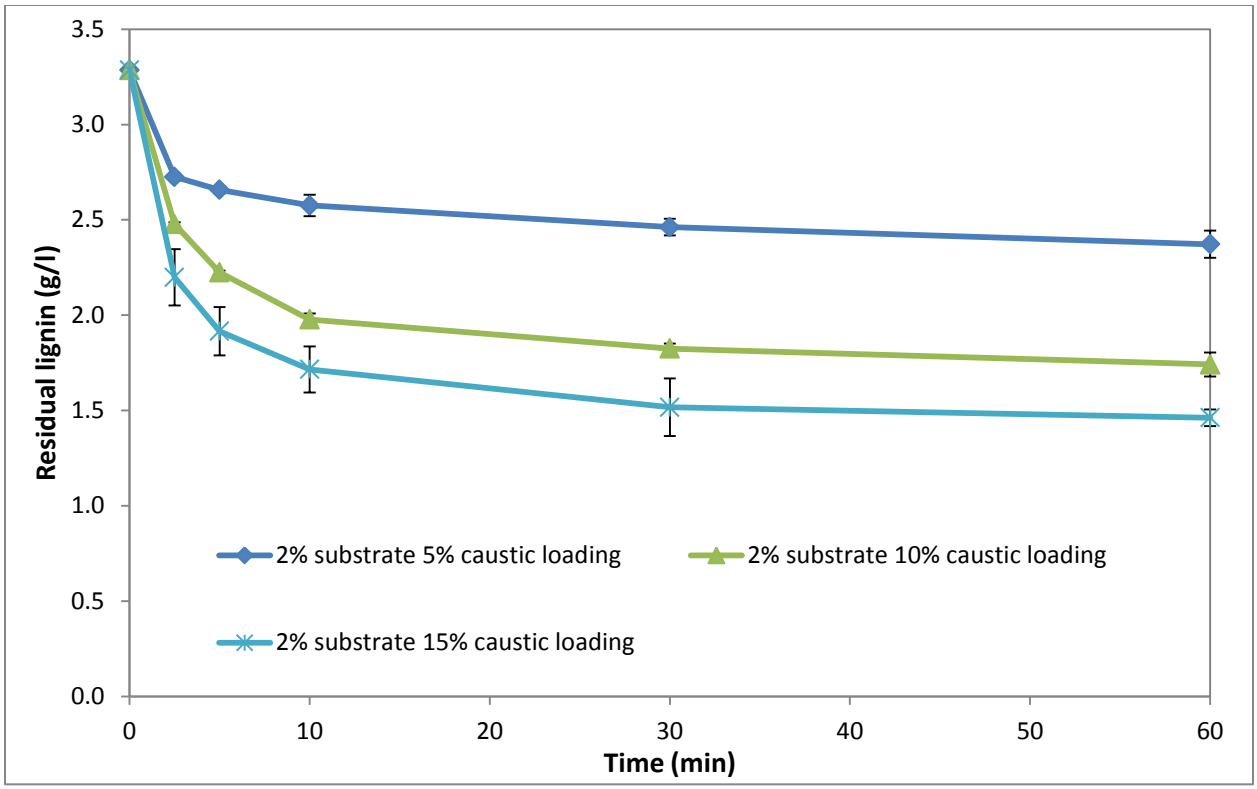

Figure 27: Delignification profile for 2% substrate loading and 110°C

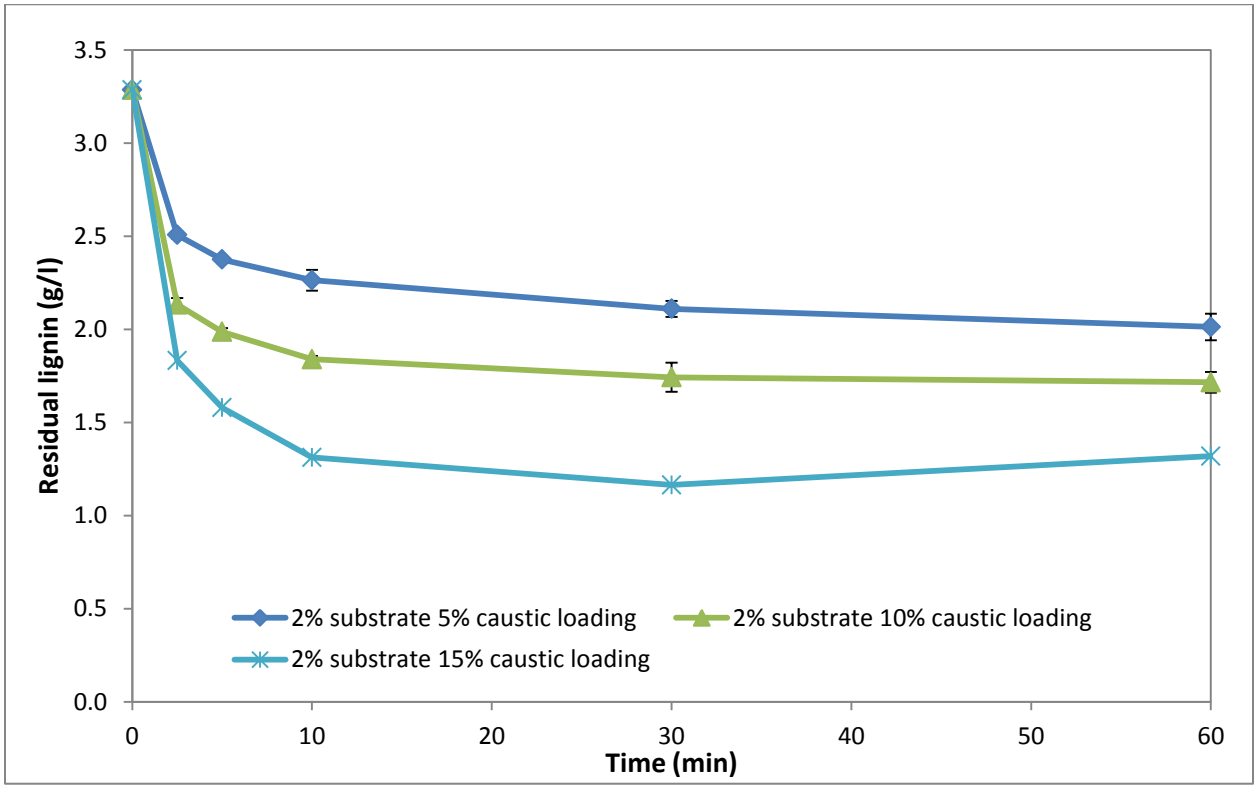

Figure 28: Delignification profile for 2% substrate loading and 130°C

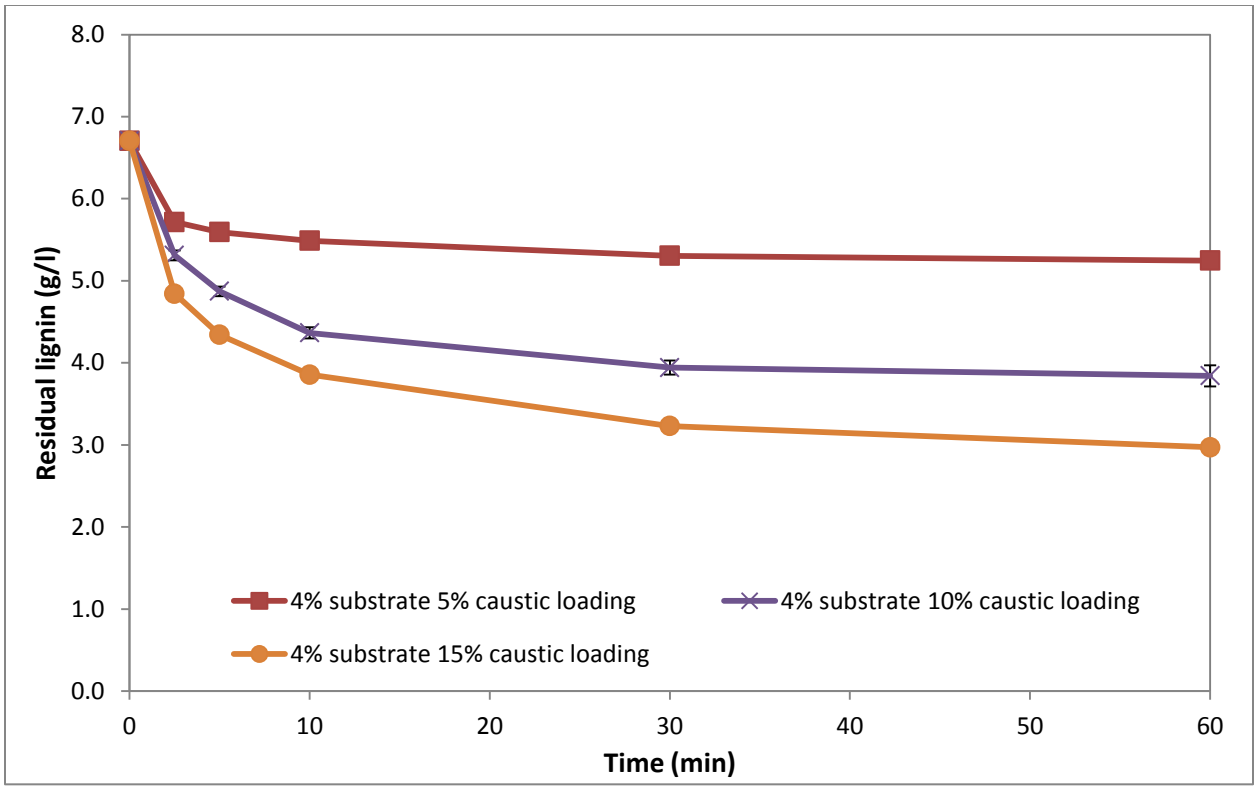

Figure 29: Delignification profile for 4% substrate loading and 90°C

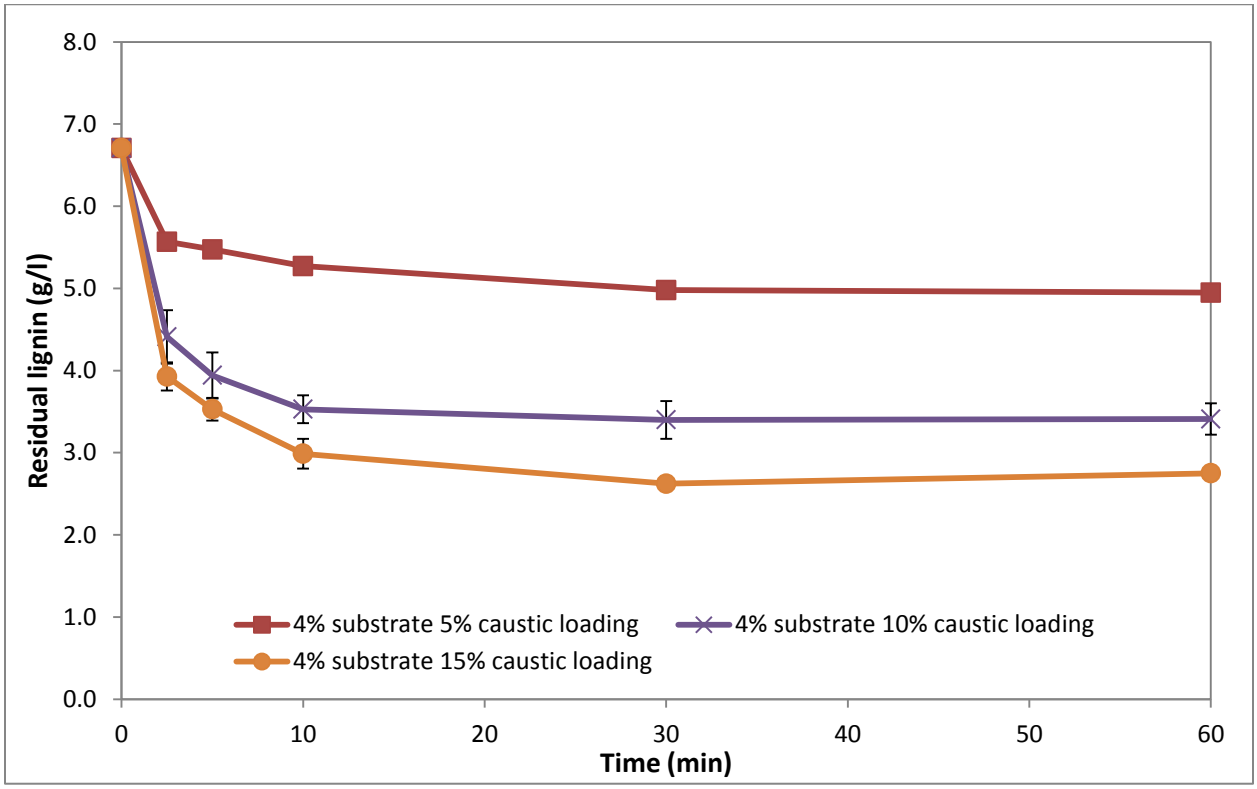

Figure 30: Delignification profile for 4% substrate loading and 110°C

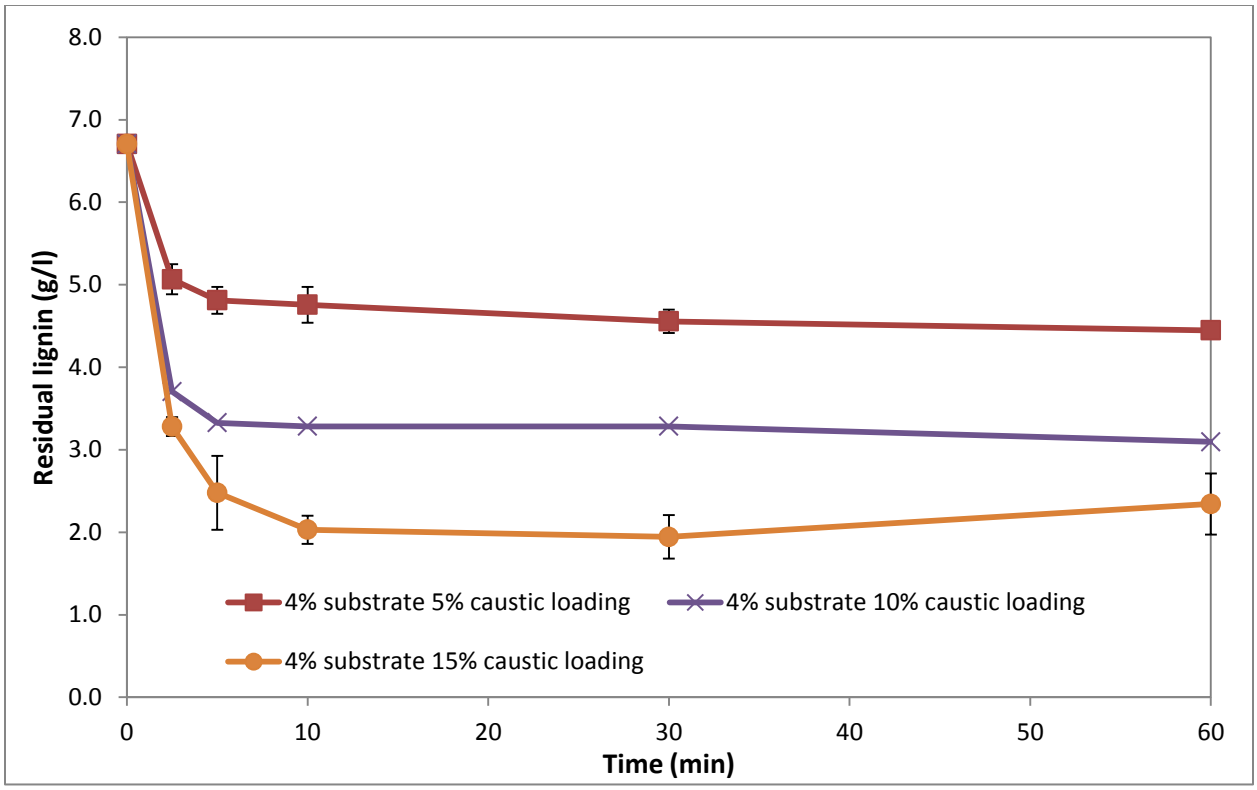

Figure 31: Delignification profile for 4% substrate loading and 130°C

The oxygen delignification profile of lignocellulosic materials could be categorized into two phases: a fast initial phase and a slow second reacting phase [**23**,**88**,**100**,**126**]. The rate of delignification plateaued off after 10 minutes of reaction, suggesting that the delignification reaction had ended [**91**]. Increasing the temperature and caustic loading increased the reaction rates of the delignification (Figure 26-31) in the first 10 minutes. The delignification profile for 2 and 4% substrate loading conditions were similar for the full range of conditions. Varying the caustic loading from 5-10% had a bigger impact on the delignification rate than increasing from 10 to 15%; however this observed effect was lessened for pretreatment conditions at 130°C. The lack of further delignification after 10 minutes showed that the reaction time for the oxygen delignification pretreatment can be reduced significantly.

5.2 Kinetic Model Development for Oxygen Delignification

5.2.1 Component Mass Balance

It was assumed that the chemical species took part in the delignification reaction were lignin, hydroxide ions (caustic) and oxygen. The kinetic model was developed by first writing the mass balance equation for these species. The reactor was modeled as a semi-batch since oxygen was sparged in continuously.

5.2.2 Mass Balance of Lignin

The mass balance of residual lignin in the solid can be written as:

$$\begin{aligned}&\text{Rate of lignin accumulation} =\\ &\text{Rate of lignin in - Rate of lignin out} +\\ &\text{Rate of lignin generation - Rate of lignin consumption}\end{aligned} \qquad 5.1$$

In a semi-batch reactor with no inlet, outlet and generation of lignin, the mass balance of residual lignin in Equation 5.1 was reduced to only the consumption term:

$$r_L = -\frac{d[L]}{dt} \qquad 5.2$$

5.2.3 Mass Balance of Hydroxide Ions

Similar to lignin mass balance, the mass balance of reacting hydroxide ions can be written as:

$$\begin{aligned}&\text{Rate of } OH^- \text{ accumulation} = \text{Rate of } OH^- \text{ in - Rate of } OH^- \text{ out} +\\ &\text{Rate of } OH^- \text{ generation - Rate of } OH^- \text{ consumption}\end{aligned} \qquad 5.3$$

Similarly, in a semi-batch reactor with no inlet, outlet and generation of hydroxide ions, the mass balance was reduced to only the consumption term:

$$r_{OH^-} = -\frac{d[OH^-]}{dt} \qquad 5.4$$

5.2.4 Mass Balance of Oxygen

The mass balance of oxygen can be written as:

$$\text{Rate of } O_2 \text{ gas accumulation} = \text{Rate of } O_2 \text{ gas in - Rate of } O_2 \text{ gas out} + \text{Rate of } O_2 \text{ gas generation - Rate of } O_2 \text{ gas consumption} - \text{Rate of } O_2 \text{ gas mass transfer into liquid} \quad (5.5)$$

and

$$\text{Rate of } O_2 \text{ liquid accumulation} = \text{Rate of } O_2 \text{ liquid in - Rate of } O_2 \text{ liquid out} + \text{Rate of } O_2 \text{liquid generation -Rate of } O_2 \text{ liquid consumption} \quad (5.6)$$

In a semi-batch reactor the oxygen gas was being sparged in continuously with an opened off gas valve. It was assumed that the reactor was well mixed and that the resistance of mass transfer was negligible. The rate of O_2 gas accumulation, generation and consumption is 0; thus the difference in the rate of O_2 gas in and out is the rate of O_2 gas mass transfer term. In Equation 5.6, the rate of O_2 liquid out and generation term is 0. The rate of O_2 liquid in is equal to the rate of O_2 gas mass transfer term. The concentration of O_2 liquid was assumed to be constant and saturated throughout the reaction; therefore the O_2 liquid accumulation term is 0. With these assumptions, combining Equation 5.5 and 5.6, the overall mass balance of O_2:

$$\text{Rate of } O_2 \text{ gas in- Rate } O_2 \text{ gas out} = \text{Rate of } O_2 \text{ gas mass transfer into liquid} = \text{Rate of } O_2 \text{ liquid consumption} = r_{O_2} \quad (5.7)$$

With the reactor setup described in section 3.5, the reacting liquid phase was assumed to be saturated with oxygen when the caustic solution was charged into the reactor. The operating pressure was set constant at 100 psig (790 kPa) and the concentration of dissolved oxygen in the presence of caustic had to be estimated. This estimation was accomplished by using Tromans' oxygen solubility model in inorganic solutions [**130**]. The estimated concentrations of the dissolved oxygen for the full range of experimental conditions are summarized in Table 15 and 16.

Table 15: Estimated dissolved oxygen concentration for 2% substrate loading

Dissolved Oxygen Concentration (mol/l)			
	Temperature (°C)		
Caustic Loading (%)	90	110	130
5	0.0181	0.0183	0.0195
10	0.0177	0.0179	0.0191
15	0.0173	0.0175	0.0187

Table 16: Estimated dissolved oxygen concentration for 4% substrate loading

Dissolved Oxygen Concentration (mol/l)			
	Temperature (°C)		
Caustic Loading (%)	90	110	130
5	0.0177	0.0179	0.0191
10	0.0169	0.0172	0.0183
15	0.0162	0.0165	0.0175

5.2.5 ODE Equation Derivation

Assuming the overall delignification reaction has the form [**125**]:

$$L + OH^- + O_2 \rightarrow L_{dissolved} + Products \qquad 5.8$$

The lignin in the solid reacted with hydroxide ions and dissolved oxygen to produce dissolved lignin and products (such as lower molecular weight phenolic molecules). The delignification rate was assumed to follow a power law model and the lignin removal rate can be written as:

$$\frac{d[L]}{dt} = -k_L[L]^{a_1}[OH^-]^{a_2}[O_2]^{a_3} \qquad 5.9$$

Where:

k_L = kinetic constant for lignin

L = lignin concentration (solid) (g/l)

OH^- = hydroxide ion concentration (g/l)

O_2 = dissolved oxygen concentration (g/l)

a_1 = exponent for lignin

a_2 = exponent for hydroxide ion

a_3 = exponent for dissolved oxygen

Since oxygen was sparged in continuously, the accumulation of oxygen was:

$$\frac{d[O_2]}{dt} = 0 \qquad 5.10$$

Therefore the oxygen concentration in Equation 5.9 was constant and can be combined into the kinetic constant k_L, to generate Equation 5.11.

$$\frac{d[L]}{dt} = -k_L[L]^{a_1}[OH^-]^{a_2} \qquad 5.11$$

The form of the rate equation for hydroxide ions is similar to Equation 5.11:

$$\frac{d[OH^-]}{dt} = -k_{OH}[L]^{a_1}[OH^-]^{a_2} \qquad 5.12$$

The kinetic parameters of the delignification reaction can be determined by measuring the change of concentrations of lignin (g/l) and hydroxide ion (g/l) with time and solving for parameters k_L, k_{OH}, a_1 and a_2 in this system of ODEs (Equation 5.11 and 5.12). The kinetic constants for the range of experimental conditions have the following abbreviation (Table 17):

Table 17: Abbreviation of kinetic constants for system of ODEs approach

Temperature (°C)	Lignin kinetic constant	Hydroxide ion kinetic constant
90	k_{L90}	k_{OH90}
110	k_{L110}	k_{OH110}
130	k_{L130}	k_{OH130}

The units for the kinetic constants for residual lignin and hydroxide ions are:

$$k_L = \frac{1}{\text{min}} * \frac{(\text{g})^{1-a_1-a_2}}{(\text{l})^{1-a_1-a_2}} \qquad 5.13$$

$$k_{OH} = \frac{1}{\text{min}} * \frac{(\text{g})^{1-a_1-a_2}}{(\text{l})^{1-a_1-a_2}} \qquad 5.14$$

5.2.6 Single ODE Approach

Alternatively, the system of ODEs (Equations 5.11 and 5.12), could be combined into a single ordinary differential equation by dividing equation 5.12 by 5.11 to obtain:

$$\frac{d[OH^-]}{dt} = \frac{k_{OH}}{k_L}\frac{d[L]}{dt} \quad 5.15$$

Where:

$$\frac{k_{OH}}{k_L} = \frac{d[OH^-]}{d[L]} = k' \quad 5.16$$

From Equation 5.16, the rate of delignification and the rate of hydroxide ion consumption can be related by the constant *k'*. Integrating equation 5.15 yields Equation 5.17:

$$[OH^-] - [OH_0^-] = k'([L] - [L_0]) \quad 5.17$$

The concentration of hydroxide ion at a given time can be calculated from the initial concentrations of hydroxide ions, initial lignin (solid) and measured lignin (solid) concentration. Substituting Equation 5.17 into 5.11 to get:

$$\frac{d[L]}{dt} = -k_L[L]^{a_1}(k'([L] - [L_0]) + [OH_0^-])^{a_2} \quad 5.18$$

The constant *k'* can be determined by plotting the rate of hydroxide ion consumption against the delignification rate [**131**], resulting in a linear relationship between two rates. For the single ODE approach, the kinetic constants for temperature 90, 110 and 130°C were abbreviated as k_{90}, k_{110}, and k_{130} and had the same units as described in Equation 5.13 and 5.14.

5.3 Solving the Kinetic Parameters

The experimental data were fitted empirically with the program EASY-FIT[Model Design] version 5.1 created by Professor Klaus Schittkowski. The residual lignin data were converted to grams per litre. The initial conditions for the hydroxide ions (caustic loading) were entered as grams per litre. The initial conditions for caustic loading corresponding to substrate loading for each operating parameter and parameter specifications used are summarized in Appendix B. Due to its simplicity, the single ODE approach model was solved first.

5.3.1 Single ODE Approach to Solve for Kinetic Parameters

The residual lignin and hydroxide ion concentration dataset from the full factorial design were first examined and used to obtain a relationship between the change in hydroxide ions and residual lignin for the single ODE approach. The oxygen delignification pretreatments were performed and samples were taken at 2.5, 5, 10, 30 and 60 minutes. The hydroxide ion concentrations were determined by a TitraLab® 854 automatic titration workstation with 0.05 M H_2SO_4 as the titrant. The rate of delignification and hydroxide ion consumption were then determined by the change in residual lignin at each sampling time divided by the sampling time difference. An example of the 2.5 to 5 minute interval for residual lignin is shown in Equation 5.19:

$$\frac{\Delta L}{\Delta t} = \frac{L_{5\,min} - L_{2.5\,min}}{5 - 2.5} \qquad 5.19$$

The rate of hydroxide ion consumption was plotted against the delignification rate and the result is shown in Figure 32. The slope in Figure 32 represent dOH^-/dL which is equal to 0.494 with a minor y intercept of 0.001 and a R^2 value of 0.843 indicating a satisfactory linear relationship between rate of delignification and hydroxide ion consumption.

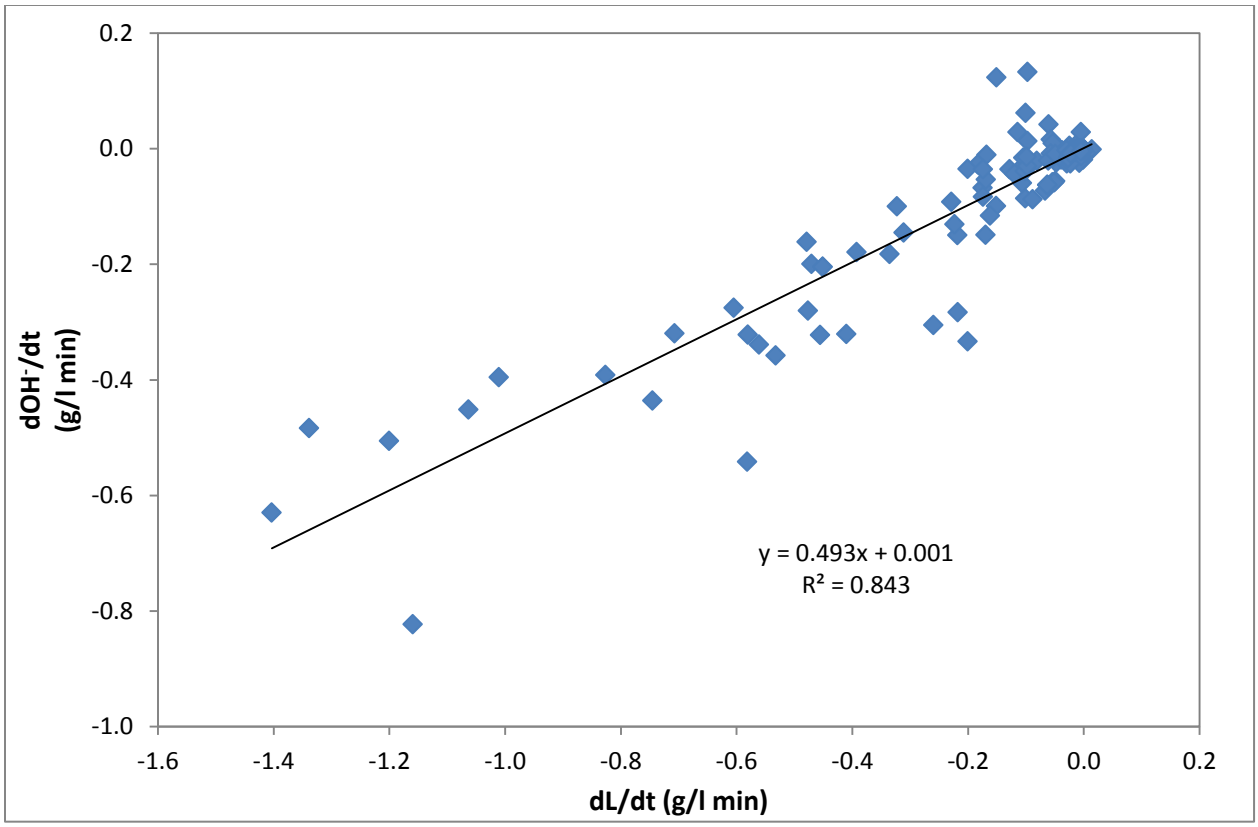

Figure 32: Relation between dOH^-/dt and dL/dt obtained from full factorial experiment dataset

The initial guesses and the final values of the solved parameters are summarized in Table 18. It is important to note that different initial guesses yielded different final values results, thus only initial guesses with convergence value that had the minimum residual values were used. The result of the solved equation is shown in Equation 5.20 and the single ODE model simulated results are shown from Figure 33-38.

$$\frac{d[L]}{dt} = -k_L[L]^{1.95}(0.493([L] - [L_0]) + [OH_0^-])^{1.18} \qquad 5.20$$

The rate constant k_L corresponded to the lignin kinetic constant at each operating temperature (90, 110 or 130°C).

Table 18: Initial guess and final values for single ODE approach with dOH^-/dL=0.493 and full factorial data

Parameter	Initial guesses	Final values
k_{90}	1.00E-01	1.04E-02
k_{110}	1.00 E-01	4.63E-02
k_{130}	1.00 E-01	1.02E-01
a_1	1.00	1.95
a_2	2.00	1.18

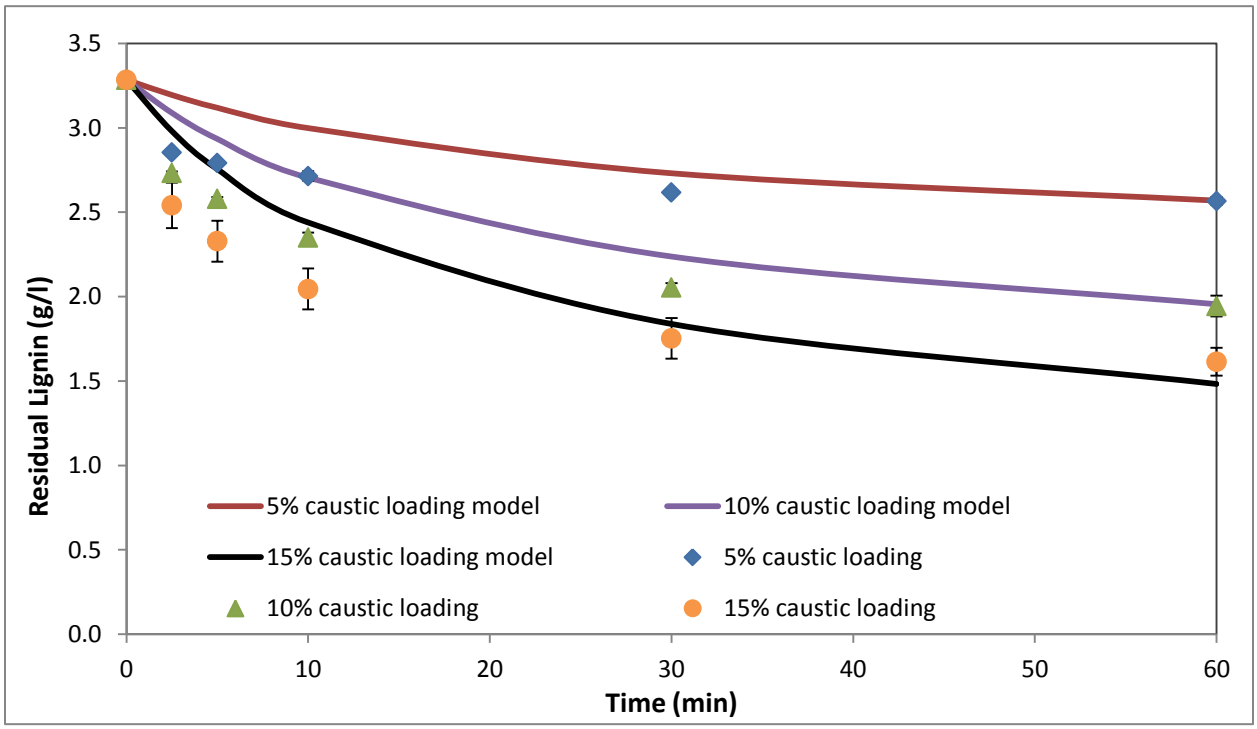

Figure 33: Simulated single ODE approach with full factorial dataset, 2% substrate loading and 90°C

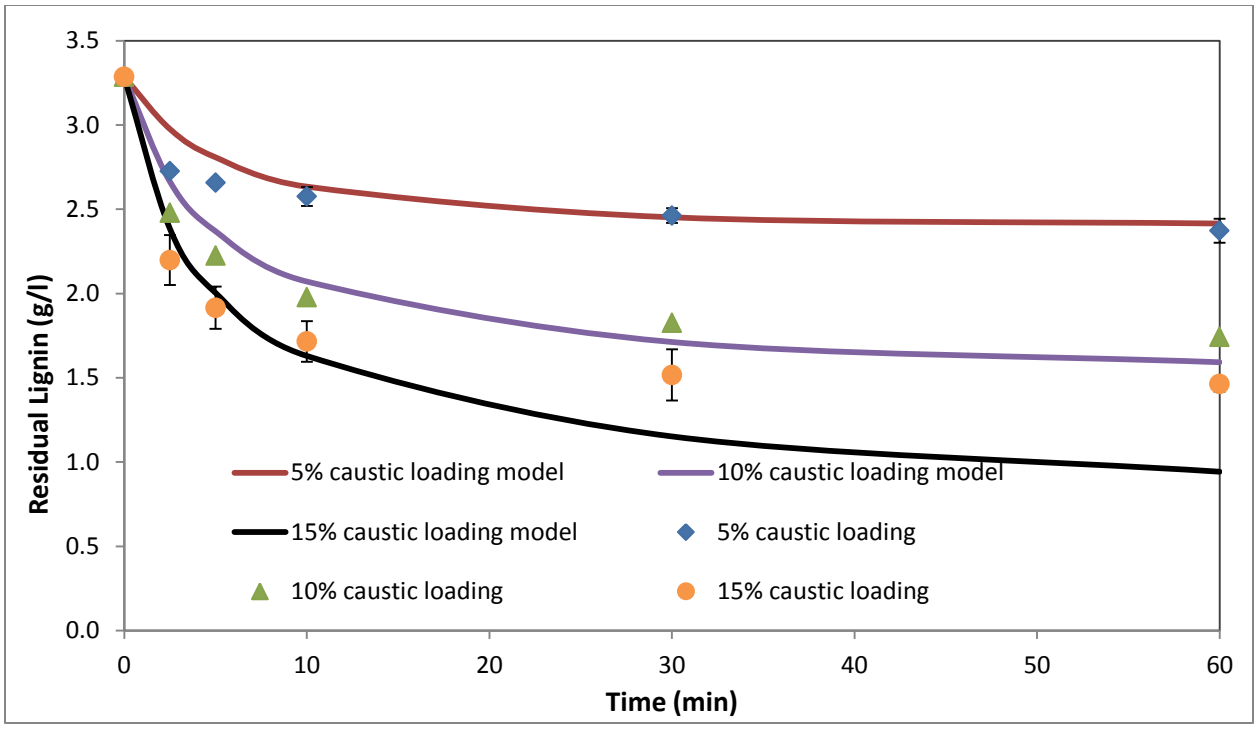

Figure 34: Simulated single ODE approach with full factorial dataset, 2% substrate loading and 110°C

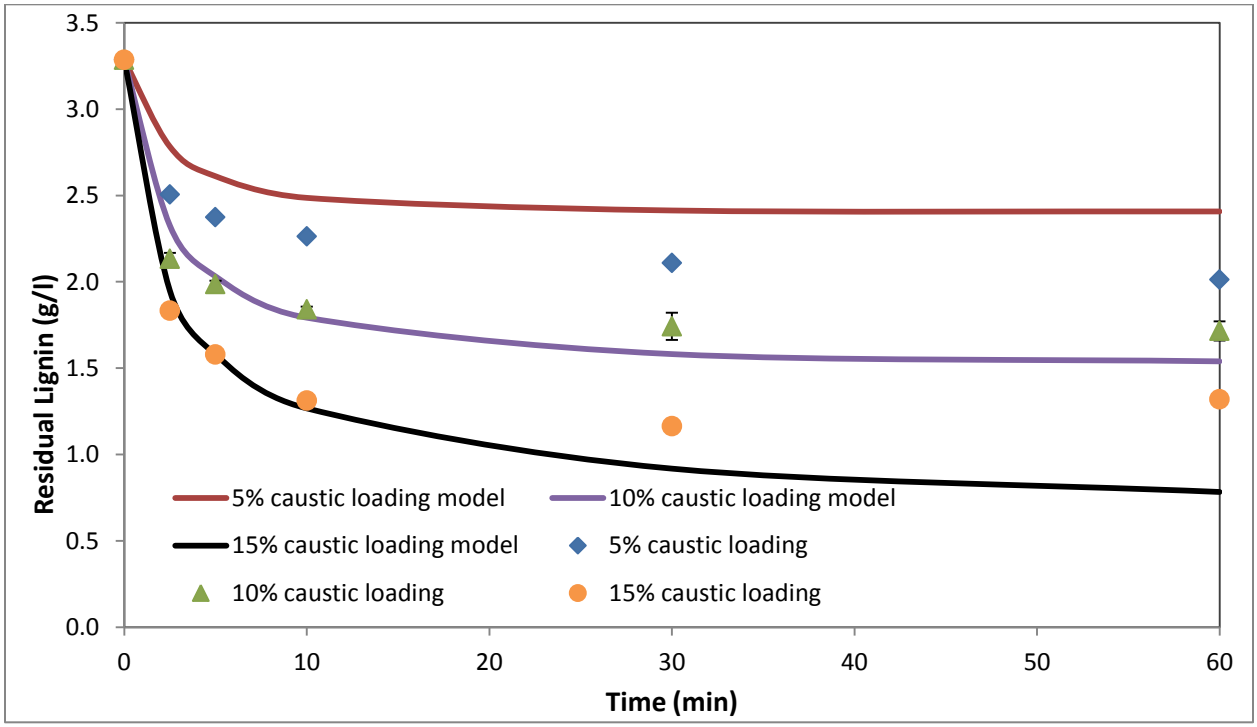

Figure 35: Simulated single ODE approach with full factorial dataset, 2% substrate loading and 130°C

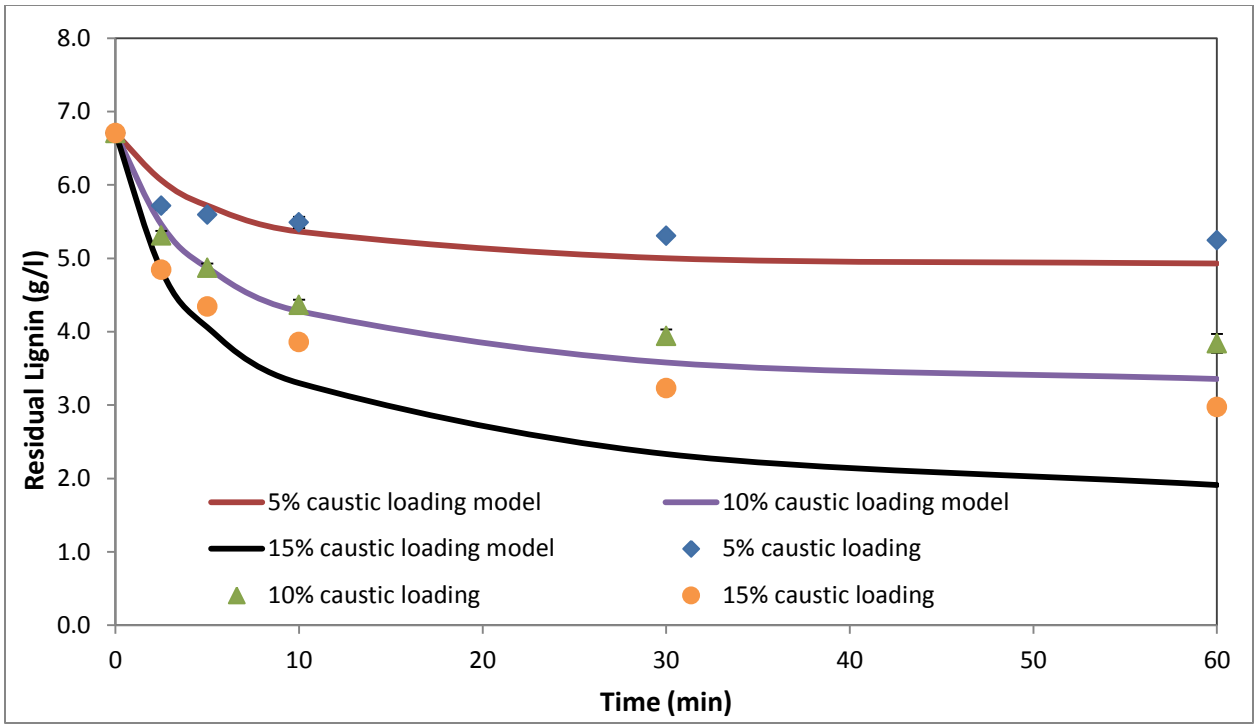

Figure 36: Simulated single ODE approach with full factorial dataset, 4% substrate loading and 90°C

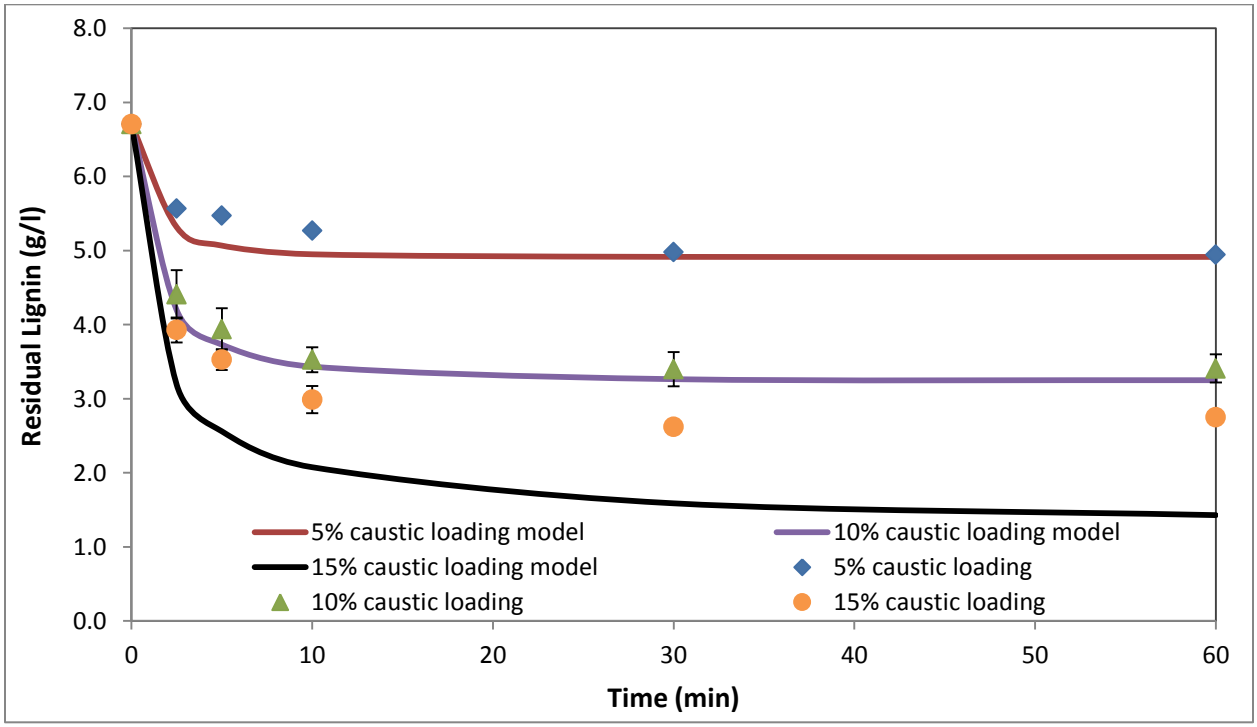

Figure 37: Simulated single ODE approach with full factorial dataset, 4% substrate loading and 110°C

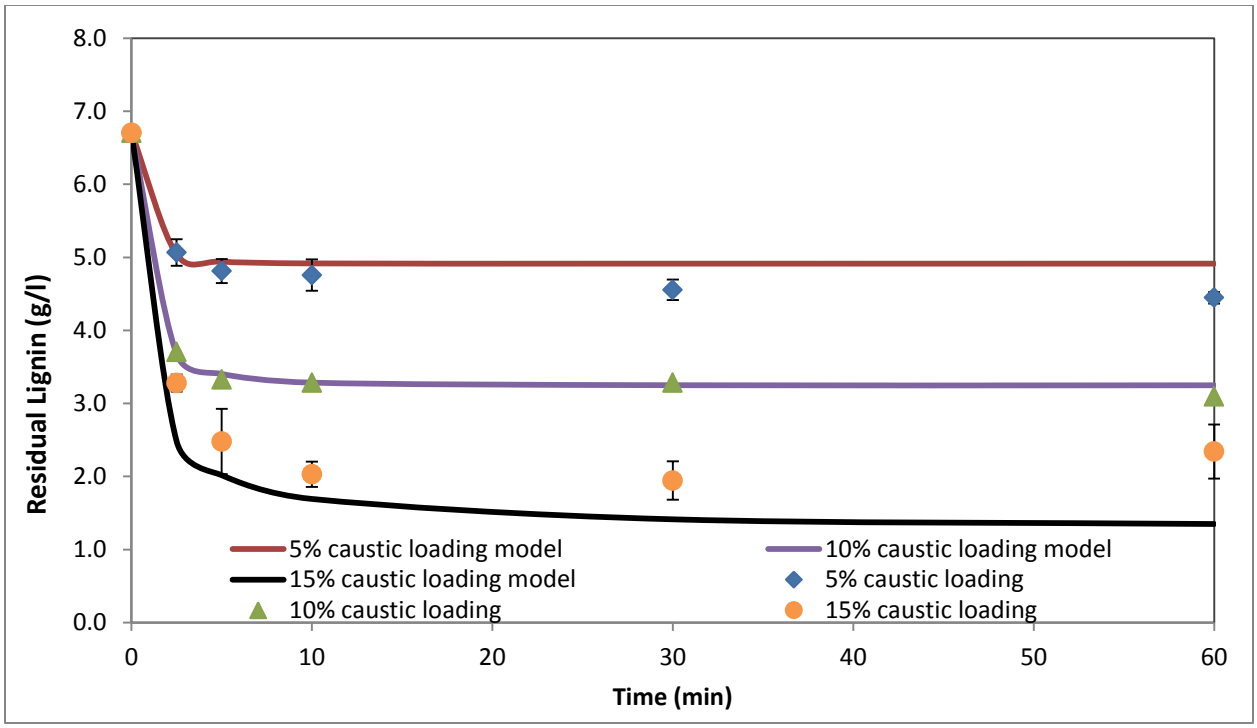

Figure 38: Simulated single ODE approach with full factorial dataset, 4% substrate loading and 130°C

The simulated single ODE approach was able to capture the general trend of the full range of pretreatment conditions. The model was situationally accurate for 5 and 10% caustic loading but was unable to predict the residual lignin concentration (solid) with 15% caustic loading. Temperature effects were adequately captured by the model for pretreatment at 5 and 10% caustic loading not at 15%. Parity plots were generated at constant caustic loading with varying temperature and substrate loading to evaluate the accuracy of the model (Figure 39-41). For pretreatment conditions performed at 5 and 10% caustic loading, the data points were scattered around the 45° line and the predicted values fell within a ±20% of the experimental data values. The model was less accurate for 15% caustic loading and the maximum error was as high as 48%, indicating an inaccurate prediction. The model was most accurate for 10% caustic loading.

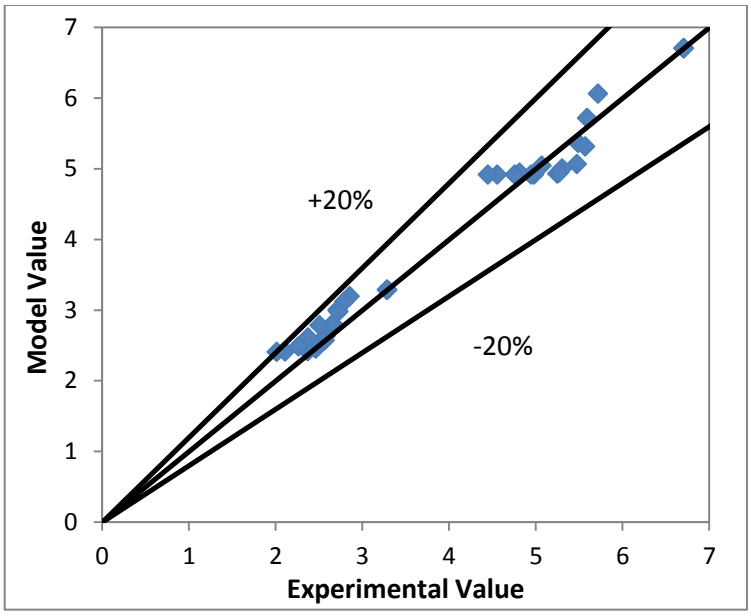

Figure 39: Single ODE approach parity plot for 5% caustic loading (±20% error) with full factorial dataset

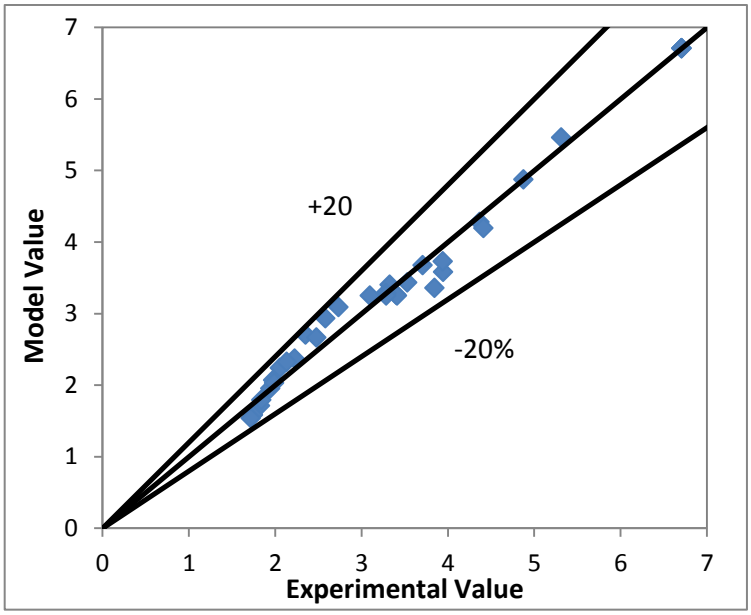

Figure 40: Single ODE approach parity plot for 10% caustic loading (±20% error) with full factorial dataset

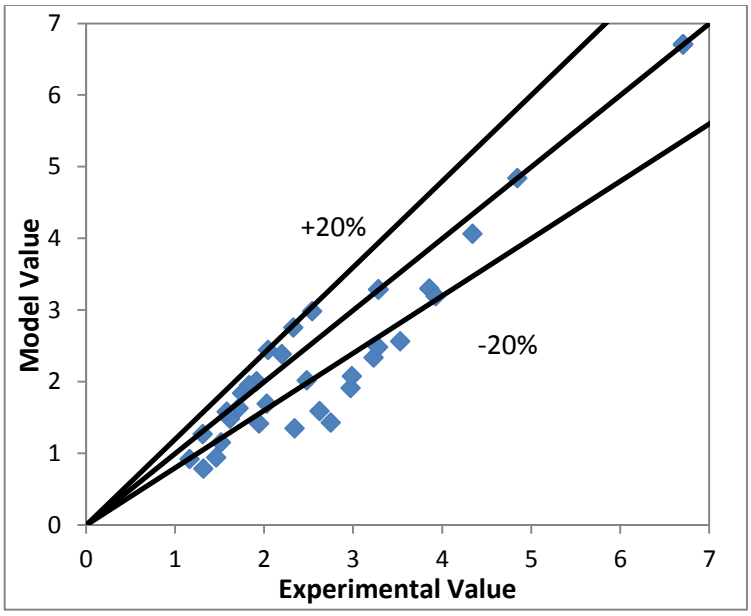

Figure 41: Single ODE approach parity plot for 15% caustic loading (±20% error) with full factorial dataset

A possible reason for the high discrepancy might be due to the duration of sample storage. Analysis of the concentration of hydroxide ions from the full factorial design samples could be inaccurate due to long storage time. Theoretically, the values of dOH^-/dL cannot be positive because hydroxide ions were being consumed over time during the reaction and thus dOH^- should always be negative. This was reflected by the positive values of dOH^-/dL values seen on Figure 32. Alternatively the model discrepancies for 15% caustic loading could be due to the saturation of hydroxide ions discussed in sections 4.2 and 4.3. Unfortunately this model (Equation 5.20) was not able capture this phenomena. In order to remedy this problem, additional experiments were performed.

5.3.2 Improvement to Single ODE Model Approach

Two hypotheses were made in order to explain the discrepancy observed:

1. Inaccurate values of dOH^-/dL caused by long sample storage
2. The hydroxide ion in the system was saturated at 15% caustic loading

In order to obtain a more accurate dOH^-/dL value, the software program JMP was used to design a 3x2x2 experiment; operating conditions are summarized in Table 19:

Table 19: Experimental conditions generated from JMP experimental design for system of ODEs approach

Temperature (°C)	Substrate Loading (% w/w)	Caustic (% w/w of substrate)
90	2	5
90	4	10
110	2	5
110	4	10
130	2	10
130	4	5

The 15% caustic loading was excluded in the JMP experimental design in order to test the hypothesized caustic saturation. The approach was to solve the model equation (Equation 5.18) with a set of new 5 and 10% caustic loading dataset and use the solved model to simulate experimental data. The rate of hydroxide ion consumption from the new dataset was plotted against the delignification rate as shown in Figure 42. The value of dOH^-/dL (slope) was equal to 0.488 with a minor y intercept of 0.005 and a R^2 value of 0.945, indicating an improvement compared to the previous value.

The values of dOH^-/dL obtained from the JMP designed dataset were all negative, indicating that the hydroxide ions readings were correct. The new dOH^-/dL value was very similar compared to the one obtained from using the full factorial design dataset (a difference of 1.1%) and was used to resolve the single ODE model (Equation 5.18).

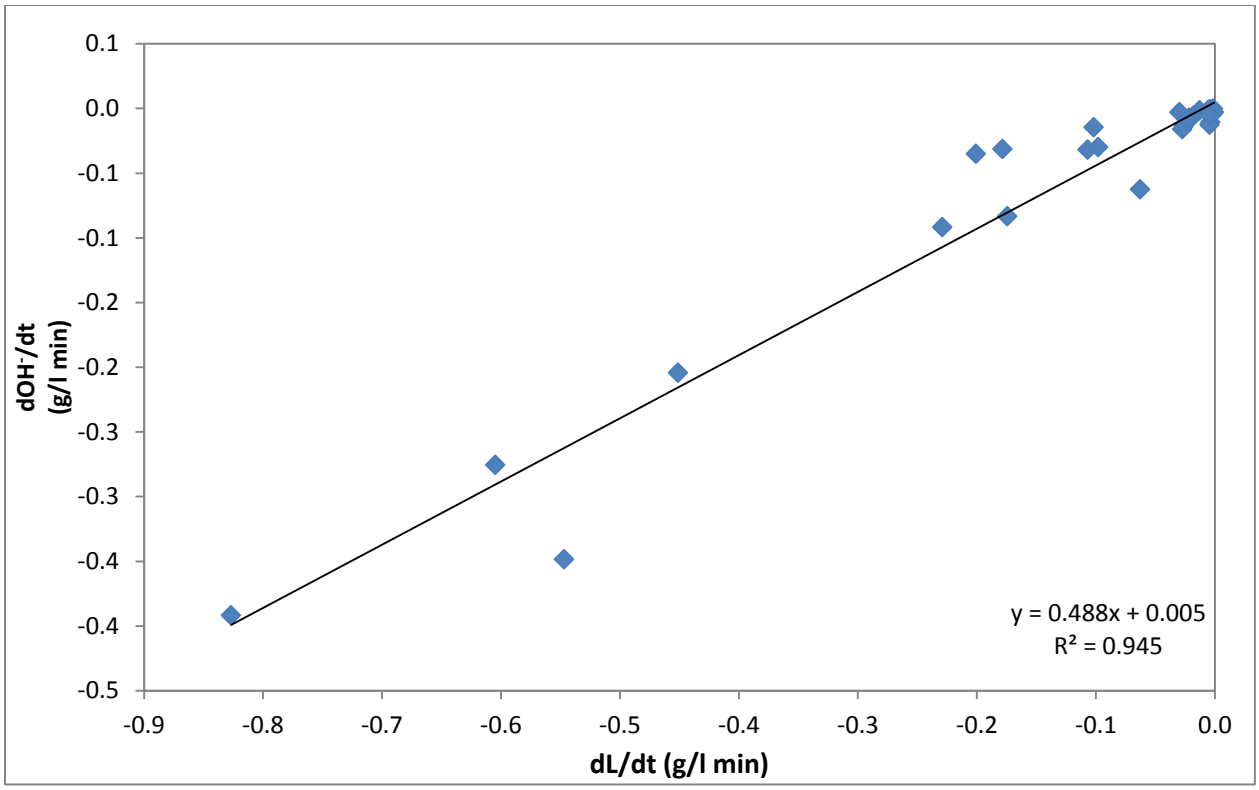

Figure 42: dOH$^-$/dt vs dL/dt results obtained from using JMP designed dataset

The single ODE model was solved with initial guesses and final values of the parameters presented in Table 20. The solved model and simulated results using JMP designed experiments are shown in Equation 5.21 and Figure 43-45 respectively. The simulated results from the newly solved model (Equation 5.21) were in good agreement with experimental data with a maximum error of 15.0%. Parity plots of the improved single ODE model and the JMP dataset are presented in Figure 46 and 47.

$$\frac{d[L]}{dt} = -k_L[L]^{0.89}(0.488([L] - [L_0]) + [OH_0^-])^{1.30} \qquad 5.21$$

The rate constant k_L corresponded to the lignin kinetic constant at each operating temperature (90, 110 or 130°C).

Table 20: Initial guess and final values for JMP designed experiment

Parameter	Initial guesses	Final values
K_{90}	1.00E-01	6.19E-02
K_{110}	1.00E-01	1.60E-01
K_{130}	1.00E-01	4.38E-01
a_1	1.00	8.85E-01
a_2	2.00	1.30

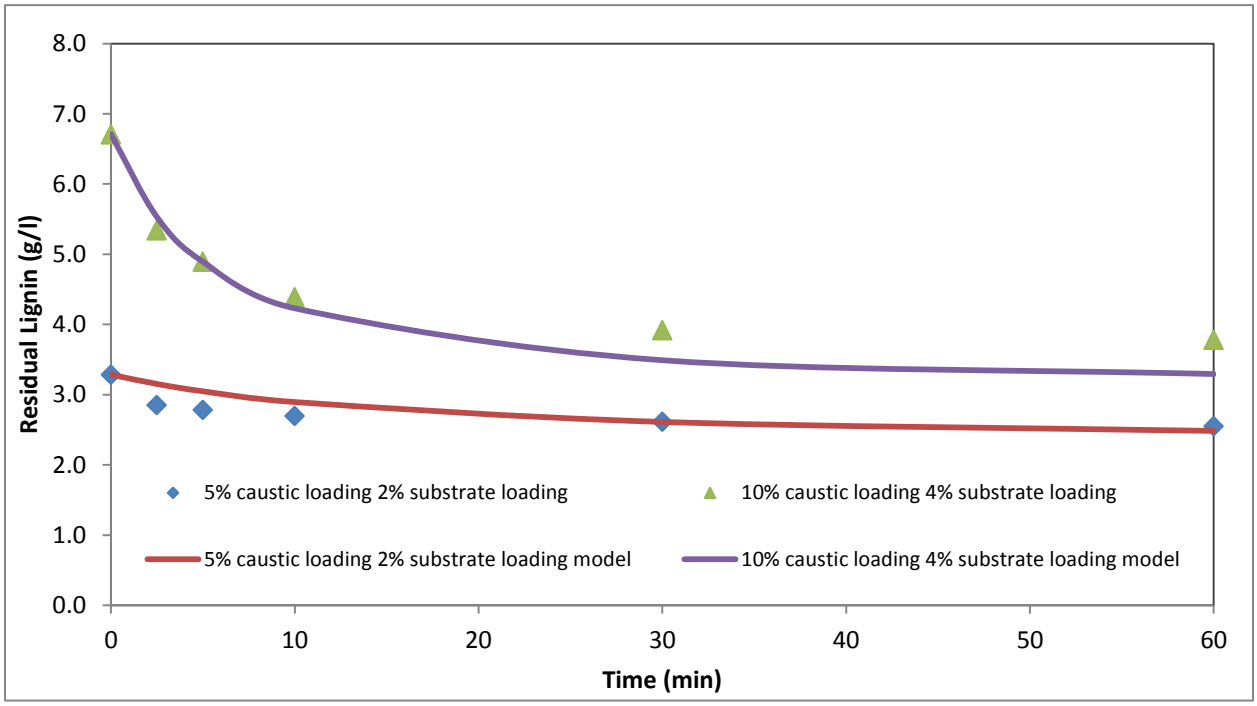

Figure 43: Simulated improved single ODE approach with JMP dataset for 90°C

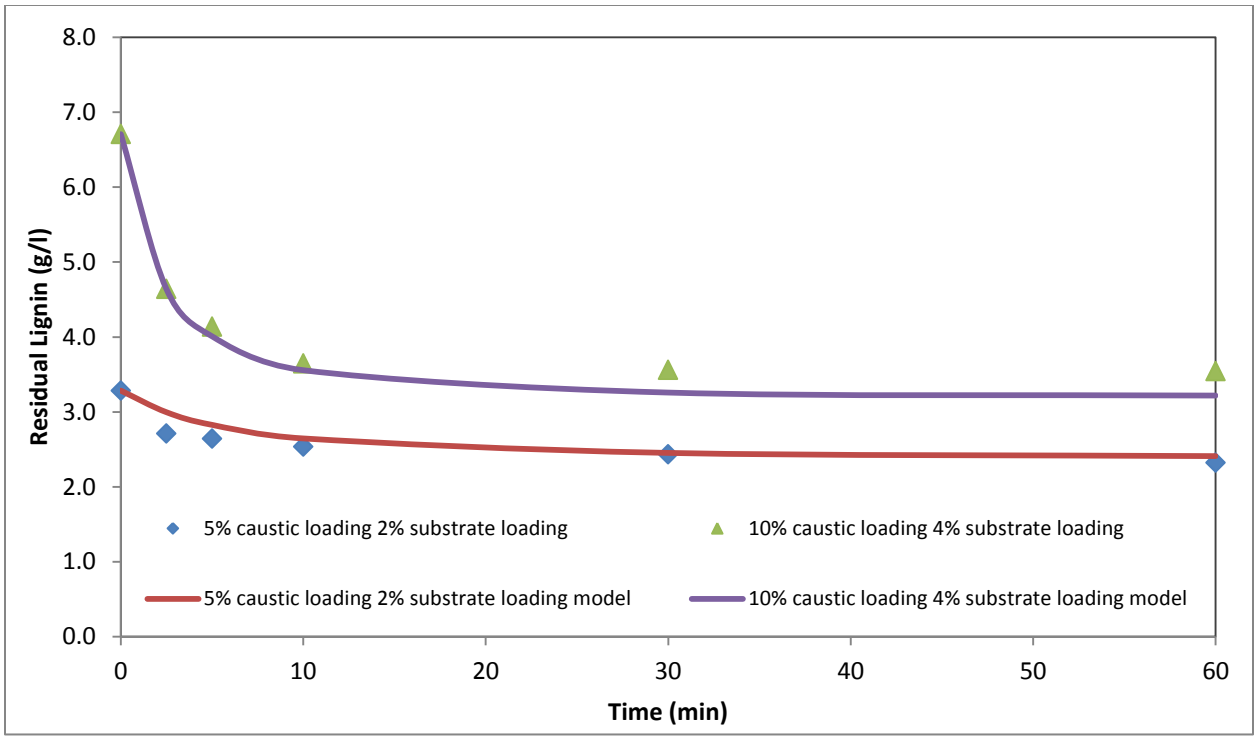

Figure 44: Simulated improved single ODE approach with JMP dataset for 110°C

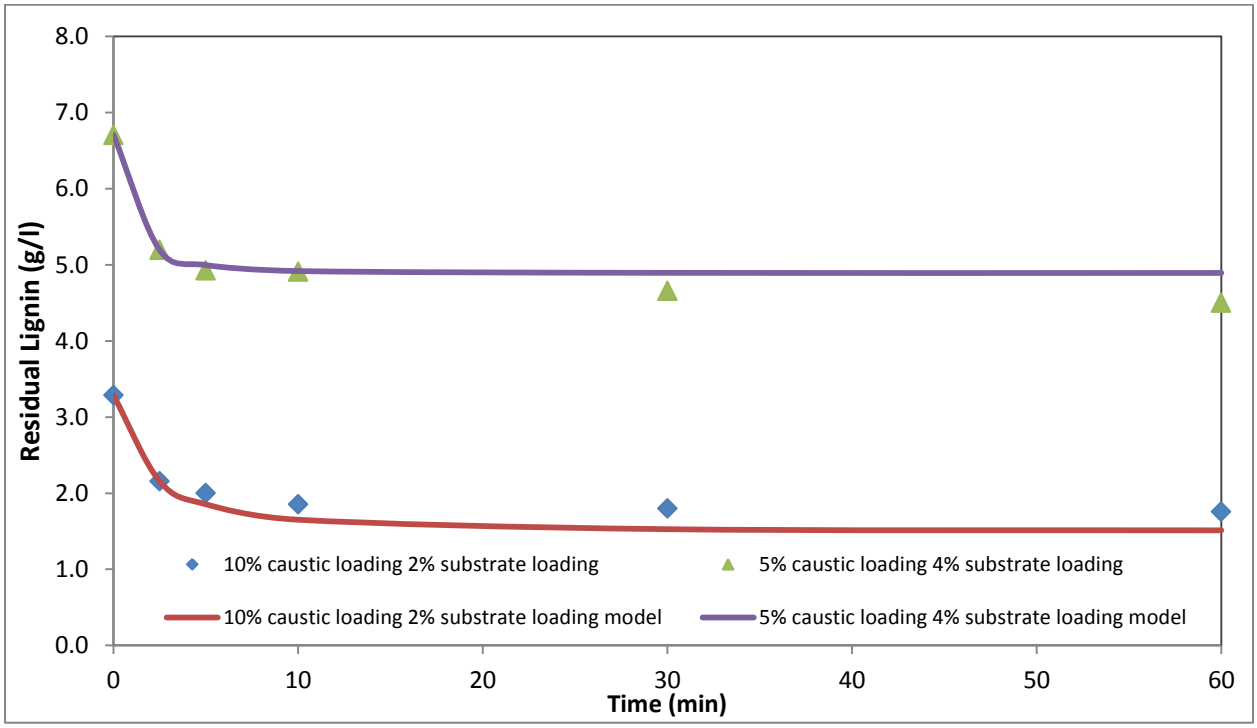

Figure 45: Simulated improved single ODE approach with JMP dataset for 130°C

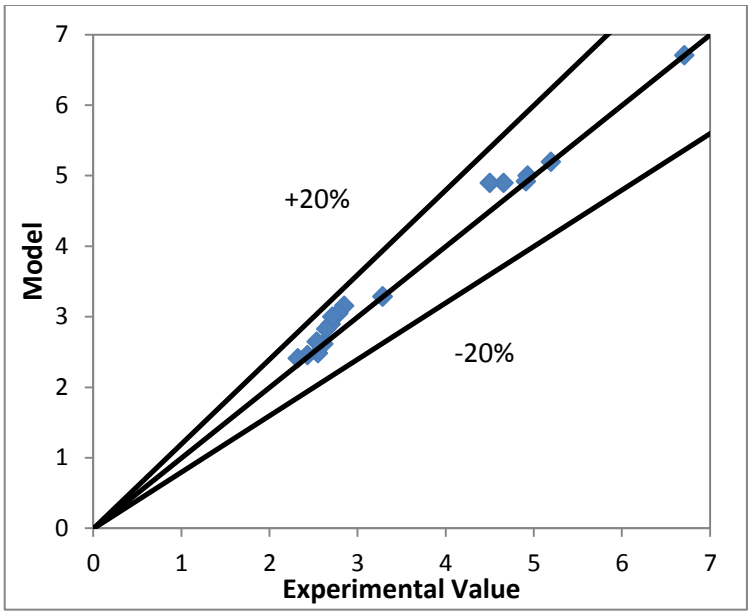

Figure 46: Improved single ODE approach parity plot for 5% caustic loading (±20% error) with JMP dataset

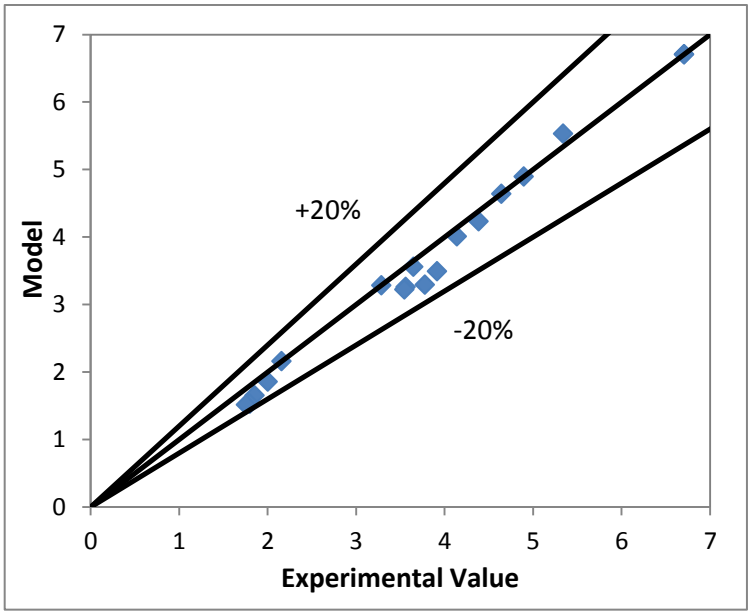

Figure 47: Improved single ODE approach parity plot for 10% caustic loading (±20% error) with JMP dataset

With the newly solved parameter values, the improved single ODE model (Equation 5.21) was used to simulate the full factorial experiment dataset (Figure 48-53) and the parity plots were also generated (

Appendix C).

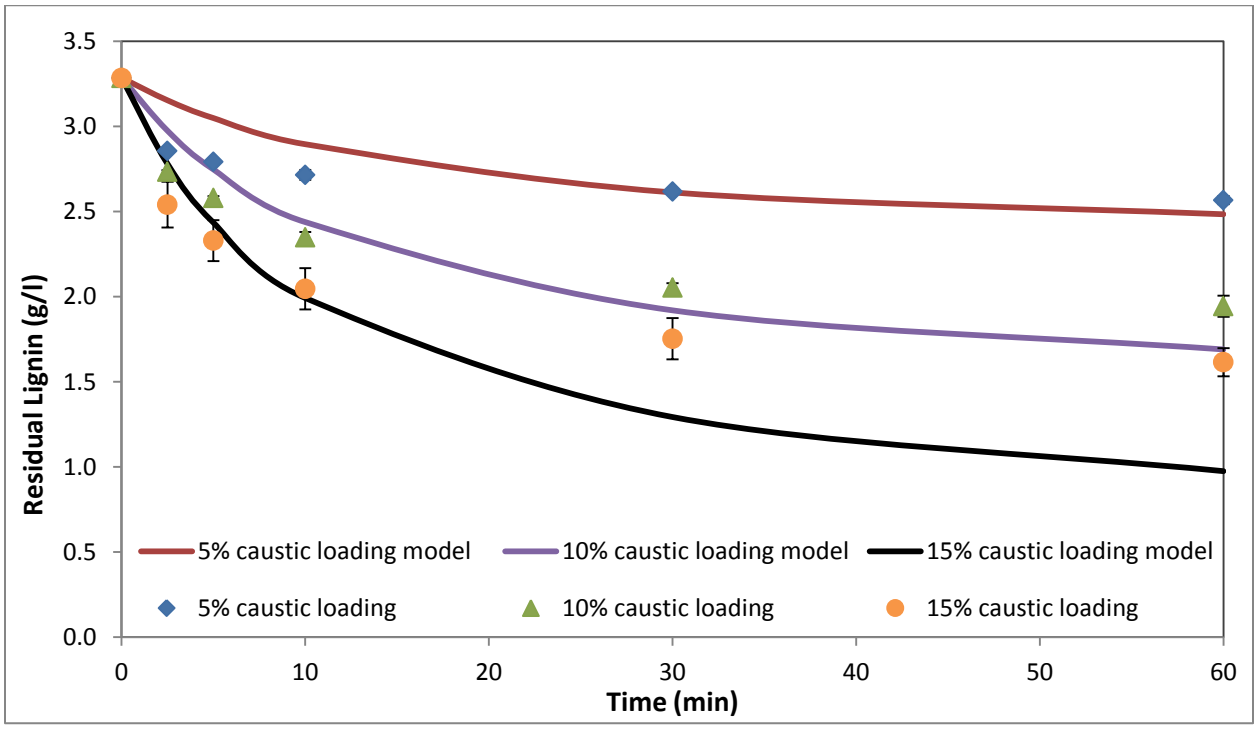

Figure 48: Simulated improved single ODE approach with full factorial dataset, 2% substrate loading and 90°C

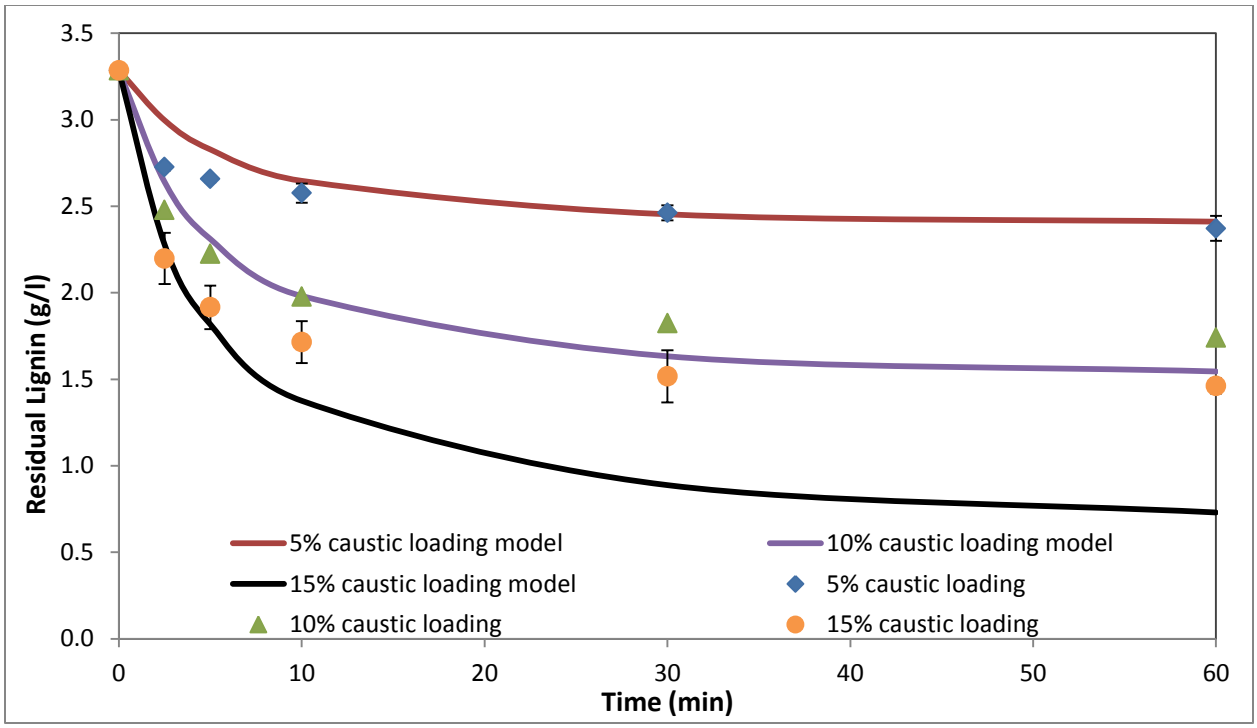

Figure 49: Simulated improved single ODE approach with full factorial dataset, 2% substrate loading and 110°C

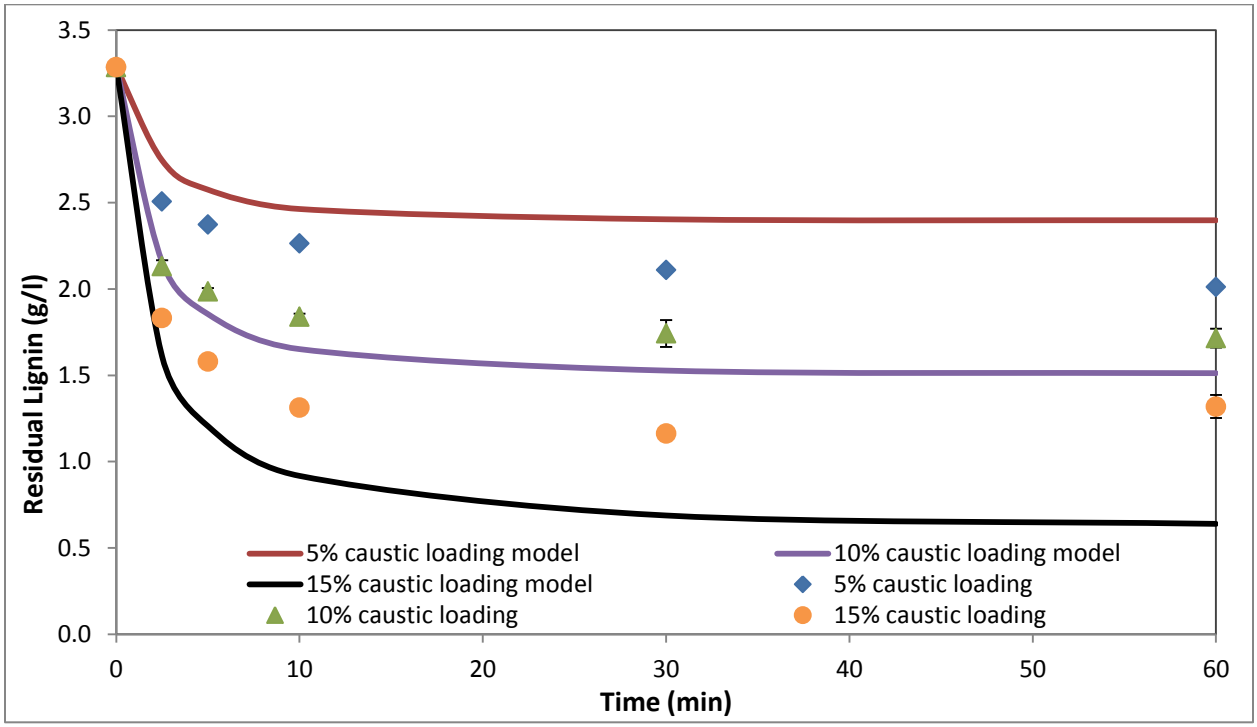

Figure 50: Simulated improved single ODE approach with full factorial dataset, 2% substrate loading and 130°C

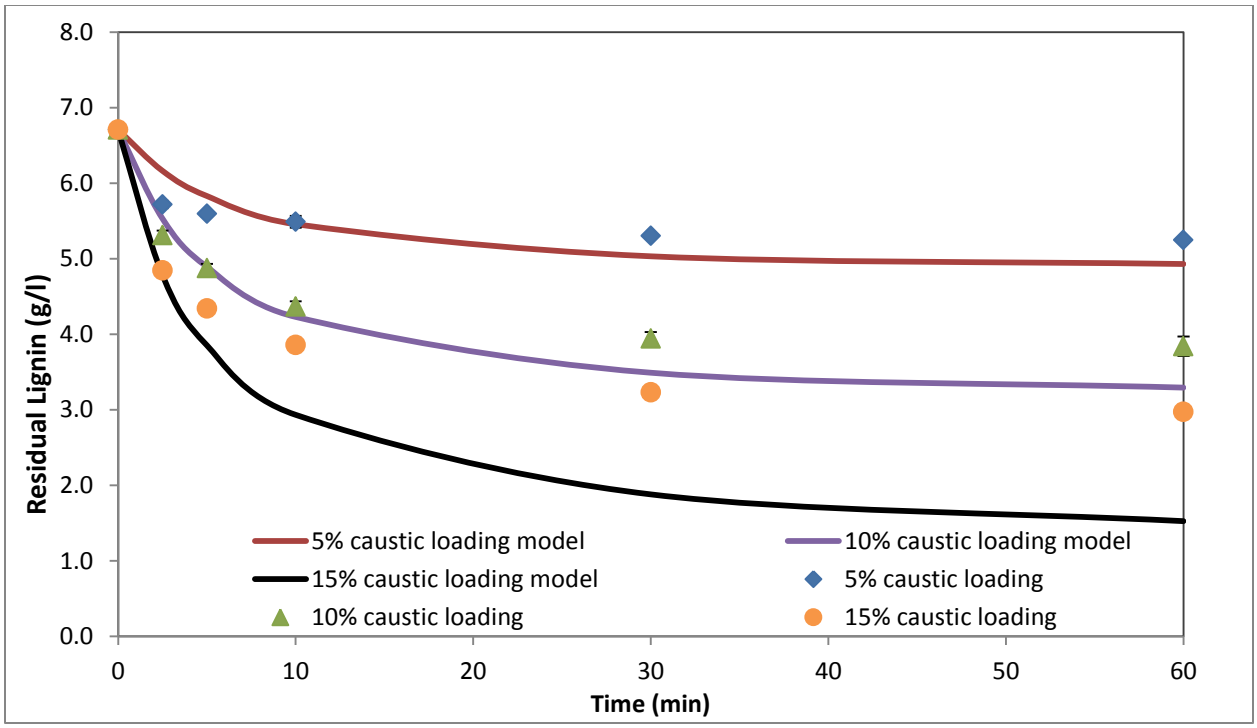

Figure 51: Simulated improved single ODE approach with full factorial dataset, 4% substrate loading and 90°C

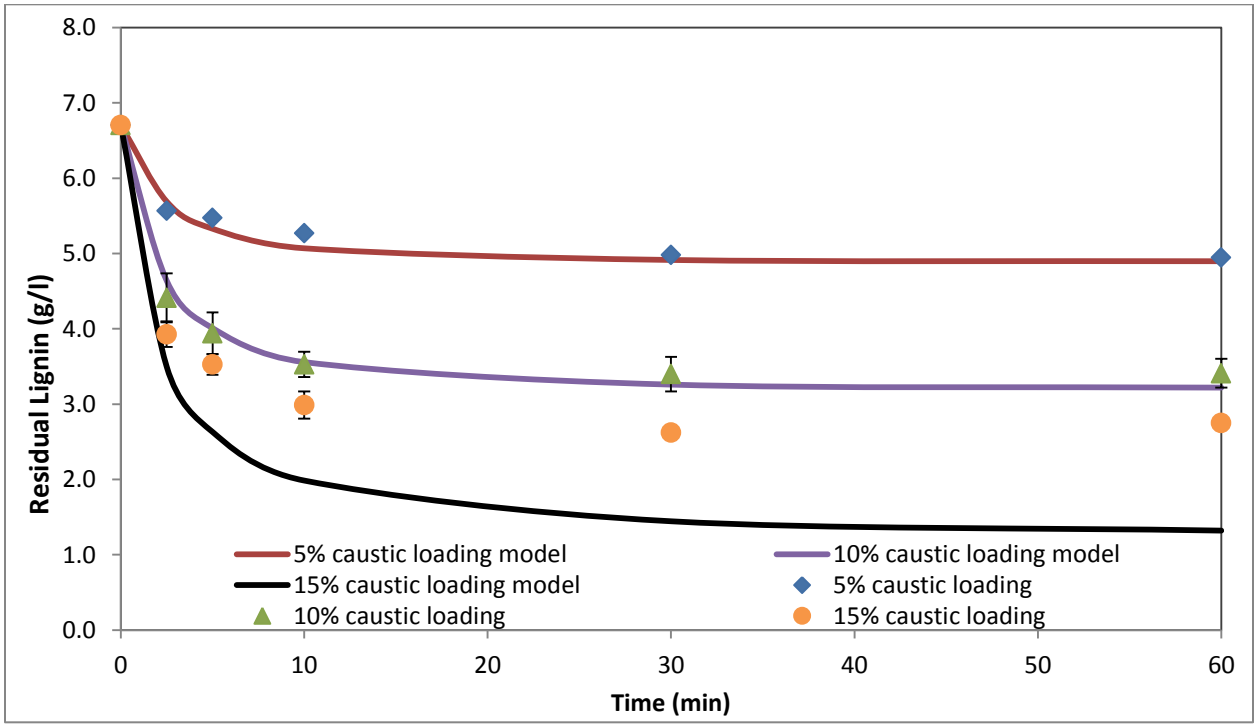

Figure 52: Simulated improved single ODE approach with full factorial dataset, 4% substrate loading and 110°C

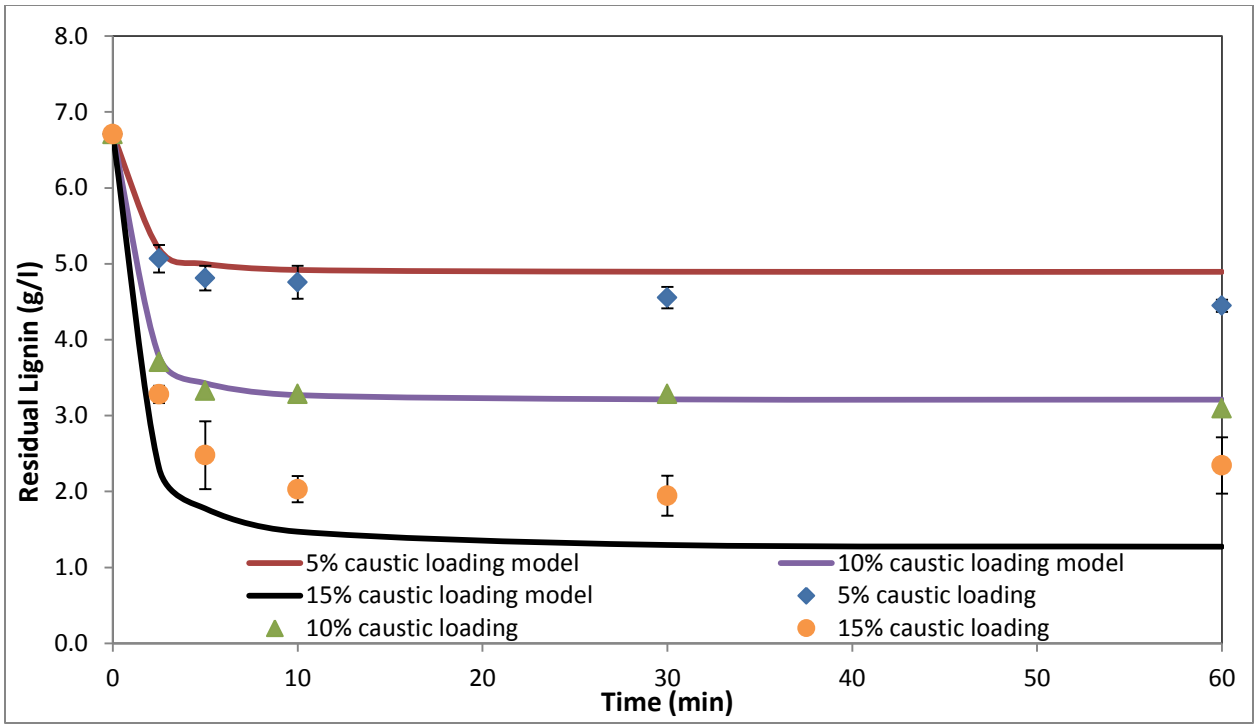

Figure 53: Simulated improved single ODE approach with full factorial dataset, 4% substrate loading and 130°C

The improved single ODE model was able to predict the experimental values with varying temperature but not at 15% caustic loading. Equation 5.21 was most accurate when caustic loading was at 10% and relative to Equation 5.20, improved the accuracy of prediction at 5% caustic loading (

Appendix C). The new dOH^-/dL did not improve residual lignin predictions at 15% caustic loadings and had a maximum error of 52%. This observation suggested the first hypothesis was false which led to the second hypothesis.

5.3.3 Test of Caustic Saturation

Additional experiments were performed in order to investigate the caustic saturation hypothesis. The conditions of the three experiments conducted are summarized in Table 21. Pretreatment was conducted at 90°C so that the reaction rate would be slow enough to distinguish between the effects of caustic loading.

Table 21: Experiment conditions for test of caustic saturation

Temperature (°C)	Caustic loading (%)	Substrate loading (%)
90	12	2
90	13	2
90	17.5	2

If the caustic loading was saturated at 15%, a similar delignification profile would be observed if the pretreatment was to be performed at a higher caustic loading. Following this reasoning, a pretreatment with 17.5% caustic loading was performed to and the results are shown in Figure 54. The residual lignin from the oxygen delignification at 17.5% caustic loading condition closely resembled 15% caustic loading with a maximum difference of 4.7%. This suggested that the hydroxide ions were saturated during the delignification reaction.

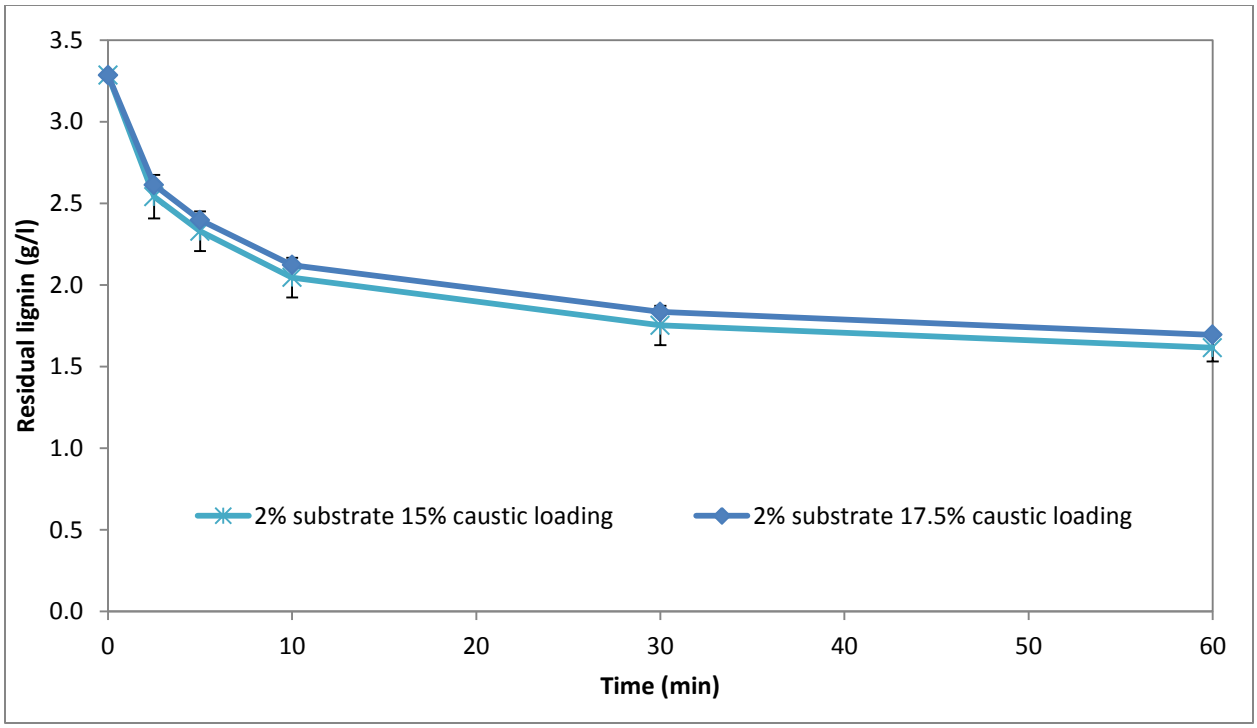

Figure 54: Delignification profile comparison between 15% and 17.5% caustic loading at 2% substrate loading 90°C

After confirming that caustic was saturated at 15% caustic loading, the next step was to approximate the caustic saturation point. This approximation was done by delignification prediction at 90°C with initial caustic loadings of 10, 11, 12, 13, 14 and 15% using the improved single ODE model (Equation 5.20) and compared the simulated results to the experimental results obtained with 15% (Figure 55). This gave a rough estimation of the caustic loading saturation point. Using minimum residual values between the model and the experimental data as the criteria, the caustic loadings at 12 and 13% were chosen to test for the caustic saturation point.

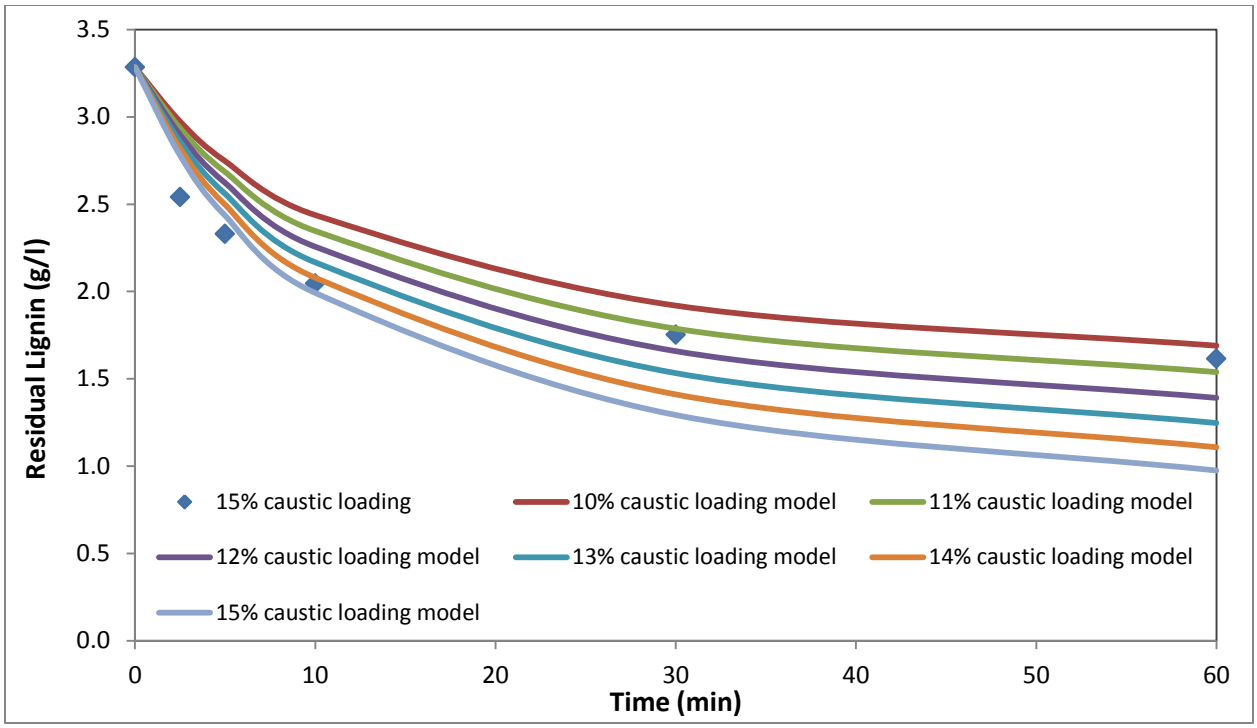

Figure 55: Estimation of caustic saturation point using the improved single ODE approach at 2% substrate loading and 90°C

The improved single ODE (Equation 5.20) was used to predict the experimental values at 90°C, 2% substrate loading, 12 and 13% caustic loading (Figure 56). Parity plot with ±20% error was plotted to examine the accuracy of the model (Figure 57). The model showed a trend of over prediction of experimental values reaction time was beyond 30 minutes. The simulated results showed a relatively good fit for 12% caustic loading (maximum error of 23.5%) with a higher deviation when caustic loading was 13% (maximum error of 30.4%).

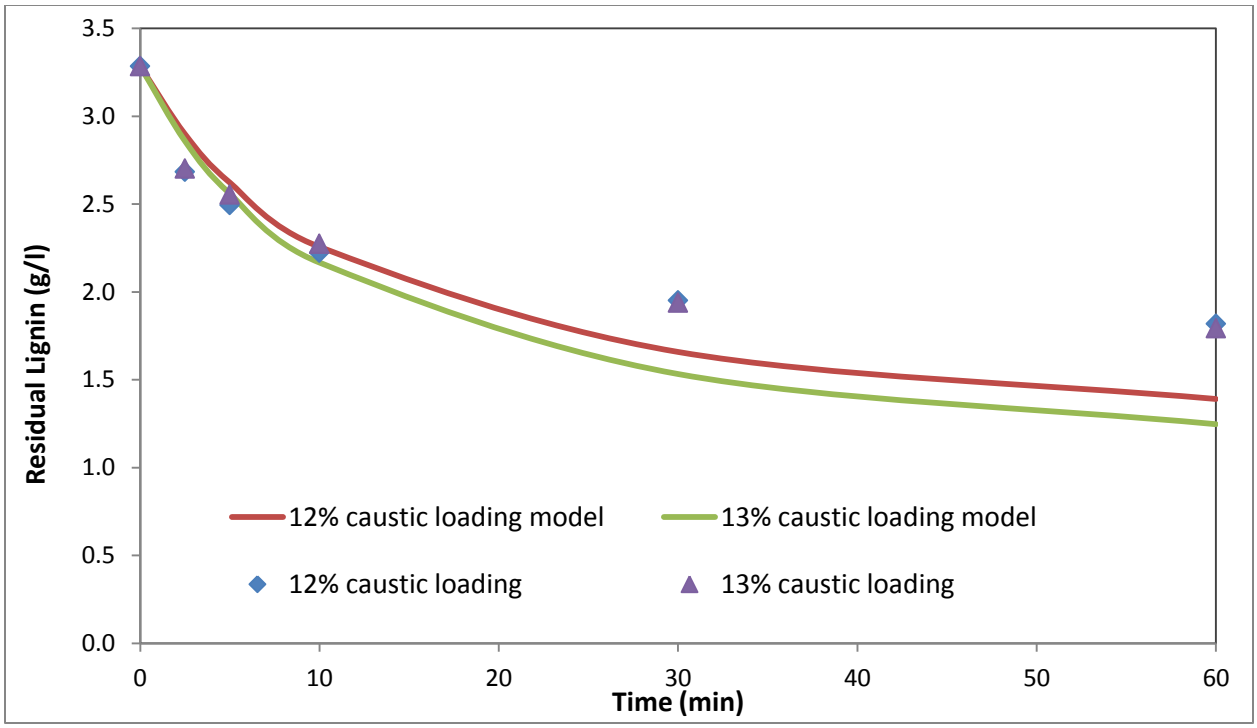

Figure 56: Simulated improved single ODE approach for 2% substrate loading at 90°C, 12 and 13% caustic loading

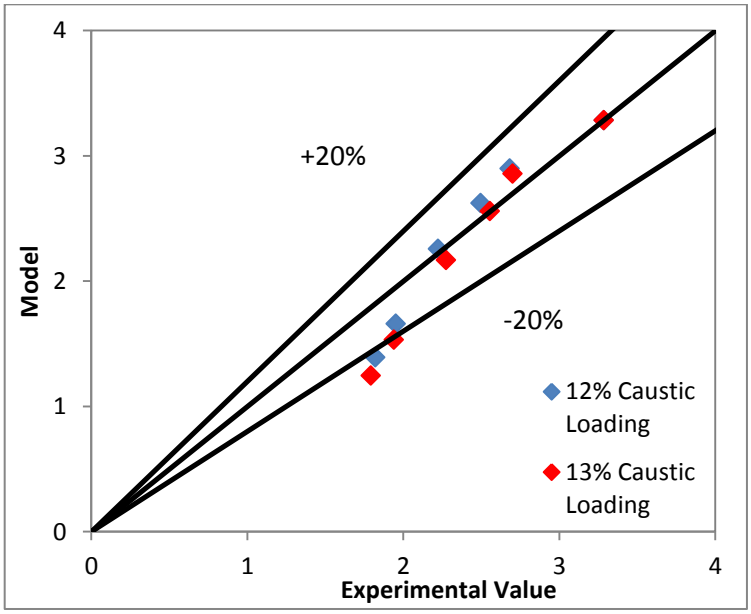

Figure 57: Improved single ODE approach parity plot with ±20% error for 2% substrate loading, 90°C, 12 and 13% caustic loading

5.3.4 System of ODEs Approach to Solve for Kinetic Parameters

The system of ODEs approach was performed with the JMP designed experimental values to solve for the kinetic parameters. In the system of ODEs approach, both Equation 5.11 and 5.12 were solved simultaneously. The initial guesses and the final values of the solved parameters are summarized in Table 22. The final form of the system of ODEs model is presented in Equation 5.22 and 5.23 and model values with the JMP dataset are shown in Figure 58-60. The parity plots of the system of ODEs model are shown in Figure 61 and 62.

$$\frac{d[L]}{dt} = -k_L[L]^{0.65}[OH^-]^{1.75} \quad 5.22$$

$$\frac{d[OH^-]}{dt} = -k_{OH}[L]^{0.65}[OH^-]^{1.75} \quad 5.23$$

The rate constants k_L and k_{OH} corresponded to kinetic constants for lignin and hydroxide ion respectively at each operating temperature (90, 110 or 130°C).

Table 22: Initial guesses and final values for system of ODEs approach using JMP designed experimental data

Parameter	Initial guesses	Final values
K_{L90}	1.00E-01	1.24E-01
K_{L110}	1.00E-01	3.51E-01
K_{L130}	1.00E-01	6.55E-01
K_{OH90}	1.00E-01	7.03E-02
K_{OH110}	1.00E-01	1.86E-01
K_{OH130}	1.00E-01	3.41E-01
α_1	1.00	0.65
α_2	2.00	1.75

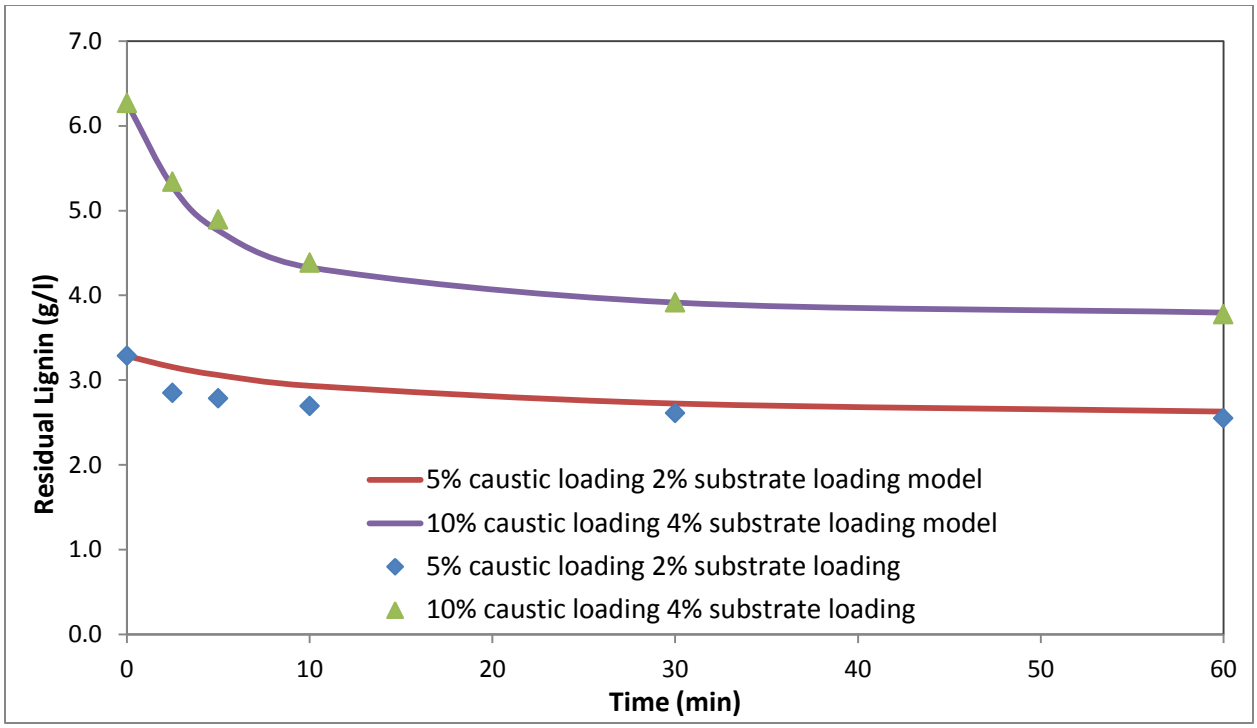

Figure 58: Simulated system of ODEs approach with JMP dataset at 90°C

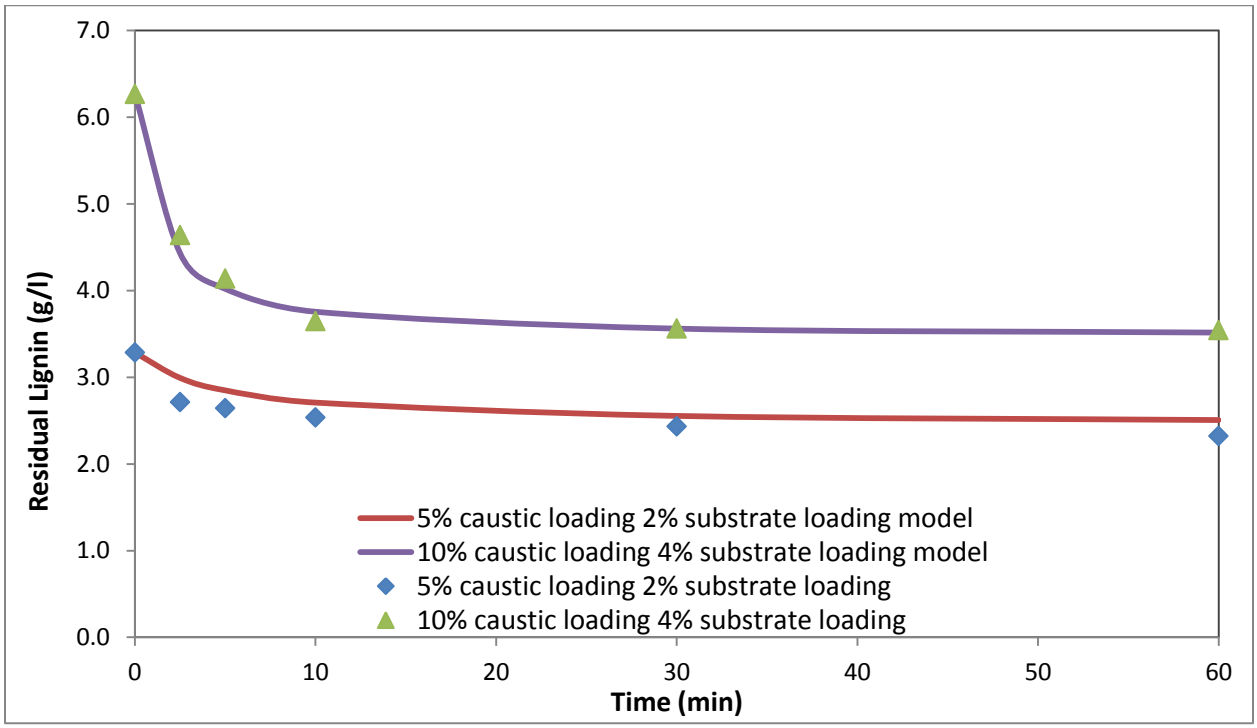

Figure 59: Simulated system of ODEs approach with JMP dataset at 110°C

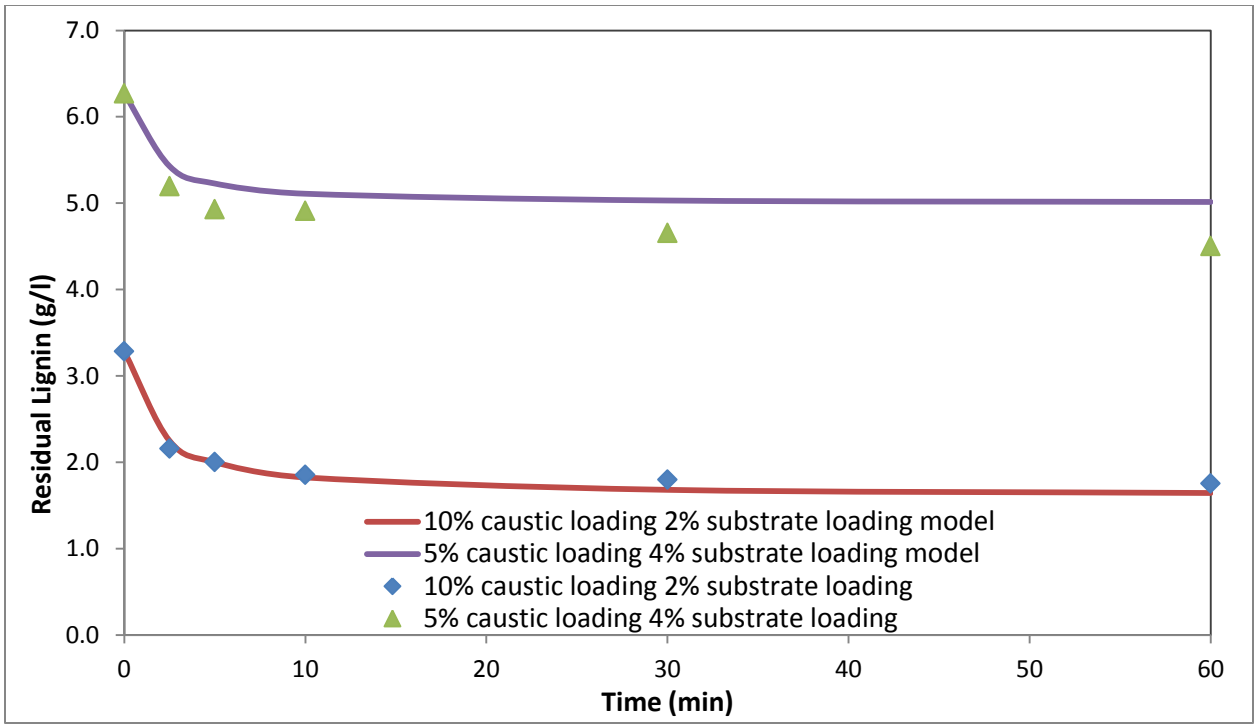

Figure 60: Simulated system of ODEs approach with JMP dataset at 130°C

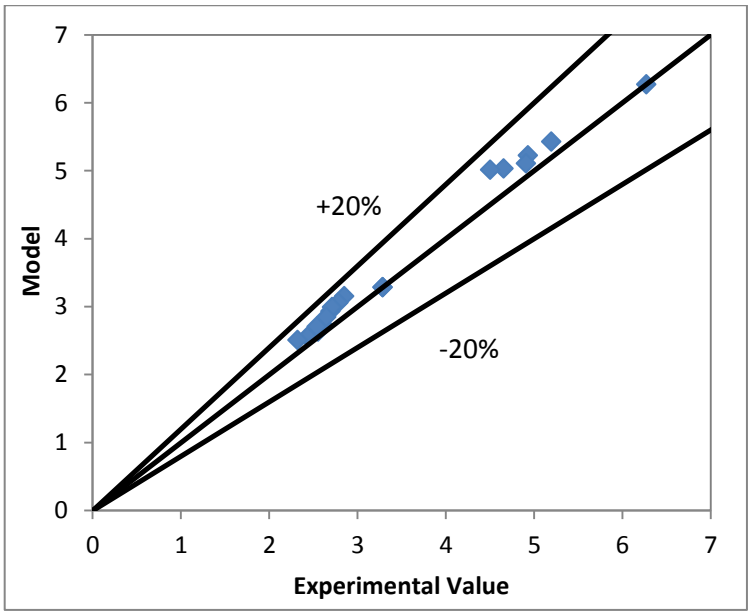

Figure 61: Parity plot with ±20% error for 5% caustic loading system of ODEs method with JMP dataset

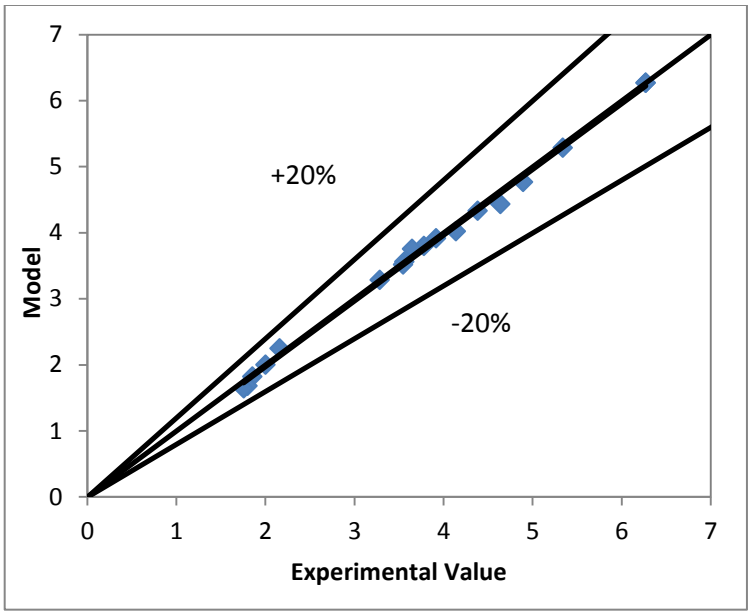

Figure 62: Parity plot with ±20% error for 10% caustic loading system of ODEs method with JMP dataset

The simulation of the system of ODEs approach produced good results for the JMP dataset with a maximum error 11.4%. The simulated results for 5% caustic loading solved by the system of ODEs approach slightly over estimated the experimental values compared to the improved single ODE approach. Improvements were made for the 10% caustic loading conditions as Figure 62 shows the data are more tightly aligned to the 45° line of the parity plot compared to Figure 47. It was believed that the improved prediction came from solving Equation 5.11 and 5.12 simultaneously. In the single ODE approach, Equation 5.20 and 5.21 were solved based on a constant average relationship between the rate of delignification and hydroxide ion consumption (dOH^-/dL). The advantage of the system of ODEs approach was the consideration of the changing relationship between the rate of delignification and rate of hydroxide ion consumption as the reaction progressed; thus the system of ODEs approach was able to provide a more accurate prediction compared to the improved single ODE approach.

The system of ODEs approach was also subjected to test the caustic saturation hypothesis. Equation 5.22 and 5.23 were used to predict the experimental values at 90°C, 2% substrate loading, 12 and 13% caustic loading (Figure 63). Parity plot with ±20% error was also plotted. Compared to the improved single ODE approach (Figure 57), the parity plot from the system of

ODEs approach were less scattered around the 45° line (Figure 64). This observation reinforced the conclusion that the system of ODEs model was the more accurate model in predicting the experimental values. The simulated results from the system of ODEs model showed a good fit with 12% caustic loading (maximum error of 11.1%) between the modeled and experimental value; however the model started to deviate when caustic loading was at 13% (maximum error of 17.6%). It was concluded that the caustic loading for oxygen delignification for wheat straw would become saturated at 15% and saturation point was between 10-12%. No attempt was made to adjust the kinetic model to capture this phenomenon.

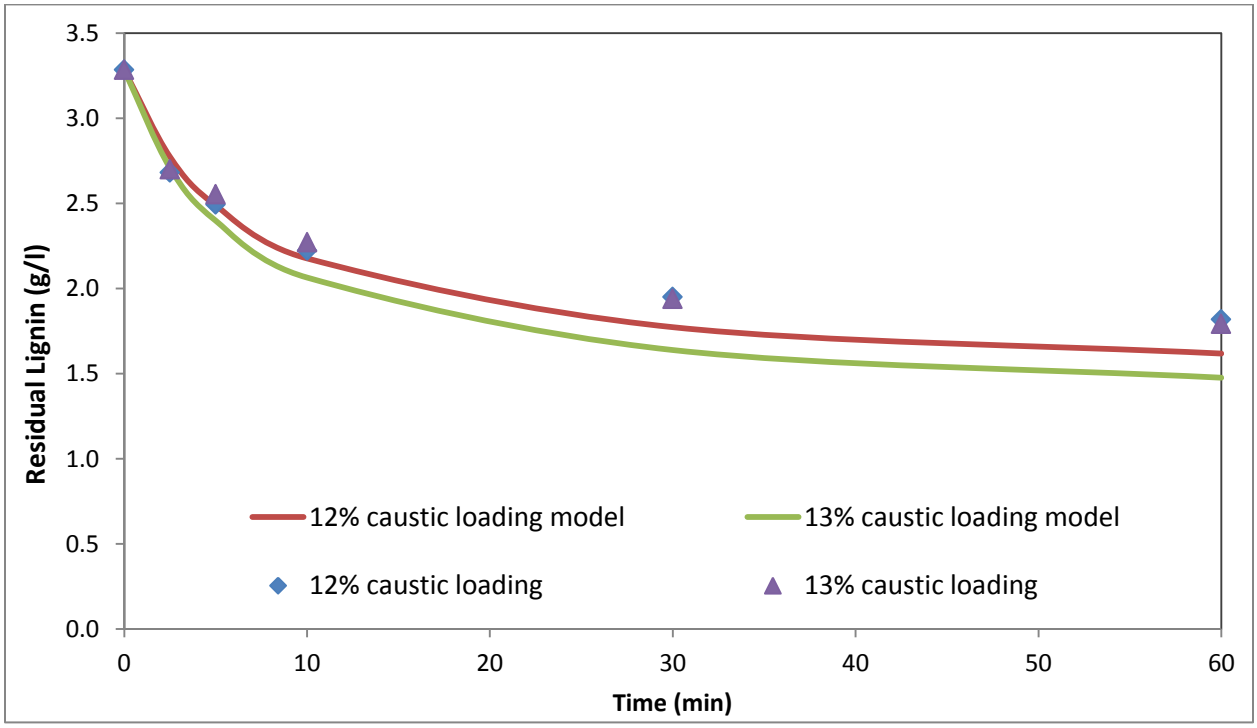

Figure 63: Simulated system of ODEs approach for 2% substrate loading at 90°C, 12, 13% caustic loading

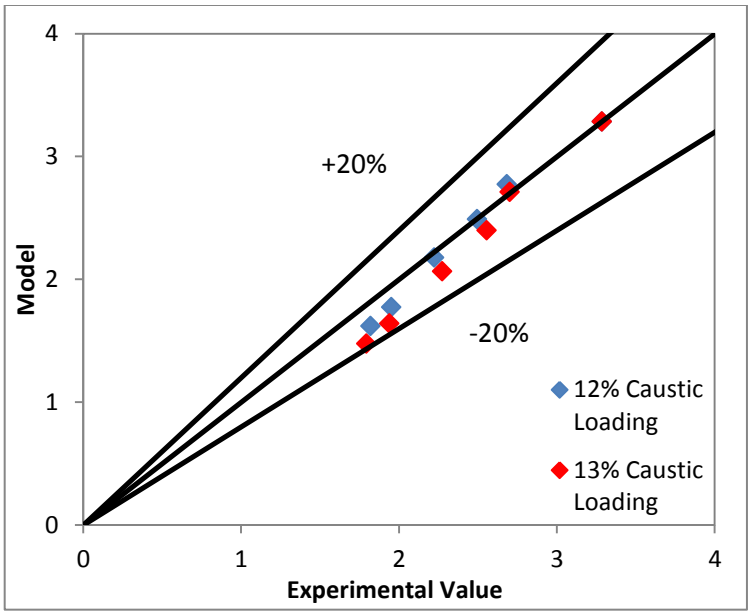

Figure 64: System of ODEs approach parity plot with ±20% error for 2% substrate loading, 90°C, 12 and 13% caustic loading

5.4 Validation of the Improved Single ODE and the System of ODEs Model

With the confirmation of the saturation at higher caustic loading (10-12%), both the improved single ODE (Equation 5.21) and the system of ODEs models (Equations 5.22 and 5.23) were validated by performing pretreatment at 90°C, 4% substrate and 7.5% caustic loading.

The delignification profile of 7.5% caustic loading fell in between the delignification curves of 5 and 10% caustic loading (Figure 65). Both the improved single ODE and system of ODEs models were used to simulate the 90°C, 7.5% caustic loading experimental values, the results and parity plots are shown in Figure 65 to 67. The improved single ODE model and the system of ODEs model had a maximum error of 6.0% and 3.5% respectively when compared to experimental values. This further supported that the system of ODEs was a more accurate model.

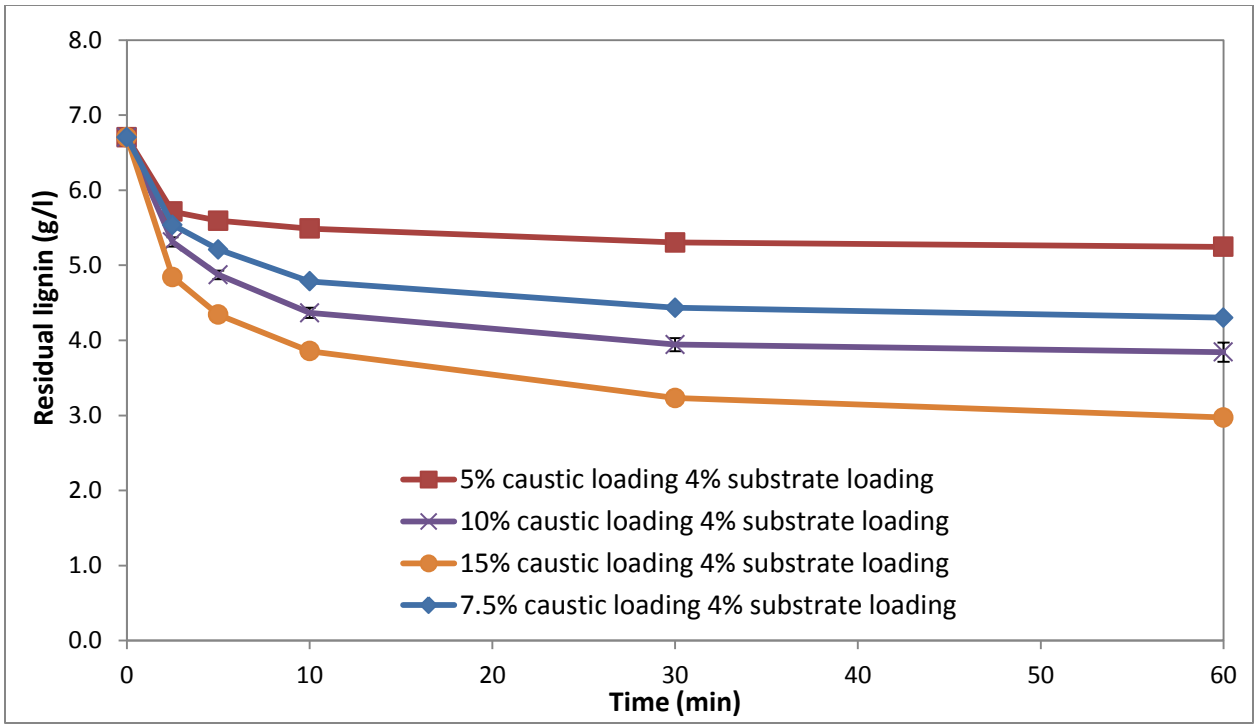

Figure 65: Delignification profile for 4% substrate at 90°C and 7.5% caustic loading

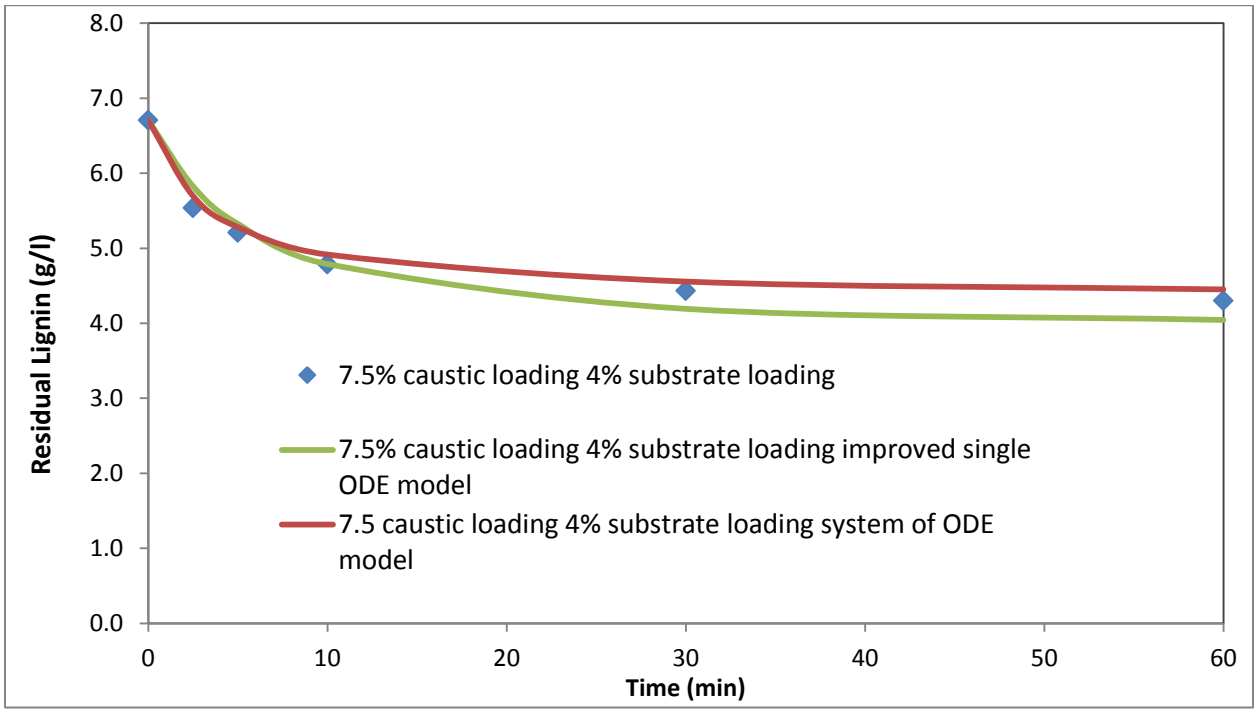

Figure 66: Simulated improved single and system of ODEs approach for 7.5% caustic loading, 4% substrate loading at 90°C

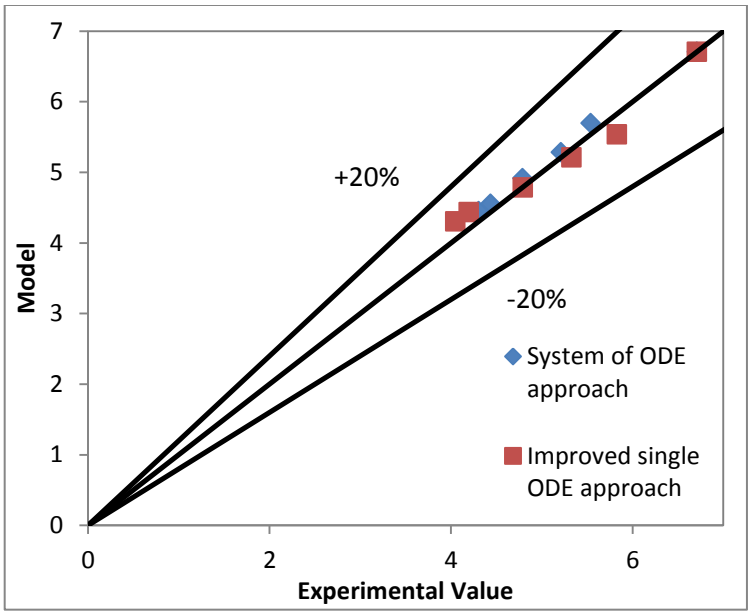

Figure 67: Improved single ODE and system of ODEs approach parity plot with ±20% error at 4% substrate loading, 7.5% caustic loading at 90°C

5.5 Activation Energy for Oxygen Delignification

In order to express the kinetic model as a function of temperature, the previous solved reaction rate constants (Table 20 and 22) were used to calculate the pre-exponential factor, *A* and activation energy E_a, required for oxygen delignification (Equation 5.24 and 5.25).

$$k = A\, e^{-\frac{E_a}{RT}} \tag{5.24}$$

$$\ln k = -\frac{E_a}{RT} + \ln A \tag{5.25}$$

In order to solve Equation 5.24, the calculated kinetic constants were plotted against the corresponding values of 1/*RT*, where *R* is 8.314 J/K mol and *T* is temperature in Kelvin. The resulting values of the slope and intercept of the line corresponded to E_a and ln *A* respectively (Figure 68). The estimated activation energies and pre-exponential factors are summarized in Table 23.

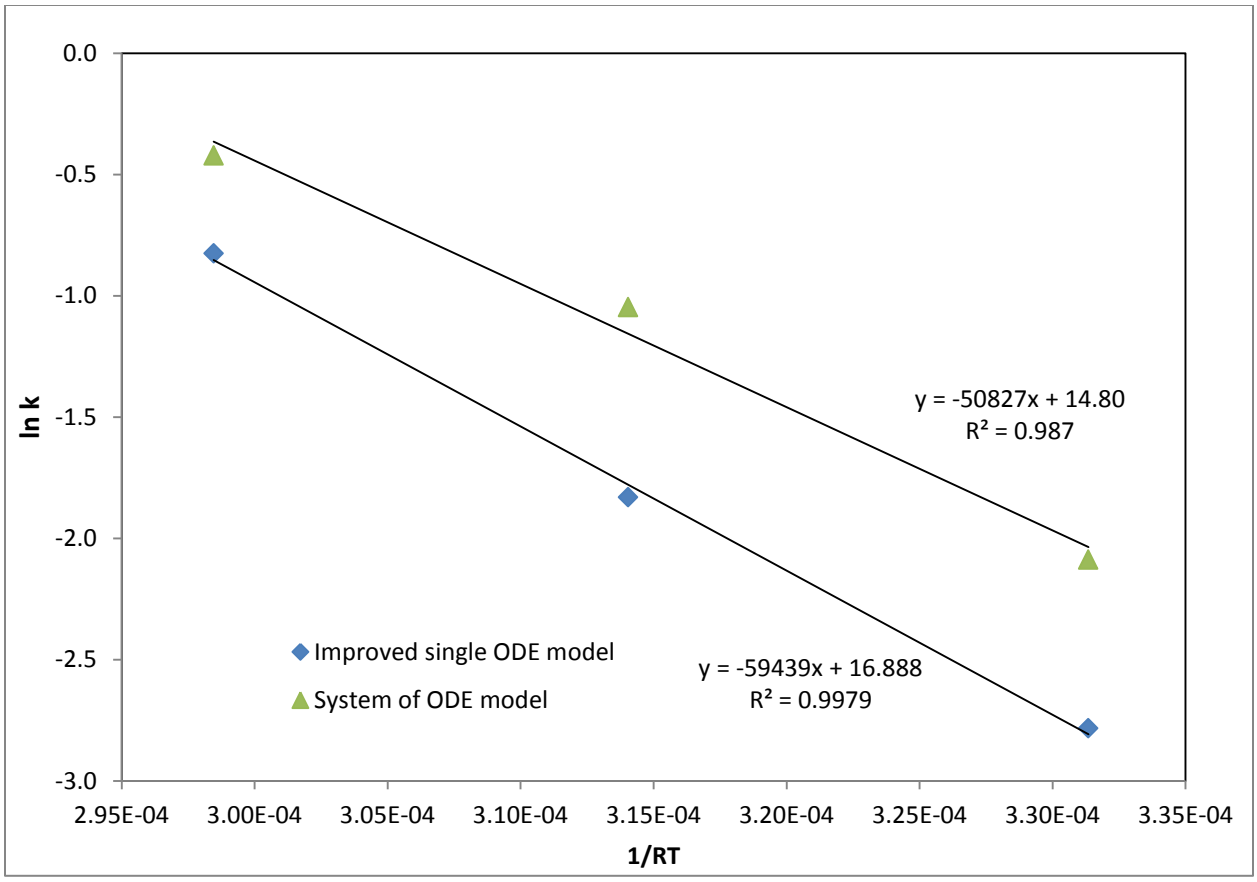

Figure 68: Activation energy for oxygen delignification

Table 23: Results of activation energy and pre-exponential factor for oxygen delignification

Model	k_{L90}	k_{L110}	k_{L130}	Activated Energy (E_a) (Joules/mol)	Pre-exponential factor A
Improved Single ODE	6.19E-02	1.60E-01	4.38E-01	59439	2.16E07
System of ODEs	1.24E-01	3.51E-01	6.55E-01	50827	2.69E06

The calculated activation energy was good as indicated by the accurate regression (Figure 68). The activation energy for oxygen delignification of wheat straw performed in this research was found to be in the ranges of 51-60 kJ/mol. This finding was similar to previously reported values in other lignocellulosic materials found in the literature (Table 24). This suggested the lignin moieties of wheat straw studied in this research were similar to those in lignocellulosic materials listed in Table 24. However, the activation energies for wheat straw delignification found in this study were substantially lower than those reported by Abdul-Karim et al. (1995) and Gonzalo et

al. (2008). The discrepancy may be due to the difference in experimental setup, sampling time and treatment of data.

Table 24: Literature reported values of activation energy in oxygen delignification process

Reference	Lignocellulosic Material	*Ea* (kJ/mol)
Perng [**142**]	Wood pulp	60
Iribane [**128**]	Wood pulp	51
Ji [**125**]	Wood pulp	53
Argawal [**100**]	Wood pulp	107.2
Ma [**143**]	Bamboo	53
Sabatier [**144**]	Bagasse	42.0
Kim [**126**]	Corn stover	50.15-54.12
Abdul-Karim [**145**]	Wheat straw	131.4
Gonzalo Epelde [**88**]	Wheat straw	93-97
Improved single ODE model	Wheat straw	60
System of ODEs model	Wheat straw	51

5.6 Comparison of the Reaction Order

The solved reaction orders with respect to residual lignin (a_1) and hydroxide ion (a_2) for oxygen delignification along with literature values are summarized in Table 25.

Table 25: Literature values of solved kinetic model exponent parameters

Reference	Material	a_1 (exponent for L)	a_2 (exponent for OH^-)
Perng [**142**]	Wood pulp	4.8	0.4
Iribane [**128**]	Wood pulp	2	0.7
Ji [**125**]	Wood pulp	1	0.426
Argawal [**100**]	Wood pulp	7.7	0.92
Ma [**143**]	Bamboo	1.1	0.9
Abdul-Karim [**145**]	Wheat straw	0.82-1.21	-
Kim [**126**]	Corn stover	1.0	-
Gonzalo Epelde [**88**]	Wheat straw	1.0	-
Schmidt [**94**]	Wheat straw	1.0	-
Single ODE model	Wheat straw	1.95	1.18
Improved single ODE model	Wheat straw	0.89	1.30
System of ODEs model	Wheat Straw	0.65	1.75

The estimated reaction order of residual lignin was approximately three times smaller than the reaction order of hydroxide ion. Other researchers had reported reaction order of opposite

trend when compared to the improved single ODE and system of ODEs model. This discrepancy may be due to how the kinetic expression was solved and the consideration of caustic saturation.

Some of the reported reaction orders in Table 25 either assumed first order reaction with respect to residual lignin [**88**,**126**,**145**] or assumed constant hydroxide ion concentration throughout the oxygen delignification process due to excess caustic [**94**]. With these assumptions, the power law kinetic model was often reduced to a single ODE similar to that of Equation 1.6 and 1.7. The results could be misleading as hydroxide ions were being consumed through the reaction; therefore it was not constant and had to be taken into account. The second equation (Equation 5.12) is especially important when delignification was conducted at or below caustic loading 10-12% (Table 26).

Table 26: Caustic loading used by different researchers

Reference	Caustic loading used (% w/w)
Ji [**125**]	2-10
Argawal [**100**]	2.5-3.5
Abdul-Karim [**145**]	10
Schmidt [**94**]	10.8

The result difference of this assumption was shown by the different reaction orders estimated by the improved single ODE (0.89) and system of ODEs model (0.65) with the latter having higher accuracy for the 5 and 10% caustic loadings. Thus, the second equation was required in order to take the changing concentration and consumption rate of hydroxide ion into account. It was confirmed in this study that there was a point where the caustic loading became saturated and the developed equations were unable to model the experimental values at 15% caustic loading. If the kinetic model was solved based on dataset from saturated caustic loading, then the solved model would only be accurate specific to the pretreatment conditions (temperature and caustic loading). A kinetic model solved in this manner might not be able to predict the experimental lignin values as soon as the caustic loading was not in excess. This was proven and shown by the comparison between the reaction orders solved with and without caustic loading being saturated (single ODE and improved single ODE).

6 Aspen Plus Simulation of Oxygen Delignification Pretreatment

Another objective in this study was to develop a simulation of the oxygen delignification pretreatment of wheat straw in a commercial simulation. The simulation program, Aspen Plus V7.3.2, was used to simulate the mass balance of the oxygen delignification pretreatment process. A stoichiometric reactor was used to model the pretreatment reactor in a continuous operation mode. Due to the unknown stoichiometric coefficients of the lignin and carbohydrate reaction with hydroxide ions, the physical properties of all components were modeled as water. This approach allowed the use of the kinetic parameters such as the activation energy, pre-exponential factor and reactant exponents to be entered into Aspen Plus and simulate the pretreatment process. Using Aspen Plus Economic Analyzer, economic analysis was performed and the capital cost was calculated for different pretreatment conditions. Sensitivity analysis was performed on the cost of biomass, caustic (NaOH) and enzyme to explore the effects on the pretreatment cost. All costs were expressed in U.S. dollar.

6.1 Equation Setup for Aspen Plus Simulation

In order to simulate the pretreatment process, the kinetic expression had to include the carbohydrate content of the pretreated substrate. The kinetic expression was resolved based on this assumed reaction:

$$\mathrm{Lig} + \mathrm{Carbo} + \mathrm{OH^-} \rightarrow \mathrm{DLig} + \mathrm{DCarbo} + \mathrm{COH^-} \qquad 6.1$$

Where:

Lig = lignin

Carbo = carbohydrate

OH^- = hydroxide ions

DLig = dissolved lignin

DCarbo = dissolved carbohydrate

COH^- = consumed hydroxide ions

The design equation for continuous process was:

$$\text{In - out} + \text{generation - consumption} = 0 \qquad 6.2$$

The mass balance equations for residual lignin, carbohydrates in the pretreated solid and hydroxide ions were expressed as:

$$C_{i,in} - C_{i,out} - \tau\, r_i = 0 \qquad 6.3$$

Where:

$C_{i,in}$ = concentration of species i going into the reactor (g/l)

$C_{i,out}$ = concentration of species i going out from the reactor (g/l)

τ = residence time (min)

r_i = rate expression of species i (g/l min)

Following the same procedure set out in section 5 along with the JMP dataset, the following rate equations for lignin and carbohydrates were derived for the Aspen Plus simulation:

$$\frac{d[L]}{dt} = -k_L[L]^{a1}[OH^-]^{a2}[Carbo]^{a4} \qquad 6.4$$

$$\frac{d[Carbo]}{dt} = -k_{Carbo}[L]^{a1}[OH^-]^{a2}[Carbo]^{a4} \qquad 6.5$$

The rate equation for hydroxide ions was eliminated by using mass balance substitution (Equation 5.17) and a value of k' = 0.488 (Figure 42).

Next EASY-FIT$^{\text{Model Design}}$ version 5.1 by Professor Klaus Schittkowski was used to solve for the constant and exponent parameters with the following initial guesses and final values (Table 27).

Table 27: Solved parameters for Aspen Plus simulation

Parameter	Initial guesses	Final values
k_{L90}	1.00E-01	4.59E-02
k_{L110}	1.00 E-01	1.19E-01
k_{L130}	1.00 E-01	2.70E-01
$k_{Carbo90}$	1.00E-01	4.10E-02
$k_{Carbo110}$	1.00 E-01	9.68E-02
$k_{Carbo130}$	1.00 E-01	2.84E-01
a_1	1.00	1.02
a_2	2.00	1.29
a_4	1.00	0.00

The activation energy and pre-exponential factor for residual lignin and carbohydrates were also solved Table 28.

Table 28: Activation energy and pre-exponential factor for Aspen Plus simulation

	Activation Energy (J/mol)	Pre-exponential Factor
Residual lignin	53919	2.65E06
Carbohydrates	58697	1.09E07

These parameters (Table 27 and 28) were used in the simulation of the oxygen delignification reaction in Aspen Plus.

6.1.1 Modeling of Enzymatic Hydrolysis Based on Pretreatment Conditions

In order to evaluate the economics of the pretreatment reactor, a unit basis had to be selected. One possible candidate was the carbohydrate content of the substrate after the pretreatment. However, it would be misleading if the pretreatment process were to be analyzed in dollar per carbohydrate basis as this would not reflect the effects the pretreatment condition had on the sugar yield. Since sugar produced after the enzymatic hydrolysis would be used directly for fermentation with subsequent distillation in the bioethanol production, it was more appropriate to use dollar per gram sugar as the unit basis to assess cost of the pretreatment. With this in mind, a model was needed to estimate the sugar yield after enzymatic hydrolysis in order to evaluate the pretreatment cost. A kinetic model for the enzymatic hydrolysis had been developed within our laboratory by Pope (2011) that estimates the sugar yield based on the lignin and carbohydrates content of the substrate [**93**].

The full derivation of this enzymatic hydrolysis kinetic model was based on enzyme absorption theory developed by Zhang et al. (2010), which predicted the product (sugar) concentration based on the initial concentration of enzyme and substrate [**146**]. The enzymatic hydrolysis kinetic model had the form:

$$P = S_0 \left\{ 1 - \left[1 + \frac{K_e E_0}{K_e + E_0} k_d t \right]^{\left(-\frac{k_2}{K_e k_d}\right)} \right\} \qquad 6.6$$

Where:

E_0 = Enzyme (initial enzyme loading)

S_0 = Substrate (initial carbohydrate content in wheat straw)

t = time

P = Product (sugar)

k_e = Equilibrium kinetic constant of the enzyme substrate reaction

k_d = Enzyme deactivation kinetic constant

k_2 = Kinetic constant of the product reaction

Equation 6.6 was modified by Pope et al. (2011) to include the lignin content of the pretreated substrate using a term called the lignin factor [**93**]. This modification was based on the hypothesis that lignin inhibits enzymatic hydrolysis. This reduction in available enzyme would decrease the rate of hydrolysis and the sugar yield. Equation 6.7 was the final equation used to estimate the sugar concentration and yield after the enzymatic hydrolysis in this research. A factor of 1.11 gram sugar per gram carbohydrate was added to account for the addition of water molecule during the hydrolysis. The unknown parameters and units are summarized in Table 29.

$$P = S_0 \left\{ 1 - \left[1 + \frac{K_e(E_0 - L_0 L_F)}{K_e + (E_0 - L_0 L_F)} k_d t \right]^{\left(-\frac{k_2}{K_e k_d}\right)} \right\} 1.11 \qquad 6.7$$

Where:

K_e = equilibrium constant

E_0 = initial concentration of enzyme

k_d = kinetic constant of the enzyme deactivation

t = time

L_0 = initial lignin concentration (solid)

L_F = lignin factor

Table 29: Units for Equation 6.7

Defined variables	Units
P, S_0, E_0, L_0	g/l
t	h
Unknown parameters	
L_F	g enzyme/g lignin
k_e	g/l
k_d	g/(l h)
k_2	1/ h

The enzymatic hydrolysis data (JMP dataset) were used to solve for the unknown parameters in Equation 6.7 by using sum of least squares method with a 48 hour hydrolysis time. The enzymatic hydrolysis model had the final form:

$$P = S_0\left\{1 - \left[1 + \frac{7.3(E_0 - 0.15L_0)}{7.3 + (E_0 - 0.15L_0)}\,2.1t\right]^{(-0.23)}\right\}1.11 \qquad 6.8$$

Enzymatic hydrolysis results with pretreatment condition 110°C and 10% caustic loading was used to validate Equation 6.8. The predicted sugar values were plotted against the experimental sugar values as shown in Figure 69. A R^2 value of 0.99 was obtained between the model and the experimental values, indicating that Equation 6.8 was able to accurately predict the sugar concentration of the enzymatic hydrolysis.

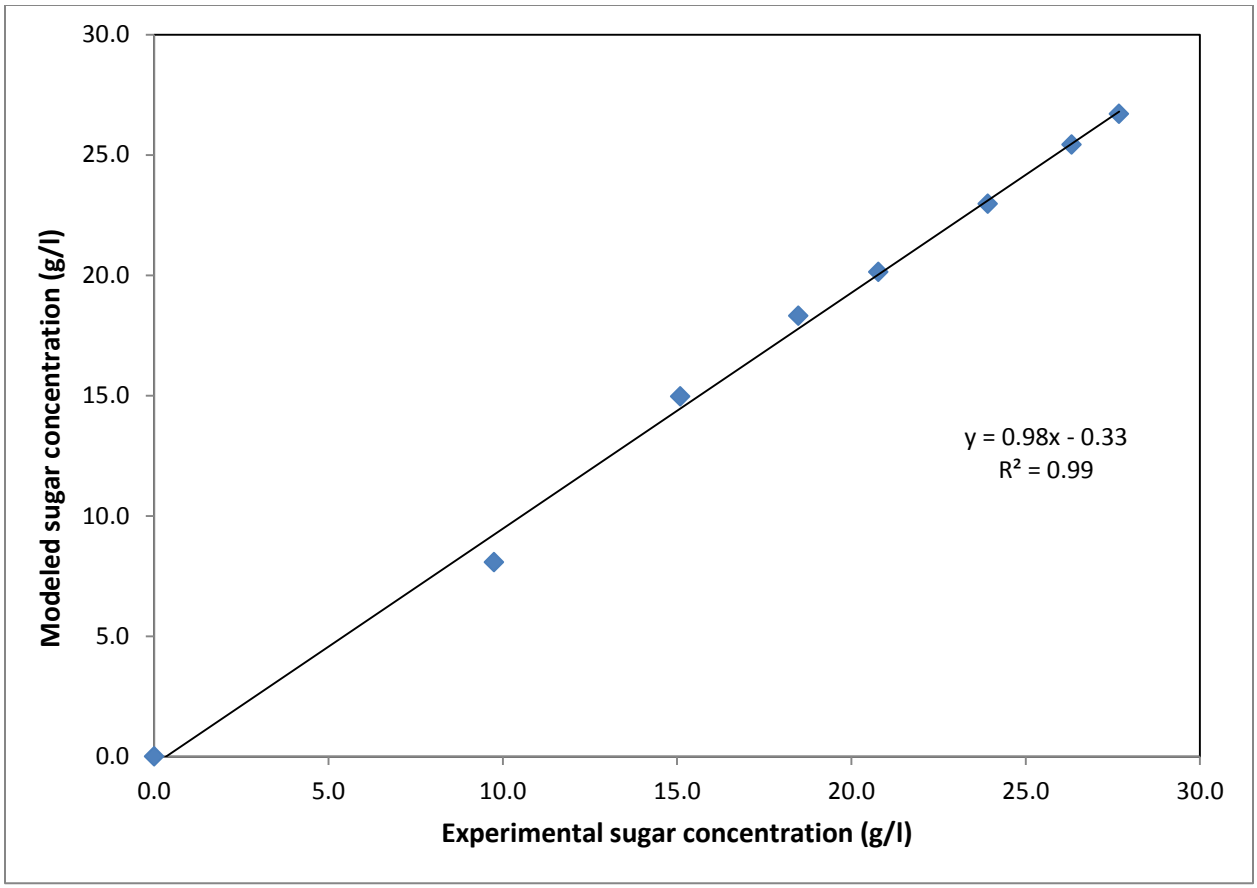

Figure 69: Validation of enzymatic hydrolysis model

6.2 Substrate Composition in Aspen Plus

A screenshot of the simulation setup in Aspen Plus is shown in Figure 70. The substrate composition (based on Table 10) was first defined in stream BIOMASS1 on a dry mass basis as the feed. A moisture content of 15% was assumed for all simulations [**147**,**148**]. The stream MOIST is an imaginary water stream that was used to adjust the substrate moisture content. Depending on BIOMASS1's flow rate, the appropriate flow rate of the MOIST stream was calculated and added into the feed stream using a FORTRAN block. For simulation purposes, all components (except oxygen) were modeled as water and a flow rate of 2200 dry ton/day of biomass was used for all simulations [**148**].

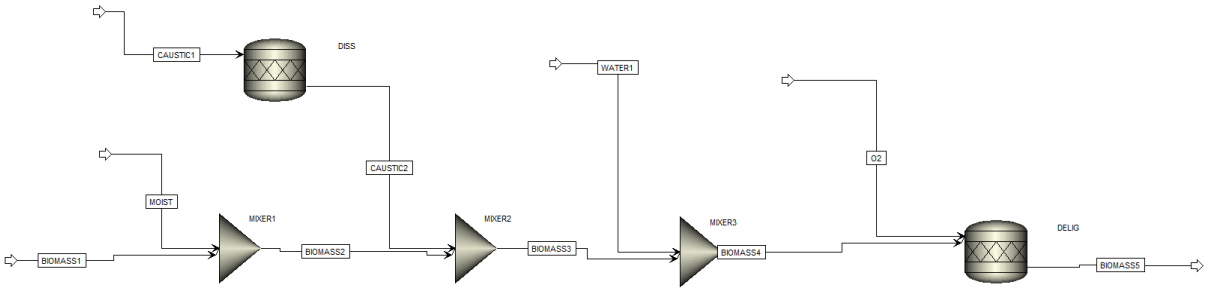

Figure 70: Aspen plus simulation setup

6.3 Simulating the Oxygen Delignification Pretreatment

The oxygen delignification pretreatment was modeled with the stoichiometric reactor DELIG. The operating temperature was specified at the DELIG reactor which was imported into a calculator block along with the flow rates of different components to calculate the out flow of residual lignin, carbohydrates and caustic. Caustic loading ranging from 5-12% was specified in stream CAUSTIC1. The DISS unit was user defined unit that separates NaOH into Na^+ and OH^- ions for mass balance purposes. The desired substrate loading was specified in the stream WATER1 and was added into the stream BIOMASS3. The flow rate of water added in was calculated in a FORTRAN block. A substrate loading of 10% was used for all simulation. The empirically solved kinetic expressions (Equations 6.4 and 6.5), along with parameters from Table 27 and 28 were incorporated into the "Excel Function" in the calculator block. The flow rates of residual lignin, carbohydrates and hydroxide ions after pretreatment were calculated based on each respective component and exported back to the DELIG reactor. The component "other" was assumed to be removed after the pretreatment.

6.4 Economic Analysis

The economic analysis of the pretreatment reactor was divided into two parts: annualization of the capital costs and operating costs of the pretreatment reactor. As mentioned previously, the unit basis for the economic evaluation of the pretreatment reactor was dollar per gram sugar produced. This approach assumed sugar produced would be sold "over the fence" and allowed the determination of pretreatment process condition that would produce the lowest pretreatment cost for bioethanol production.

The capital cost of the pretreatment reactor was calculated using the Aspen Plus Economic Analyzer. First the pretreatment reactor was defined using the Unit Mapping function. The pretreatment reactor was mapped as an enclosed agitator operating at a continuous mode. Stainless steel 316 was used as the material of construction due to the corrosive nature of caustic.

The capital cost of the pretreatment reactor was a function of reactor size and, in turn, was a function of the volumetric flow rate of the feed and residence time. The volumetric flow rate of the feed stream into the reactor was dependent on the specified solid suspension. The reactor's dimensions and the capital cost for 10% substrate loading was calculated at different residence times and the results are summarized in Table 30. The calculated reactor volume included a disengagement height of 1.22 meters. The equipment cost represented the "off the shelf" price of the reactor whereas the total direct cost represented the reactor cost, labor, installation and associated cost related to the reactor. The annualized capital cost was calculated based on a 10 year loan at 8% interest rate. A sample calculation of the annualized cost can be found in

Appendix A. The assumed total direct capital cost of the enzymatic hydrolysis was $ 8,006,772 and the annualized cost was $ 1,193,245 [**148**]. It was possible to adopt this from Humbird et al. (2011) as both simulations used a feed rate of 2200 dry ton biomass per day.

Table 30: Pretreatment reactor capital cost and size with 10% substrate loading

Residence time (min)	Diameter (m)	Vessel height (m)	Capacity (m^3)	Equipment cost ($ million)	Total direct cost ($ million)	Annualized total direct cost ($ million/year)
2	2.29	8.53	35.03	0.42	0.65	0.10
5	3.20	11.28	90.72	0.85	1.14	0.17
10	3.96	13.87	171.02	1.18	1.53	0.23
15	4.57	15.70	257.71	1.76	2.16	0.32
30	5.64	19.66	490.95	2.87	3.37	0.50
60	7.16	24.38	982.57	5.20	5.85	0.87

6.4.1 Operating Cost of the Pretreatment Reactor

The operating cost of the oxygen delignification pretreatment reactor was calculated using the economic analysis tool in Aspen Plus. A base case scenario for the material and utility costs that were associated with the pretreatment reactor were established and summarized in Table 31.

Table 31: Base case scenario for material and utility costs

Material/Utility cost	Value
Biomass ($/ton)	36
Process water ($/kg)	1.3E-05
Caustic soda($/ton)	420
Steam (50 psig) ($/kg)	0.0055
Oxygen ($/kg)	0.103
Lignin income ($/kg)	0.079

The cost of biomass was calculated based on a price of $20 per bale and 1100 lb per bale and it was assumed this cost included price of shipping, handling, size reduction etc. This information was retrieved from the "Straw for Sale Listing" from the government of Alberta's agriculture and rural development [**149**]. The cost of caustic soda (NaOH) was retrieved from ICIS and the price ranged from 420-850 $/ton [**150**]. Pressurized steam was used as the heating utility for the pretreatment reactor and the cost was retrieved from Seider et al. [**151**]. It was assumed that the steam was fully saturated with pressure at 50 psig (446 kPa) with 2121.31 kJ/kgW as the latent heat of vaporization.

The cost of the oxygen delignification pretreatment was calculated with reference to Professor Wilcox [**152**]. The calculation was based on the assumption of commercial arrangement with

Praxair where an onsite oxygen plant is owned and operated by Praxair and the customer pays a fixed monthly facility fee. The capital cost and annualized electricity fee were calculated based on required O_2 flow rate, whereas the annualized facility fee was calculated based on the capital cost. The required O_2 flow rate used was 22 kg O_2/ton biomass [**153**]. Assumptions and the results of the oxygen plant costs are summarized in Table 32 and Table 33 respectively. Sample calculations of the O_2 plant capital cost, annualized facility and electricity can be found in Appendix A.

Table 32: Oxygen plant costs assumptions

Assumption	Costs
Capital cost for 1000 ton/day O_2 plant ($)	27 million
Monthly facility fee (% of capital)	2.75
Power consumption per oxygen flow rate (kWh/m^3)	0.53
Electricity fee ($/kWh)	0.04
Scaling factor	0.6

Table 33: Oxygen feed cost

Costs	
Capital cost based on calculated 53.35 tons O_2/day ($)	4.65 million
Annualized facility fee ($/yr)	1.54 million
Annualized electricity fee ($/yr)	0.28 million
Annual cost of O_2 ($/yr)	1.82 million
Cost of O_2 ($/kg)	0.103

The cost of enzyme was calculated based on the work put forth by Aden et al. (2002). Using a cost of 0.50 $/gallon ethanol [**106**], the cost was back calculated to be 12.08 $/million FPU. An enzyme loading of 20 FPU per gram glucan was used to calculate the enzyme cost. The calculation of the enzyme cost can be found in

Appendix A. Lignin residues recovered after enzymatic hydrolysis were assumed to be combusted to generate electricity. The assumed selling price of electricity was 0.040 $/kWh with 28% efficiency [**154**] and the lignin heating value was 25.4 MJ/kg [**28**].

With these assumptions, the lignin by-product had a credit of 0.079 $/kg and the calculation can be found in

Appendix A. The enzyme cost and lignin credit for each pretreatment condition, in combination with different residence times, were calculated and added to the annualized operating cost. The total cost of different pretreatment conditions was first analyzed with residence time fixed at 60 minutes, with the results summarized in Table 34.

Table 34: Annualized pretreatment cost with 60 minutes residence time

Temperature (°C)	Substrate loading (%)	Caustic loading (%)	¢/lb sugar
90	10	5	26.20
110	10	5	26.47
130	10	5	26.85
90	10	10	27.24
110	10	10	27.62
130	10	10	28.07
90	10	12	28.10
110	10	12	28.53
130	10	12	29.04

It was clear that increasing the severity of the pretreatment conditions increased pretreatment cost. Although higher reaction temperatures increased the sugar yield, the increased yields did not compensate for the increased cost of steam and caustic loading. The pretreatment condition that resulted in lowest cost was found to be 90°C and 5% caustic loading. This "optimum" pretreatment condition was based on the total sugar produced from the enzymatic hydrolysis; however this might not be the global optimum as less severe pretreatment conditions were not tested. After the pretreatment condition was selected, the residence time was varied from 2 to 60 minutes in order to determine reactor size for this pretreatment condition and the results are presented in Table 35.

Table 35: Pretreatment cost to Condition 90°C, 10% substrate loading, 5% caustic loading

Residence time (minutes)	Total cost for pretreatment cost ($ million /yr)	Sugar produced from hydrolysis (million lb/yr)	Pretreatment cost to produce a pound of sugar (¢/lb sugar)
2	160.26	532.20	28.79
5	158.69	556.50	27.42
10	157.71	567.87	26.80
15	157.31	572.45	26.56
30	156.84	577.76	26.30
60	156.76	580.74	26.20

The economics of the pretreatment process improved as the residence time increased. This was due to the decreased enzyme loading with lower carbohydrate content in the pretreated substrate. Based on this evaluation, the pretreatment condition at 90°C and 5% caustic loading with 60 minutes residence time was found to have the lowest pretreatment cost at 26.20 ¢/lb. The cost and revenue for each component that contributed to this pretreatment cost is shown in Figure 71.

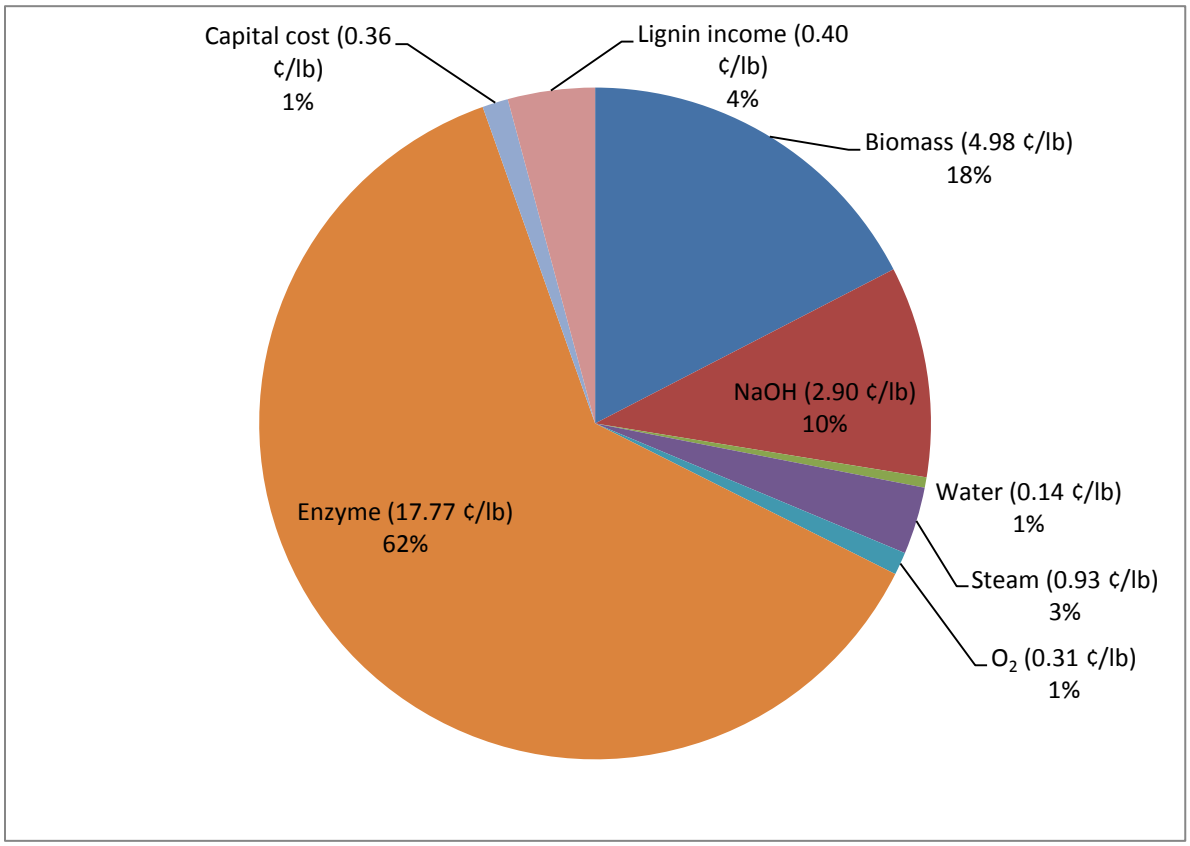

Figure 71: Economic breakdown of pretreatment cost

It was found that the cost of enzyme, biomass and NaOH (caustic) accounted for 90% of the pretreatment cost. These costs were subjected to sensitivity analysis and their effects on the pretreatment cost will be discussed in the section 6.5.

Wyman (1994) had suggested that the pretreatment cost had to be well below 20 ¢/lb in order for the bioethanol to be economically viable. Ruth et al. (2000), Aden et al. (2002) and Humbird et al. (2011) had calculated a pretreatment cost of 3.2 to 11.58 ¢/lb when lignocellulosic biomass was pretreated with dilute acid. The calculated sugar price (26.20 ¢/lb) in this study was at least double those reported in literature and did not meet baseline recommendation set out by Wyman. The calculated pretreatment cost was not economically competitive compared to the literature reported prices. Although the calculated sugar price was higher, the reported literature values in Table 36 assumed an enzyme cost of less than 0.50 $/gal ethanol and a 90% sugar yield during hydrolysis. These assumed values are optimistic compared to the ones used in this study and will be addressed in the sensitivity analysis.

Table 36: Pretreatment cost from literature

Reference	Pretreatment cost (¢/lb)	Method
Wyman (1994) [**155**]	<20	Recommended baseline
Ruth et al. (2000) [**156**]	3.2-7.5	Dilute acid
Aden et al. (2002) [**157**]	5.6-6.4	Dilute acid
Humbird et al. (2011) [**148**]	11.58	Dilute acid

The bulk sugar price was compared in order to determine if the calculated sugar price was competitive if sugar was to be sold “over the fence”. The bulk sugar price had been relatively stable for the last decade; however sugar price had been volatile since 2007 and saw a historical high of 38.12 ¢/lb in 2011 (Figure 72) [**158**]. The calculated pretreatment cost (26.20 ¢/lb) indicated the oxygen delignification pretreatment process was economically viable if sugar from wheat straw were to be produced and sold “over the fence” for bioethanol production.

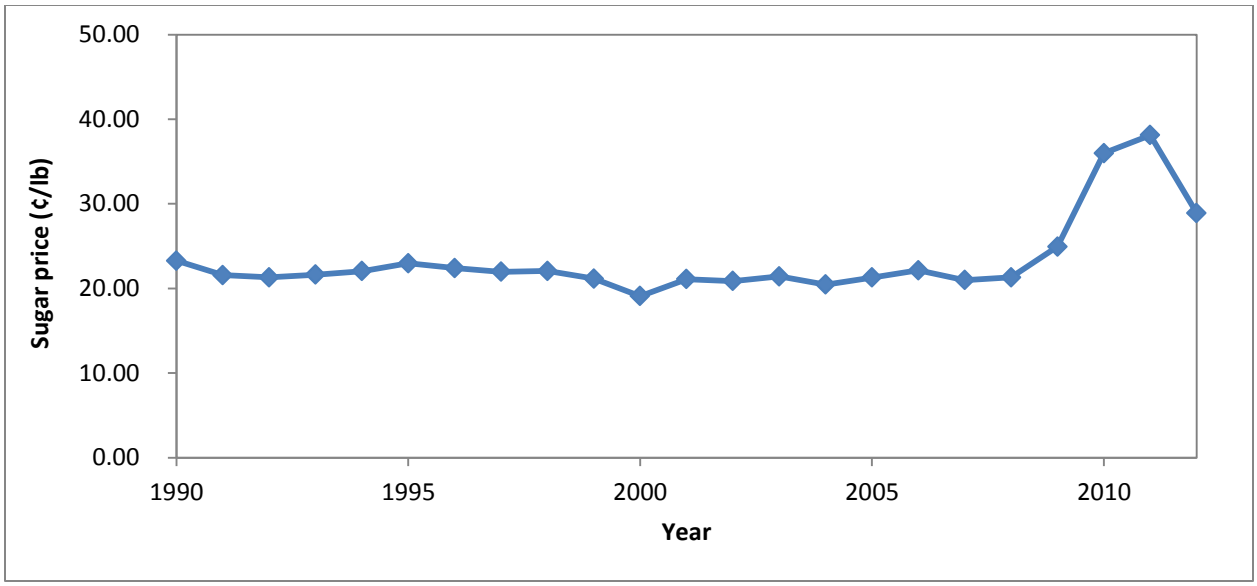

Figure 72: Historical raw sugar price adapted from U.S. Department of Agriculture [158**]**

6.5 Sensitivity Analysis of Biomass, Caustic and Enzyme Cost

A sensitivity analysis was performed on the cost of the biomass feed, the caustic loading and enzyme. This was to evaluate the effect of price fluctuation of the feed stream had on the best pretreatment condition that produced the lowest pretreatment cost (26.20 ¢/lb). The varied ranges for these three parameters are listed in Table 37.

Table 37: Price range of parameter for sensitivity analysis

Parameter	Value
Enzyme ($/million FPU)	2.41, 12.08, 35.52
Biomass feed ($/ton)	20, 40, 60
Caustic ($/ton)	420, 635, 850

The enzyme cost was selected because it contributed the largest (62%) to the total pretreatment cost. The enzyme cost calculated in the base case scenario was based on Novozyme's estimate of 0.50 $/gallon of ethanol produced which corresponded to 12.08 $/million FPU [**106**]. Aden et al. (2002) reported an optimistic enzyme cost of 0.10 $/gallon ethanol while Klein-Marcuschamer et al. (2011) claimed that a more realistic enzyme cost was 1.47 $/gallon ethanol [**157**,**159**]. These selected enzyme costs were used for the sensitivity analysis in order to observe the effects on the cost of pretreatment. The enzyme cost presented in Table 37 corresponded to 0.1, 0.5 and 1.47 dollar per gallon respectively [**106**,**157**,**159**].

Sensitivity analysis was performed on the cost of biomass because it represented the second largest contribution (18%) to the cost of the pretreatment process. A price range between 40-127 $/ton dry mass of lignocellulosic material had been reported in the literature [**148**,**157**,**160**]. The cost of biomass feedstock is likely to fluctuate due to factors such as: location, collection, storage, processing and handling fees [**148**]. Since 36 $/dry ton biomass was used as the cost of biomass feedstock in the base scenario, a price range of 20-60 $/dry ton biomass was used in order to observe the effect of this parameter on the economics of the pretreatment process.

As discussed previously, increasing the caustic loading during pretreatment had a positive effect on sugar yield and ultimately the cost of the pretreatment process. Caustic loading contributed to 18% of the total pretreatment cost in the base case scenario (420 $/ton). With the uncertain price range between 420-850 $/ton of caustic reported by ICIS [**150**], the cost of caustic could significantly affect the economics of the optimized pretreatment condition.

The effect of each parameter had on the best pretreatment condition is shown in Figure 73 and the tabulated data can be found in Appendix B.

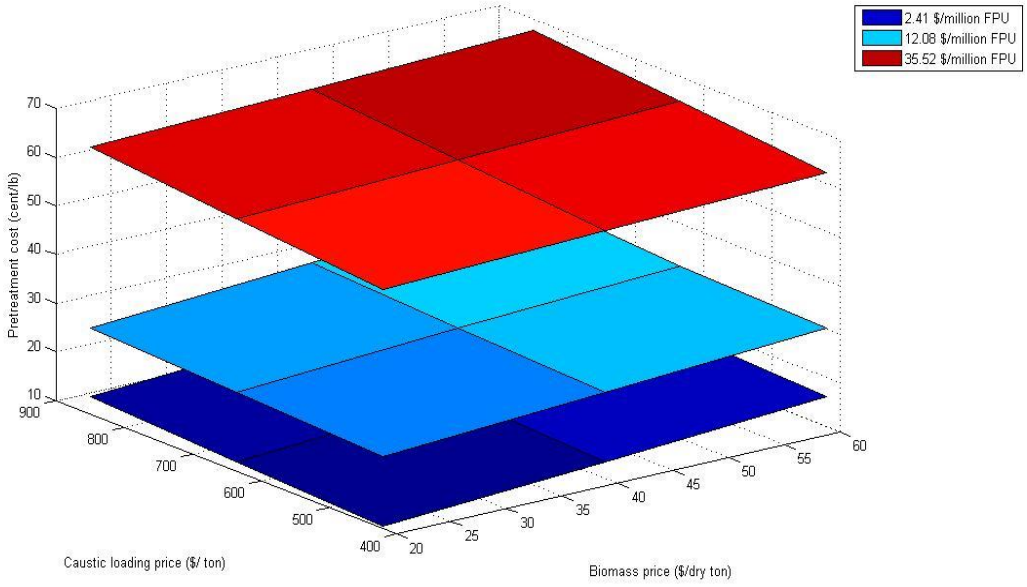

Figure 73: Sensitivity analysis of enzyme cost for pretreatment condition 90°C, 5% caustic loading, 60 minutes residence time

In this sensitivity analysis, it was found that the maximum increase in biomass, caustic and enzyme cost, while the other two parameters were held constant at base case values, increased the pretreatment cost by a maximum of 3.31, 2.98 and 34.5 (¢/lb sugar) respectively over the full range of the tested condition. The sensitivity of each parameter was determined by dividing the change in pretreatment cost by the change in unit price of that parameter while holding the other two constant (Table 38).

Table 38: Sensitivity of biomass, caustic and enzyme cost on pretreatment cost

Sensitivity parameter	Value	Unit
Biomass	0.138	(¢/lb sugar)/($/dry ton biomass)
Caustic	6.93×10^{-3}	(¢/lb sugar)/($/ton caustic)
Enzyme	1.47	(¢/lb sugar)/($/million FPU)

It was observed that the change in the enzyme cost had the most significant impact on the pretreatment cost. The biomass and caustic cost had at least ten times lower impact compared to enzyme cost.

The enzyme cost was investigated further to determine how dominating the enzyme cost was to the pretreatment cost. This was done by setting the lower and higher end of the cost for biomass (20 and 60 $/dry ton) and caustic (420 and 850 $/ton) while varying the cost of enzyme. Through this analysis the cost of enzyme was found to be crucial to the economics of the pretreatment process (Table 39). The pretreatment cost was dominated by the enzyme cost (from 19.5 to 89.4% of the pretreatment cost). Thus, in order for the oxygen delignification process to be economically viable as a pretreatment for bioethanol production, the enzyme cost must be as low as possible [**157**].

Table 39: Effect of enzyme cost on total pretreatment cost

Enzyme cost ($/gallon ethanol	Enzyme cost ($/million FPU)	Pretreatment cost (¢/lb sugar)	Percentage of pretreatment cost (%)	Pretreatment cost (¢/lb sugar)	Percentage of pretreatment cost (%)
		Biomass cost: 20 $/dry ton Caustic cost: 420 $/ton		Biomass cost: 60 $/dry ton Caustic cost: 850 $/ton	
0.10 [**157**]	2.41	9.76	36.4	18.2	19.5
0.50 [**106**]	12.08	24.0	74.1	32.5	54.7

1.47 [**159**]	35.52	58.5	89.4	67.0	78.0

Due to the significant role of enzyme cost played in the pretreatment cost, a sensitivity analysis was also performed on the yield of enzymatic hydrolysis. A fixed pretreatment condition 90°C, 5% caustic loading and 60 minutes residence time was used for this analysis. The sugar hydrolysis yield was varied from 10-90% and an exponential relationship between the sugar yield and cost of pretreatment was observed. Increasing the sugar yield from 20% (untreated wheat straw) to 60-70% was able to decrease (66.7-71.4%) the pretreatment cost significantly (Figure 74). This demonstrated that high hydrolysis yield was also essential to the economics of the pretreatment process.

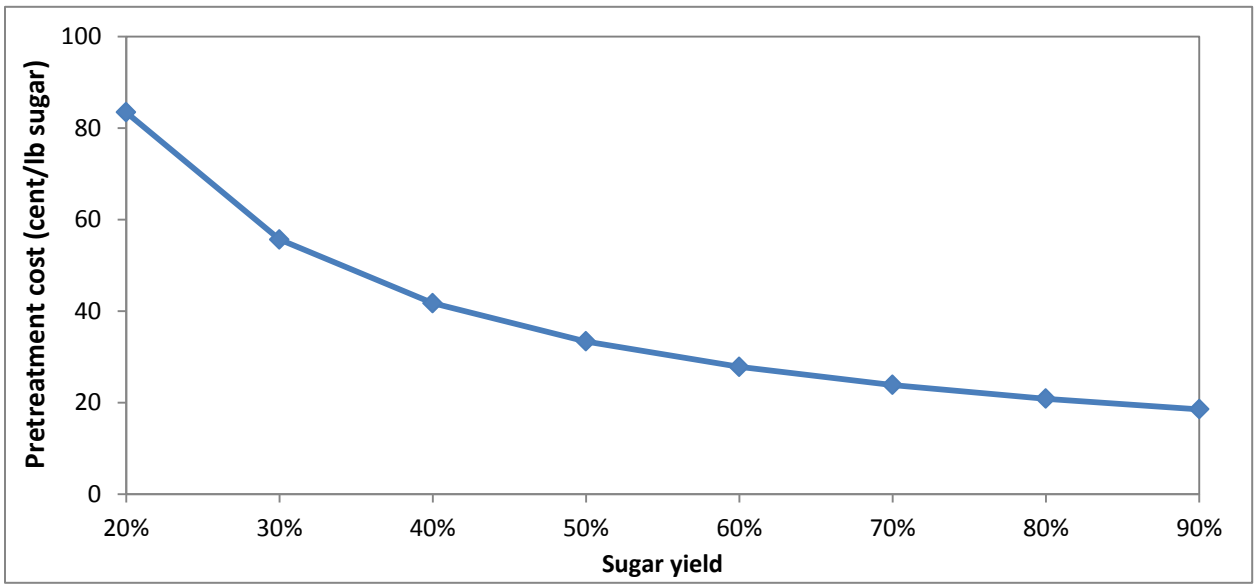

Figure 74: Effect of sugar yield on pretreatment cost for condition 90°C, 5% caustic loading, 60 minutes residence time

From this sensitivity analysis, it showed that an increased cost in the biomass, caustic or enzyme would definitely lower the economic viability of the oxygen delignification process. Compared to the cost of biomass and caustic, the cost of enzyme was found to be at least ten times more important to the cost of pretreatment. The need for pretreatment was further reinforced with the observed exponential relationship found between the cost of pretreatment and sugar yield. The cost of enzyme has shown its dominance and was the parameter that has the most significant effect on the cost of pretreatment.

7 Conclusions

During oxygen delignification of wheat straw, a decrease in the pretreated substrate lignin content was observed when the operating temperature (90-130°C), caustic loading (5-15%) and reaction time (2.5-60 minutes) were increased. Increasing the substrate loading from 2 to 4 % w/w did not have any major effect on the observed delignification. Of all the operating parameters, caustic loading was found to be the most significant in solubilization of lignin. Approximately 39.8 to 82.4% of lignin was solubilized after 60 minutes of reaction for the full range of pretreatment conditions. The most severe pretreatment condition (130°C, 15% caustic loading, 2% substrate loading) produced substrate with the highest carbohydrate and lowest lignin content (80.1% and 6.5 % respectively). The pretreatment condition with the highest sugar yield (85.0%) was 110°C, 15% caustic loading and 2% substrate loading.

Carbohydrate degradation is inevitable during oxygen delignification as radicals and hydroxide ions attack lignin and carbohydrate indiscriminately. Analysis of the pretreated liquor had shown that carbohydrate recovery was between 66.5-83.3% over the full range of pretreatment conditions. Further analysis revealed that the lower carbohydrate recovery was due to longer reaction time (60 minutes) compared to the literature (10-15 minutes). The operating parameter that affected the recovery of carbohydrates the most was caustic loading.

It was observed that the rate of delignification was separated into two distinct reacting phases (fast and slow). The rate of delignification was at its highest in the first 10 minutes of the reaction and approached zero after 10 minutes of reaction over the full range of pretreatment conditions. Increasing both temperature and caustic loading increased the rate of delignification in the first 10 minutes of the reaction. It was also observed that the caustic loading had the biggest effect on the rate of delignification.

The kinetics of the oxygen delignification was studied and a general power law model was developed to predict the lignin content of the pretreated substrate. The empirical kinetic model was solved in two ways: using a single ODE and system of ODEs. The major difference between the two approaches was that the single ODE approach assumed constant hydroxide ion

consumption while the system of ODEs method did not. In the single ODE approach, the kinetic model was expressed by Equation 5.18.

$$\frac{d[L]}{dt} = -k_L[L]^{a_1}(k'([L] - [L_0]) + [OH_0^-])^{a_2}$$

Where:

k_L = kinetic constant for lignin

k' = k_{OH}/k_L

L = lignin concentration (solid) (g/l)

$L_{0\,=}$ Initial lignin concentration (solid) (g/l)

OH^-_0 = Initial hydroxide ion concentration (g/l)

a_1 = exponent for lignin concentration

a_2 = exponent for hydroxide concentration

The system of ODEs approach was to solve the rate equation of delignification and hydroxide ion consumption simultaneously. The kinetic model for this approach was expressed by Equation 5.11 and 5.12.

$$\frac{d[L]}{dt} = -k_L[L]^{a_1}[OH^-]^{a_2}$$

$$\frac{d[OH^-]}{dt} = -k_{OH}[L]^{a_1}[OH^-]^{a_2}$$

Where:

k_L = kinetic constant for lignin

k_{OH} = kinetic constant for hydroxide ion

L = lignin concentration (solid) (g/l)

OH^- = hydroxide ion concentration (g/l)

a_1 = exponent for lignin

a_2 = exponent for hydroxide ion

The unknown parameters were solved by fitting the model equations by using the program EASY-FIT[Model Design]. The reaction orders for lignin and hydroxide ion were 0.89 and 1.30 for single

ODE, 0.65 and 1.75 for system of ODEs respectively. The activation energy for delignification was found to be 60 and 51 kJ/mol for single ODE and system of ODEs respectively. The maximum error for the single and system of ODEs approach were 15.0 and 11.4% respectively. The delignification models had satisfactory results (±20%) in predicting the experimental results for 5 and 10%, but not for 15%, caustic loading.

Both models were validated with pretreatment condition at 90°C, 7.5% caustic loading and 4% substrate loading. Overall, the system of ODEs approach showed more accurate prediction of experimental data compared to single ODE approach. This improvement was believed to be due to incorporation of changing concentration and rate of consumption of hydroxide ions.

The single ODE model showed a poor fit when caustic loading was at 15% which led to the theory of possible caustic saturation. This assumption stemmed from the observed "diminishing" effects of delignification, enzymatic hydrolysis, carbohydrate recovery and delignification rate when the caustic loading was 15% or greater. It was found that the lignin content in the substrate after delignification at 15% caustic was similar to that after delignification with 17.5% caustic loading. After further testing, it was determined that the saturation point for caustic loading for the delignification of wheat straw was between 10-12%. The theory of caustic saturation helped explain the observed diminishing effects and why the developed kinetic model did not fit well at 15% caustic loading. It was also demonstrated that the predicted kinetic parameters would be different if data from excess caustic loading conditions were excluded. Amongst all the operating parameters, the caustic loading had the greatest effect on the pretreatment performance.

The kinetic model was incorporated into Aspen Plus to simulate the oxygen delignification pretreatment process of wheat straw. Utilizing the economic analysis tool in Aspen Plus, the pretreatment cost was evaluated based on the production of sugar produced after the enzymatic hydrolysis. Based on 60 minutes of residence time, it was found that the pretreatment condition that produced the lowest pretreatment cost (26.20 ¢/lb) was at 90°C and 5% caustic loading. Increasing the severity of the pretreatment conditions increased the sugar production however it did not overcome the increased cost of steam (form 90 to 130°C) and caustic loading (5-12%).

The residence time was varied and the residence time and reactor size that produced the lowest pretreatment cost was found to be at 60 minutes and 982.57 m^3 respectively. It was also found that the pretreatment cost decreased with increasing residence time from 2 to 60 minutes. Based on the best pretreatment condition, the cost of enzyme, biomass and caustic contributed 90% (62, 18 and 10% respectively) of the total pretreatment cost. This led to a sensitivity analysis on the cost of these parameters.

In the sensitivity analysis, the cost of enzyme, biomass and caustic were varied. It was observed that the pretreatment cost was at least ten times more sensitive to the enzyme cost when compared to the cost of biomass and caustic. It was important to have high sugar yield during the enzymatic hydrolysis as an exponential relationship between sugar yield and pretreatment cost was observed. This further reinforced the need of pretreatment as it enhances sugar yield during enzymatic hydrolysis. The sensitivity analysis demonstrated that the cost of enzyme dominated the cost of pretreatment and the cost had to be at least as low as 0.1 $/gallon ethanol in order for the process to be economically viable.

8 Future Work

Different modeling approaches were deployed into obtaining the kinetics of oxygen delignification. The values of the solved kinetic parameters were different depending on the dataset used.

Excess caustic concentration has to be taken into account when developing the kinetic model. The assumption of the caustic term being combined with the kinetic constant when it is in excess will lead to erroneous results if the kinetic model is not modified. Further experiments can be done to pin point the exact caustic saturation point. The kinetic parameters are also highly dependent on the sampling time. Shorter sampling intervals are highly desirable, especially in the first 10 to 15 minutes of the delignification, where the delignification reaction is fast and highly nonlinear. A more thorough study on the kinetics of the solubilization of carbohydrates should be performed. Also, if components such as the oligomers in the pretreated liquor can be quantified in real time, a more accurate and complete kinetic model can be developed. This will not only offer improvements on prediction of oxygen delignification, but it can also give a more accurate simulation in Aspen Plus for better economic estimation.

The carbohydrates are converted into assorted sugar oligomers, monomers and hydrolysis inhibitors (such as furans and carboxylic acid) in the pretreated liquor during the pretreatment process [**98**,**161**]. The oligomers and monomers can be potentially recovered from the liquor to further increase the sugar production should be examined. The effect of, or potential to replace a portion of the buffer solution during enzymatic hydrolysis with the oligomer-rich liquor (with or without inhibitor removal) to enhance sugar production should also be explored.

The primary advantage of bioethanol production through enzymatic hydrolysis for it to be renewable and sustainable; however commercialization is not viable if enzyme is too expensive. The cost of enzyme has been demonstrated to be the dominating factor in the economics of the process. The effect of optimizing the enzyme loading on the pretreatment cost should be explored. The activity of enzyme through the course of hydrolysis could also be examined as this will determine the optimal enzymatic hydrolysis time and loading. Ultimately, the enzyme

"cocktail" formula can also be modified as some research has shown enhanced hydrolysis yield results with the addition of xylanase [**113**].

Recovery of several key components should be considered to improve the economics of the pretreatment process. First, heat and energy integration should be considered as heat recovered throughout the process can be used to lower the cost of the steam utility for the pretreatment. Given the high price range of caustic, the recovery of caustic from pretreated liquor has great potential to further improve the process economics. Finally, a cost effective way to recover and reuse enzyme should be examined and researched thoroughly as a minor percentage cost reduction from enzyme could greatly improve the economic viability of bioethanol production.

Bibliography

[1] S.N. Naik, V. V. Goud, P. K. Rout, and A. K. Dalai, "Production of First and Second Generation Biofuels: A Comprehensive Review," *Renewable and Sustainable Energy Reviews*, vol. 14, no. 2, pp. 578-597, February 2010.

[2] B. Kamm, P. R. Gruber, and M. Kamm, *Biorefinery Industrial Processes and Products: Status Quo and Future Direction*. Weinheim: Wiley-VCH Verlag GmbH, 2006.

[3] BP, "BP Statistical Review of World Energy June 2009," 2009.

[4] Central Intelligence Agency, "The World Factbook," 2008.

[5] O. J. Sanchez and C. A. Cardona, "Trends in Biotechnological Production of Fuel Ethanol from Different Feedstocks," *Bioresource Technology*, vol. 99, no. 13, pp. 5270-5295, September 2008.

[6] J. T. Houghton et al., "IPCC 2001: Clmite Change 2001: The Scientific Basis. Contribution of Working Group I to the Thrid Assessment Report of the Intergovernmental Panel on Climate Change," *Cambridge University Press, Cambridge, United Kingdom and New York, NY, USA*, pp. 1-881, 2001.

[7] U.S. Energy Information Administration, "Petroleum Marketing Monthly," U.S. Department of Energy, Washington, 2012.

[8] N. Momayezi and R. B. Rosenburg, "Oil, the Middle East and U.S. Naional Security," *International Journal of Humanities and Social Science*, vol. 1, no. 10, pp. 1-7, August 2011.

[9] P. Dwivedi, L. Pankaj, and J. R. R. Alavalapati, "Cellulosic Ethanol Production in the United States: Conversion Technologies, Current Production Status, Economics, and Emerging Developments," *Energy for Sustainable Development*, vol. 13, no. 3, pp. 174-182, September 2009.

[10] Energy Information Administration. (2008) State Carbon dioxide Emissions: By Energy Sectors. [Online]. http://www.eia.doe.gov/environment

[11] K. T. Tan, K. T. Lee, and A. R. Mohamed, "Role of Energy Policy in Renewable Energy Accomplishment: The Case of Second-Generation Bioethanol," *Energy Policy*, vol. 36, no. 9, pp. 3360-3365, September 2008.

[12] R. E.H. Sims, W. Mabee, J. N. Saddler, and M. Taylor, "An Overview of Second Generation

Biofuel Technologies," *Bioresource Technology*, vol. 101, no. 6, pp. 1570-1580, 2010.

[13] Y. Sun and J. Cheng, "Hydrolysis of Lignocellulosic Materials for Ethanol Production: A Review," *Bioresource Technology*, vol. 83, no. 1, pp. 1-11, May 2002.

[14] T. Hatton, "Canada's Wood Residues: A Profiel of Current Surplus and Regional Concentrations," Canadian Forest Service, Prepared for the National Climate Change Process, Forest Sector Tabble 1999.

[15] K. M. Draude, C. B. Kurniawan, and S. J. B. Duff, "Effect of Oxygen Delignification on the Rate and Extent of Enzymatic Hydrolysis of Lignocellulosic Material," *Bioresources Technology*, vol. 79, no. 2, pp. 113-120, September 2001.

[16] C. W. Hall and O. Kitani, *Biomass Handbook*, C. W. Hall and O. Kitani, Eds. New York: Gordon and BreakScience Publishers, 1989.

[17] C. E. Wyman, "Ethanol Production From Lignocellulosic Biomass: Overview," in *Handbook on Bioethanol: Production and Utilization*, C. E. Wyman, Ed. Washington: Taylor & Francis, 1996.

[18] A. Wingren, M. Galbe, and G. Zacchi, "Energy Considerations for a SSF-Based Softwood Ethanol Plant," *Bioresources Technology*, vol. 99, no. 7, pp. 2121-2131, May 2008.

[19] "Accelerating Industry Innovation 2012 Ethanol Industry Outlook," Renewable Fules Association, 2012.

[20] M. Wang, C. Saricks, and D. Santini, "Effects of Fuel Ethanol use on Fuel-Cycle Energy and Greenhous Gas Emissions," Argonne National Laboratory, Argonne, IL, 1999.

[21] IEA, "Medium Term Oil-Market Report," International Energy Agency, IEA/OECD, Paris, 2009.

[22] P. Alvira, E. Tomax-Pejo, M. Ballesteros, and M. J. Negro, "Pretreatment Technologies for an Efficient Bioethanol Production Process Based on Enzymatic Hydrolysis: A Review," *Bioresource Technology*, vol. 101, no. 13, pp. 4851-4861, July 2010.

[23] H. J. Huang, S. Ramaswamy, U. W. Tschirner, and B. V. Ramarao, "A Review of Separation Technologies in Current and Future Biorefineries," *Separation and Purification Technology*, vol. 62, no. 1, pp. 1-21, August 2008.

[24] D. Michell, A Note on Rising Food Prices, 2008.

[25] D. Pimentael and T. W. Patzek, "Ethanol Production Using Corn, Switchgrass, and Wood; Biodiesel Production Using Soybean and Sunflower," *Natural Resource Research*, vol. 14, no. 1, pp. 65-76, March 2005.

[26] L. Luo, E. Voet, and G. Huppes, "Life Cycle Assessment and Life Cycle Costing of Bioethanol From Sugarcane in Brazil," *Renewable and Sustainable Energy Reviews*, vol. 13, no. 6-7, pp. 1613-1619, August 2009.

[27] L. Ryan, F. Convery, and S. Ferreira, "Stimulating the Use of Biofuels in the European Union: Implications for Climate Change Policy," *Energy Policy*, vol. 34, no. 17, pp. 3184-3194, July 2006.

[28] S. Banerjee et al., "Commercializing Lignocellulosic Bioethanol: Technology Bottlenecks and Possible Remedies," *Biofuels, Bioproducts & Biorefining*, vol. 4, no. 1, pp. 77-93, January 2010.

[29] A. E. Farrell et al., "Ethanol Can Contribute To Energy and Environmental Goals," *Science*, vol. 311, pp. 506-508, January 2006.

[30] M. Pualy and K. Keegstra, "Cell-Wall Carbohydrates and Their Modification as a Resource for Biofuels," *Plant Journal*, vol. 54, no. 4, pp. 559-568, May 2008.

[31] K. Stamatelatou, G. Antonopoulou, I, Ntaikou, and G. Lyberatos, "The Effect of Physical, Chemical and Biological Pretreatments of Biomass on its Anaerobic Digestibility and Biogas Production," in *Biogas Production: Pretreatment Methods in Anaerobic Digestion*, A. Mudhoo, Ed.: John Wiley & Sons, Inc., 2012, pp. 55-90.

[32] N. Moiser et al., "Features of Promising Technologies for Pretreatment of Lignocellulosic Biomass," *Bioresource Technology*, vol. 96, no. 6, pp. 673-686, April 2005.

[33] H. Inoue, S. Yano, T. Endo, T. Sakai, and S. Sawayama, "Combining Hot-Compressed Water and Ball Milling Pretreatments to Improve the Efficiency of the Enzymatic Hydrolysis of Eucalyptus," *Biotechnology for Biofuels*, vol. 1, no. 1, April 2008.

[34] V. Putsche and D. Sandor, "Strateic, Economic, and Environmental Issues for Transporation Fuels," in *Handbook on Bioethanol: Production and Utilization*, C. E. Wyman, Ed. Washington: Taylor & Francis, 1996.

[35] L. Olm and A. Tedder, "The Kinetics of Oxygen Bleaching," *TAPPI Journal*, vol. 62, no. 12, pp. 43-46, 1979.

[36] M. Von Sivers and G. Zacchi, "Ethanol From Lignocellulosics: A Review of the Economy," *Bioresource Technology*, vol. 56, no. 2, pp. 131-140, May 1996.

[37] W. T. Mckean and R. S. Jacbos, "Wheat Straw as a Paper Fiber Source," Clean Washington Center, Seattle, 1997.

[38] P. Kumar, D. M. Barrett, M. J. Delwihe, and P. Stroeve, "Methods for Pretreatment of Lignocellulosic Biomass for Efficient Hydrolysis and Biofuel Production," *Industrial Engineering Chemistry Research*, vol. 48, no. 8, pp. 3713-3729, March 2009.

[39] S. H. Ali, S. M. Asghar, and A. U. Shabbir, "Neutral Sulphite Pulping of Wheat Straw," , Atlanta, GA, 1991.

[40] S. I. Aronovsky, A. J. Ernst, H. M. Stucliffe, and G. H. Nelson, "Agricultural Residue Pulps Comparison of Pulping Processes," *Paper Trade Journal*, vol. 126, no. 26, p. 78, June 1948.

[41] R. Mohan, R. Prasad, R. Yadav, K. K. Ray, and N. J. Rao, "Pulping Studies of Wheat Straw Using Soda and Soda-Anthraquinone Processes," , vol. Beijing, Beijing, 1988, p. 339.

[42] B. Utne and L. Hegbom, "Microscopy Studies of Wheat Straw and Rice Straw as Raw Materials for the Pulp and Paper Industry," , Beijing, 1992.

[43] K. D. Misra, "Cereal Straw," in *Pulp and Paper Manufacture: Secondary Fibers and Non-Wood Fibers*, TAPPI Press, Ed. Atlanta: F. Hamilton and B. Leopold, 1987.

[44] M. Petersen, J. Larsen, and M. H. Thomsen, "Optimization of Hydrothermal Pretreatment of Wheat Straw for Production of Bioethanol at Low Water Consumption Without Addition of Chemicals," *Biomass Bioenergy*, vol. 33, no. 5, pp. 834-840, 2009.

[45] (2013) Iogen Corporation. [Online]. http://www.iogen.ca/company/demo_plant/

[46] Kris Bevill. (2001, Septembeer) Ethanol Producer Magazine. [Online]. http://ethanolproducer.com/articles/8176/abengoa-begins-building-23-mmgy-cellulosic-ethanol-plant

[47] (2012, July) Environment News Service. [Online]. http://www.ens-newswire.com/ens/jul2012/2012-07-26-01.html

[48] Lisa Gibson. (2009, November) Biomass Magazine. [Online]. http://www.biomassmagazine.com/articles/3251/bioethanol-plant-in-denmark-inaugurated/

[49] P. Albersheim, A. Darvill, K. Roberts, R. Sederoff, and A. Staehelin, *Plant Cell Walls From Chemistry to Biology*, Peter Albersheim, Ed. New York: Garland Science, Taylor & Francis Group, LLC, 2011.

[50] Z. Jin, K. S. Katsumata, T. B. Lam, and K. Iiyama, "Covalent Linkages Between Cellulose and Lignin in Cell Wall of Coniferous and Nonconiferious Woods," *Biopolymers*, vol. 83, no. 2, pp. 103-110, October 2006.

[51] M. Galbe and G. Zacchi, "Pretreatment of Lignocellulosic Materials for Efficient Bioethanol Production," *Advances in Biochemical EngineeringéBiotechnology*, vol. 108, pp. 41-65, 2007.

[52] P. Harsen, W. Huijgen, L. Bermudez, and R. Bakker, "Literature Review of Physical and Chemical Pretreatment Processes for Lignocellulosic Biomass," Wageningen UR Food & Biobased Research, 2010.

[53] V. Arantes and J. N. Saddler, "Access to Cellulose Limits the Efficiency of Enzymatic Hydrolysis: The Role of Amorphogensis," *Biotechnology for Biofuel*, vol. 3, no. 1, February 2010.

[54] R. F. Brown, F. K. Agbogbo, and M. T. Holtzapple, "Comparison Mechanistic Models in the Initial Rate Enzymatic Hydrolysis of AFEX-Treated Wheat Straw," *Biotechnology for Biofuels*, vol. 3, no. 1, March 2010.

[55] R. Malcolm JR. Brown, "Cellulose Structure and Biosynthesis: What is in Store for the 21st Century?," *Journal of Polymer Science*, vol. 42, no. 3, pp. 487-495, February 2004.

[56] J. S. Brigham, W. S. Adney, and M. E. Himmel, "Hemicellulases: Diversity and Application," in *Handbook on Bioethanol*, Charles Wyman, Ed. Washington: Tyalor & Francis, 1996.

[57] J. Chen, W. Zhang, T. Li, T. Wang, and G. He, "Optimization of Metabolic Pathways for Bioconversion of Lignocellulose to Ethanol Through Genetic Engineering," *Biotechnology Advances*, vol. 27, no. 5, pp. 593-598, September 2009.

[58] H. Palonen, "Role of Lignin in the Enzymatic Hydrolysis of Lignocellulose," *Espo 2004. VTT*

Publications 520, 2004.

[59] J. Ruffel, "Pretreatment and Hydrolysis of Recovered Fiber for Ethanol Production," UBC, Master Thesis, 2008.

[60] A. Wiselogel, S. Tyson, and D. Johnson, "Biomass Feedstock Resources and Composition," in *Handbook on Bioethanol: Production and Utilization*, C. E. Wyman, Ed. Washington: Taylor & Francis, 1996.

[61] G. P. Philippidis, "Cellulose Bioconversion Technlogy," in *Handbook on bioethanol: Production and Utilization*, Charles Wyman, Ed. Washington: Taylor & Francis, 1996.

[62] S. K. Picataggio and M. Zhang, "Biocatalyst Development for Bioethanol Prodcution from Hydrolysates," in *Handbook on Bioethanol: Production and Utilization*, C. E. Wyman, Ed. Washington: Taylor & Francis, 1996.

[63] I. Tanczos, C. Schwarzinger, H. Schmidt, and J. Balla, "THM-GC/MS Analysis of Model Uronic Acids of Pectin and Hemicelluloses," *Journal of Analytical and Applied Pyrolysis*, vol. 68-69, pp. 151-162, August 2003.

[64] R. Sun, J. M. Lawther, and W. B. Banks, "A Tentative Chemical Structure of Wheat Straw Lignin," *Industrial Crops and Products*, vol. 6, no. 1, pp. 1-8, February 1997.

[65] J. S. Han and J. S. Rowell, "Chemical Composition of Fibers," in *Paper and Composites from Agro-Based Resources*, R. M. Rowell, R. A. Young, and J. Rowell, Eds. Madison: CRC Press, 1996.

[66] G. Lissens, H. Klinke, W. Verstratete, B. Ahring, and A. B. Thomsen, "Wet Oxidation Treatment of Organic Household Waste Enriched with Wheat Straw for Simultaneous Saccharification and Fermentation into Ethanol," *Environmental Technology*, vol. 25, no. 6, pp. 647-655, June 2004.

[67] S. I. Mussatto, M. Fernandes, and I. C. Roberto, "Lignin Recovery From Brewer's Spent Grain Black Liquor," *Carbohydrate Polymers*, vol. 70, no. 2, pp. 218-223, September 2007.

[68] L. R. Lynd et al., "How Biotech can Transform Biofuels," *Nature Biotechnolgy*, vol. 26, pp. 169-172, 2008.

[69] H. Hatakeyama and T. Hatakeyama, "Lignin Structure, Properties, and Applications," *Advance Polymer in Science*, vol. 232, pp. 1-63, 2010.

[70] B. Yang and C. E. Wyman, "Pretreatment: the Key to Unlocking Low-Cost Cellulosic Ethanol," *Biofuels Bioproducts & Biorefining*, vol. 2, no. 1, pp. 26-40, 2008.

[71] B. Bals, C. Rogers, M. Jin, V. Balan, and B. Dale, "Evaluation of Ammonia Fibre Expansion (AFEX) Pretreatment for Enzymatic Hydrolysis of Switchgrass Harvested in Different Seasons and Locations," *Biotechnology for Biofuels*, vol. 3, no. 1, January 2010.

[72] Y. Zheng, Z.i Pan, and R. Zhang, "Overview of Biomass Pretreatment for Cellulosic Ethanol Production," *International Journal of Agricultural and Biological Engineering*, vol. 2, no. 3, pp. 51-68, 2009.

[73] G. Banerjee, S. Car, J. S. Scott-Craig, D. Hodge, and J. Walton, "Alkaline Peroxide Pretreatment of Corn Stover: Effects of Biomass, Peroxide, and Enzyme Loading and Composition on Yields of Glucose and Xylose," *Biotechnology for Biofuels*, vol. 4, no. 1, June 2011.

[74] Teh-An Hsu, "Pretreatment of biomass," in *Handbook on Bioethanol*, Charles Wyman, Ed. Washington: Taylor & Francis, 1996.

[75] R. Silverstein, Y. Chen, R. Sharma-Shivappa, M. Boyette, and J. Osborne, "A Comparison of Chemical Pretreatment Methods for Improving Saccharification of Cotton Stalks," *Bioresource Technology*, vol. 98, no. 16, pp. 3000-3011, November 2007.

[76] R. Wooley, M. Ruth, D. Glassner, and J. Sheehan, "Process Design and Costing of Bioethanol Technology: A Tool for Determining the Status and Direction of Research and Development," *Biotechnlogy Progress*, vol. 15, no. 5, pp. 764-803, 1999.

[77] M. W. Lau, C. Gunawan, and B. E. Dale, "The Impacts of Pretreatment on the Fermentability of Pretreated Lignocellulosic Biomass: A Comparative Evaluation Between Ammonia Fiber Expansion and Dilute Acid Pretreatment," *Biotechnology for Biofuels*, vol. 2, no. 1, December 2009.

[78] G. D. McGinnis, W. W. Wilson, and C. E. Mullen, "Biomass Pretreatment With Water and High-Pressure Oxygen. The Wet-Oxidation Process," *Industrial & Engineering Chemistry Product Research and Development*, vol. 22, no. 2, pp. 352-357, June 1983.

[79] W. H. Chen, B. L.i Pen, C. T. Yu, and W. S. Hwang, "Pretreatment Efficiency and Structural Characterization of Rice Straw by an Integrated Process of Dilute-Acid and Steam Explosion for Bioethanol Production," *Bioresource Technology*, vol. 102, no. 3, pp. 2916-2924,

February 2011.

[80] H. W. Liu, H. K. Walter, G. M. Vogt, H. S. Vogt, and B. E. Holbein, "Steam Pressure Disruption of Municipal Solid Waste Enhances with Wheat Straw for simultaneous Saccharification and Fermentation into Ethanol," *Biotechnolgy and Bioengineering*, vol. 77, no. 2, pp. 121-130, January 2002.

[81] H. K. Murnen et al., "Optimization of Ammonia Fiber Expansion (AFEX) Pretreatment and Enzymatic Hydrolysis of Miscanthus x giganteus to Fermentable Sugars," *Biotechnology Progress*, vol. 23, no. 4, pp. 846-850, 2007.

[82] F. Teymouri, L. Laureano-Perez, H. Alizadeh, and B. E. Dale, "Optimization of the Ammonia Fiber Explosion (AFEX) Treatment Parameters for Enzmatic Hydrolysis of Corn Stover," *Bioresource Technology*, vol. 96, no. 18, pp. 2014-2018, February 2005.

[83] P. J. Morjanoff and P. P. Gray, "Optimization of Steam Explosion as a Method for Increasing Susceptibility of Sugarcane Bagasse to Enzymatic Saccharification," *Biotechnology and Bioengineering*, vol. 29, no. 6, pp. 733-741, April 1987.

[84] D. J. Schell, J. Farmer, M. Newman, and J. McMillian, "Dilute-Sulfuric Acid Pretreatment of Corn Stover in Pilot-Scale Reactor," in *Biotecnologyy for Fuels and Chemicals*, B. H. Davison et al., Eds.: Human Press, 2003, vol. 105, pp. 69-85.

[85] V. Chang, W. Kaar, B. Barry, and M. T. Holtzapple, "Simultaneous Saccharification and Fermentation of Lime-Treated Biomass," *Biotechnology Letters*, vol. 23, no. 16, pp. 1327-1333, August 2001.

[86] V. Chang, C. H. K. Kim, and M. T. Holtzapple, "Oxidative Lime Pretreatment of High-Lignin Biomass," *Applied Biochemistry and Biotechnology*, vol. 94, no. 1, pp. 1-28, April 2001.

[87] H. Klinke, B. Ahring, A. Schmidt, and A. Thomsen, "Characterization of Degradation Products from Alkaline Wet Oxidation of Wheat Straw," *Bioresource Technology*, vol. 82, no. 1, pp. 15-26, March 2002.

[88] I. Gonzalo Epelde, C. T. Lindgren, and M. E. Lindstorm, "Kinetics of Wheat Straw Delignification in Soda and Kraft Pulping," *Journal of Wood Chemistry and Technology*, vol. 18, no. 1, pp. 69-82, 2008.

[89] R. Sierra, C. B. Granda, and M. T. Holtzapple, "Lime Pretreatment," in *Biofuels*, J. R.

Mielenz, Ed.: Human Press, 2010.

[90] T. J. Mcdonough, "Oxygen Bleaching Processes," *TAPPI Journal*, vol. 69, no. 6, pp. 46-52, June 1986.

[91] N. Charles, S. D. Mansfield, O. Mircochnik, and S. J. B. Duff, "Effect of Oxygen Delignification Operating Parameters on Downstream Enzymatic Hydrolysis of Softwood Substrates," *Biotechnology Progress*, vol. 19, no. 5, pp. 1606-1611, September 2003.

[92] H. M. Baudel, Claudio Zaror, and C. A.M. de Abreu, "Improving the Value of Sugarcane Bagasse Wastes Via Integrated Chemical Production Systems: An Environmentally Friendly Approach," *Industrial Crops and Products*, vol. 21, no. 3, pp. 309-315, May 2005.

[93] D. Pope, "Assessing the Potential for Biothanol Production from Oxygen Delignified corn Stover and Wheat Straw," UBC, Master Thesis 2011.

[94] A. S. Schmidt and A. B. Thomsen, "Optimization of Wet Oxidation Pretreatment of Wheat Straw," *Bioresource Technology*, vol. 64, no. 2, pp. 139-151, May 1998.

[95] B. K. Ahring, K. Jensen, P. Nielsen, A. B. Bjerre, and A. S. Schmidt, "Pretreatment of Wheat Straw and Conversion of Xylose and Xylan to Ethanol By Thermophilic Anaerobic Bacteria," *Bioresource Technology*, vol. 58, no. 2, pp. 107-113, November 1996.

[96] G. Panagiotou and L. Olsson, "Effect of Compounds Released During Pretreatment of Wheat Straw on Microbial Growth and Enzymatic Hydrolysis Rates," *Biotechnology and Bioengineering*, vol. 96, no. 2, pp. 250-258, February 2007.

[97] A. B. Bjerre, A. B. Olesen, T. Fernqvist, A. Ploger, and A. S. Schmidt, "Pretreatment of Wheat Straw Using Combined Wet Oxidation and Alkaline Hydrolysis Resulting in Convertible Cellulose and Hemicellulose," *Biotechnology and Bioengineering*, vol. 49, no. 5, pp. 568-577, March 1996.

[98] C. Martin, H. B. Klinke, and A. B. Thomsen, "Wet Oxidation As a Pretreatment Method For Enhancing the Enzymatic Convertibility Of Sugarcane Bagasse," *Enzyme and Microbial Technology*, vol. 40, no. 3, pp. 426-432, February 2007.

[99] E. Varga, Z. Szengyel, and K. Reczey, "Chemical Pretreatments of Corn Stover for Enhancing Enzymatic Digestibility," *Applied Biochemistry and Biotechnology*, vol. 98, no. 1-9, pp. 73-87, 2002.

[100] S. B. Argawal, J. M. Genco, B. J. W. Cole, and W. Miller, "Kinetics of Oxygen Delignification," *Journal of Pulp and Paper Science*, vol. 25, no. 10, pp. 361-366, 1999.

[101] M. J. Taherzadeh and K. Karimi, "Acid-Based Hydrolysis Processes for Ethanol From Lignocellulosic Materials: A Review," *BioResources*, vol. 2, no. 3, pp. 472-499, 2007.

[102] K. Karimi, S. Kheradmandinia, and M. J. Taherzadeh, "Conversion of Rice Straw to Sugars by Dilute-Acid Hydrolysis," *Biomass and Bioenergy*, vol. 30, no. 3, pp. 247-253, March 2006.

[103] A. Aden and T. Foust, "Technoeconomic Analysis of the Dilute Sulfuric Acid and Enzymatic Hydrolysis Process for the Conversion of Corn Stover to Ethanol," *Cellulose*, vol. 16, no. 4, pp. 535-545, August 2009.

[104] A. Dutta, N. Dowe, K. N. Ibsen, D. J. Schell, and A. Aden, "An Economic Comparison of Different Fermentation Configurations to Convert Corn Stover to Ethanol Using Z. mobilis and Saccharomyces," *Biotechnology Progress*, vol. 26, no. 1, pp. 64-72, January 2010.

[105] F. K. Kazi et al., "Techno-Economic Comparison of Process Technologies For Biochemical Ethanol Production from Corn Stover," *Fuel*, vol. 89, pp. S20-S28, November 2010.

[106] R. Smith, Novozymes Reports Enzyme Breakthrough For Biofuel Production, 2010.

[107] J. D. Wright, C. E. Wyman, and K. Grohmann, "Simultaneous Saccharification and Fermentation of Cellulose: Process Evaluation," *Applied Biochemistry and Biotechnology*, vol. 18, no. 1, pp. 75-90, 1988.

[108] Lee R. Lynd, Paul J. Weimer, W. H. van Zyl, and I. S. Pretorius, "Microbial Cellulose Utilization: Fundamentals and Biotechnology," *Microbiology and Molecular Biology Reviews*, vol. 66, no. 3, pp. 506-577, September 2002.

[109] T. T. Teeri, "Crystalline Cellulose Degradation: New Insight into the Function of Cellobiohydrolases," *Trends in Biotechnology*, vol. 15, no. 5, pp. 160-167, May 1997.

[110] M. Chauve et al., "Comparative Kinetic Analysis of Two Fungal B-Glucosidases," *Biotechnology and Biofuels*, vol. 3, no. 1, February 2010.

[111] F. C. Corazza, L.PlV. Calsavara, F.F. Moraes, G.M. Zanin, and I. Neitzel, "Determination of Inhibition in the Enzymatic Hydrolysis of Cellobiose Using Hybrid Neural Modeling," *Brazilian Journal of Chemical Engineering*, vol. 22, no. 1, pp. 19-29, March 2005.

[112] Z. Yue, W. Bin, Y. Baixu, and G. Peiji, "Mechanism of Cellobiose Inhibition in Cellulose Hydrolysis by C1ellobiohydrolase," *Science in China Series C: Life Sciences*, vol. 47, no. 1, pp. 18-24, 2004.

[113] J. Hu, V. Arantes, and J. N. Saddler, "The Enhancement of Enzymatic Hydrolysis of Lignocellulosic Substrates by the Addition of Accessory Enzymes Such as Xylanase: Is It an Additive or Synergistic Effect?," *Biotechnology for Biofuels*, vol. 4, no. 1, October 2011.

[114] Saumita Banerjee et al., "Commercializing lignocellulosic bioethanol: technology bottlenecks and possible remedies," *Biofules, Bioprod. Bioref.*, vol. 4, pp. 77-93, 2010.

[115] George P. Philippidis, "Cellulose Bioconversion Technlogy," in *Handbook on bioethanol: Production and Utilization*, Charles Wyman, Ed. Washington: Taylor & Francis, 1996.

[116] L. A. Lucia and R. S. Smereck, "Effect of Lignin Content and Magnesium-To-Manganese Radio on the Selectivity of Oxygen Delignification in Softwood Kraft Pulp," *Pure and Applied Chemistry*, vol. 73, no. 12, pp. 2059-2065, 2001.

[117] J. Gierer, T. Reitberger, E. Yang, and B. H. Yoon, "Formation and Involvement of Radicals in Oxygen Delignification Studied by the Autoxidation of Lignin and Carbohydrate Model Compounds," *Journal of Wood Cehmistry and Technology*, vol. 21, no. 4, pp. 313-341, 2001.

[118] J. Gierer, "Formation and Involvement of Superoxide and Hydroxyl Radicals in TCF Bleaching Processes: A Review," *Holzforschung*, vol. 51, no. 1, pp. 34-46, 1997.

[119] "Kappa Number of Pulp," *TAPPI Test Method T236 cm-85*, 1996.

[120] Li Tao, "Oxygen Delignification for Southern Softwood Kraft Pulps with High Lignin," University of Maine, Master Thesis, 2005.

[121] P. J. Kleppe, H. M. Chang, and R. C. Eckert, "Delignification of High Yield Pulp with Oxygen and Alkali. I. Preliminary Studies of Southern Pines," *Pulp Paper Magazine of Canada*, vol. 73, no. 12, pp. 102-106, 1972.

[122] E. Johansson and S. Ljunggren, "The Kinetics of Lignin Reactions during Oxygen Bleaching. IV. The Reactivities of Different Lignin Model Compounds and the Influence of Metal Ions on the Rate of Degradation," *Journal of Wood Chemistry and Technology*, vol. 14, no. 4, pp. 507-525, August 1994.

[123] R. Sierra-Ramirez, L. A. Garcia, and M. T. Holtzapple, "Selectivity and Delignification Kinetics for Oxidative Short-Term Lime Pretreatment of Poplar Wood, Part I: Constant-Pressure," *Biotechnology Progress*, vol. 27, no. 4, pp. 976-985, 2011.

[124] R. Yang, L. Lucia, A. J. Ragauskas, and H. Jameel, "Oxygen Delignification Chemistry and Its Impact on Pulp Fibers," *Journal of Wood Chemistry and Technology*, vol. 23, no. 1, pp. 13-29, 2003.

[125] Y. Ji, "Kinetics and Mechanism of Oxygen Delignification," University of Maine, PhD Thesis, 2007.

[126] S. Kim and M. T. Holtzapple, "Delignification Kinetics of Corn Stover in Lime Pretreatment," *Bioresource Technology*, vol. 97, no. 5, pp. 778-785, March 2006.

[127] M. Lee, "Lignin Model Compound Approach to Modeling Oxygen Delignification Reaction Kinetics," UBC, Master Thesis, 2005.

[128] J. Iribarne and L. R. Schroeder, "High-Pressure Oxygen Delignification of Kraft Pulps, Part 1: Kinetics," *TAPPI Journal*, vol. 80, no. 10, pp. 241-250, 1997.

[129] A. H.D. Vincent, L. K. Nguyen, and F. F. Mathews, "Kinetics of Oxygen Delignification of Eucalyptus Kraft Pulp," *Appita Journal*, vol. 47, no. 3, pp. 217-220, 1994.

[130] D. Tromans, "Oxygen Solubility Modeling in Inorganic Solutions: Concentration, Temperature and Pressure Effects," *Hydrometallurgy*, vol. 50, no. 3, pp. 279-296, September 1998.

[131] S. M. Violette, "Oxygen Delignification Kinetics and Selectivity Improvement," University of Maine, Master Thesis, 2003.

[132] H. J. Jung and D. Himmelsbach, "Isolation and Characterization of Wheat Straw Lignin," *Journal of Agricultural and Food Chemistry*, vol. 37, no. 1, pp. 81-87, January 1989.

[133] A. Sluiter, R. Ruiz, C. Scarlata, J. Sluiter, and D. Templeton, "Determination of Extractives in Biomass," National Renewable Energy Laboratory, Golden, Technical Report 2005.

[134] A. Sluiter et al., "Determination of Ash in Biomass," National Renewable Energy Laboratory, Golden, Technical Report 2005.

[135] B. Hames et al., "Preparation of Samples for Compositional Analysis," NREL, Golden,

Technical Report 2008.

[136] A. Sluiter et al., "Determination of Structural Carbohydrates and Lignin in Biomass," National Renewable Energy Laboratory, Golden, Technical Report 2008.

[137] A. Sluiter et al., "Determination of Sugars, Byproducts, and Degradation Products in Liquid Fraction Process Samples," National Renewable Energy Laboratory, Golden, Technical Report 2006.

[138] T. Kondo, T. Ohshita, and T. Kyuma, "Comparison of Characteristics of Soluble Lignins from Untreated and Ammonia-Treated Wheat Straw," *Animal Feed Science and Technology*, vol. 39, no. 3-4, pp. 253-263, November 1992.

[139] W. G. Campbell and I. R. C. McDonald, "The Chemistry of the Wood Cell Wall. Part II.* The Isolation of Beech and Spruce Acid-Soluble and Modified Lignins," , Appleton, Wisconsin, 1951.

[140] M. O. Bagby, R. L. Cunningham, and R. L. Maloney, "Ultraviolet Spectral Determination of Lignin," *Tappi*, vol. 56, no. 4, pp. 162-163, April 1973.

[141] R. S. Fukishima and R. D. Hatfield, "Extraction and Isolation of Lignin for Utilization as a Standard to Determine Lignin Concentration Using the Acetyl Bromide Spectrophotometric Method," *Journal of Agricultural and Food Chemistry*, vol. 49, no. 7, pp. 3133-3139, July 2001.

[142] Y. S. Perng and C. W. Oloman, "Kinetics of Oxygen Bleaching Mediated by Electrochemically Generated Ferricyanide," *Tappi*, vol. 77, no. 7, pp. 115-126, 1994.

[143] X. Ma et al., "Preparation of Dissolving Pulp from Bamboo for Textile Applications. Part 2. Optimization of Pulping Conditions of Hydrolyzed Bamboo and its Kinetics," *BioResources*, vol. 7, no. 2, pp. 1866-1875, 2012.

[144] J. Sabatier, C. Peniche, and N. Fernandez, "Soda Pulping of Bagasse: Delignification Phases and Kinetics," *Holzforschung*, vol. 47, no. 4, pp. 313-317, 1993.

[145] L. A. Abdul-Karim, A. Rab, E. Polyanszky, and I. Rusznak, "Kinetics of Delignification in Kraft Pulping of Wheat Straw and Hemp," *Tappi Journal*, vol. 78, no. 8, pp. 161-164, August 1995.

[146] Y. Zhang, J. L. Xu, H. J. Xu, Z. H. Yuan, and Y. Guo, "Cellulase Deactivation Based Kinetic

Modeling of Enzymatic Hydrolysis of Steam-Exploded Wheat Straw," *Bioresource Technology*, vol. 101, no. 21, pp. 8261-8266, November 2010.

[147] E. Gnansounou and A. Dauriat, "Techno-Economic Analysis of Lignocellulosic Ethanol: A Review," *Bioresource Technolgy*, vol. 101, no. 13, pp. 4980-4991, July 2010.

[148] D. Humbird et al., "Process Design and Economics for Biochemical Conversion of Lignocellulosic Biomass to Ethanol," National Renewable Energy Laboratory, Golden, Technical Report 2011.

[149] (2013, April) Alberta Agriculture and Rural Development. [Online]. http://www.agric.gov.ab.ca/app68/hay?cat=For%20Sale&cat1=Straw

[150] J. Chang. (2013, March) ICIS. [Online]. http://www.icis.com/chemicals/channel-info-chemicals-a-z/

[151] W. D. Seider, J. D. Seader, and D. R. Lewin, *Product and Process Design Principles: Synthesis, Analysis and Evaluation 2ed*, Bill Zobrist, Ed. New York: John Wiley and Sons, Inc., 1999.

[152] W. R. Wilcox. (2005, December) Oxygen Costs. [Online]. http://people.clarkson.edu/~wwilcox/Design/oxycost.htm#_ftn2

[153] A. Ragauskas. (2013, March) Georgia Institute of Paper Science Tech and Technology. [Online]. http://www.ipst.gatech.edu/faculty/ragauskas_art/technical_reviews/O2%20delig.pdf#page=1&zoom=auto,-7,0

[154] P. Taylor, O. Lavagne d'Ortigue, N. Trudeau, and M. Francoeur, "Energy Efficiency Indicators for Public Electricity Production from Fossil Fuels," OECD/IEA, Paris, 2008.

[155] C. E. Wyman, "Alternative Fuels from Biomass and Their Impact on Carbon Dioxide Accumulation," *Applied Biochemistry and Biotechnology*, vol. 45-46, no. 1, pp. 897-915, 1994.

[156] M. F. Ruth and R.J. Wooley, "The Potential Cost of Lignocellulosic Sugar for Commodity Chemical Production," , Washington, DC, 2000.

[157] A. Aden et al., "Lignocellullosic Biomass to Ethanol Process Design and Economics Utilizing Co-Current Dilute Acid Prehydrolysis and Enzymatic Hydrolysis for Corn Stover," National

Renewable Energy Laboratory, Golden, Technical Report 2002.

[158] S. Haley. (2013, May) USDA Economic Research Service. [Online]. http://www.ers.usda.gov/data-products/sugar-and-sweeteners-yearbook-tables.aspx#.UaRDzNK1EwB

[159] D. Klein-Marcuschmaer, P. Oleskowicz-Popiel, B. A. Simmons, and H. W. Blanch, "The Challenge of Enzyme Cost in the Production of Lignocellulosic Biofuels," *Biotechnology and Bioengineering*, vol. 109, no. 4, pp. 1083-1087, April 2012.

[160] H. J. Huang, S. Ramaswamy, W. Al-Dajani, U. Tschirner, and R. A. Cairncross, "Effect of Biomass Species and Plant Size on Cellulosic Ethanol: A Comparative Process Economic Analysis," *Biomass and Bioenergy*, vol. 33, no. 2, pp. 234-246, February 2009.

[161] L. Bjorklund, S. Larsson, L. J. Jonsson, A. Reimann, and N-O. Nilvebrant, "Treatment with Lignin Residue," *Applied Biochemistry and Biotechnology*, vol. 98-100, no. 1-9, pp. 563-575, 2002.

[162] Metro Vancouver, "Metro Vancouver Sustainability Report 2009," Vancouver, 2009.

[163] K. Kovasin, P. Uusitalo, and M. Villo, "Dimensioning of Oxygen Delignification Reactor," , Atlanta, 1987.

[164] A. Teder and L. Olm, "Extended Delignification by Combination of Modified Kraft Pulping and Oxygen Bleaching," *Paperi ja Puu*, vol. 63, no. 4a, pp. 315-326, 1981.

[165] J. E. Evans, V. Venkatesh, J. S. Gratzl, and H. M. Chang, "The Kinetic of Low-Consistency Oxygen Delignification: Kraft and Soda-Anthraquinone Pulps," *TAPPI Journal*, vol. 62, no. 6, pp. 37-39, 1979.

[166] G Franz and W Blackshek, "The Glucan Chains of Cellulose Microfibrils All Have the Same Orientation," in *Plant Cell Walls from Chmeistry to Biology*, P. Albersheim et al., Eds. New York: Garland Science, Taylor & Francis Group, LLC, 2011.

[167] T. K. Ghose, "Measurement of Cellulase Activities," *International Union of Pure and Applied Chemistry*, vol. 59, no. 2, pp. 257-268, 1987.

[168] L. D. Gomez, C. G. Steele-King, and S. J. McQueen-Mason, "Sustainable Liquid Biofuels from Biomass: The Writing's on the Walls," *The New Phytologist*, vol. 178, no. 3, pp. 473-485, 2008.

[169] T. W. Jeffries, "Fermentation of D-Xylose and Cellobiose," in *Handbook on Bioethanol*, Charles Wyman, Ed. Washington: Taylor and Francis, 1996.

[170] K. L. Kadam, "Cellulase Production," in *Handbook on Bioethanol*, Charles Wyman, Ed. Washington: Taylor & Francis, 1996.

[171] C. Laine, "Structures Of Hemicelluloses and Pectins in Wood and Pulp," Helsinki University of Technology, Doctoral Thesis, 2005.

[172] J. M. Lawther, R. C. Sun, and W. B. Banks, "Rapid Isolation and Structural Characterization of Alkali-Soluble Lignins During Alkaline Treatment and Atmospheric Refining of Wheat Straw," *Industrial Crops and Products*, vol. 5, no. 2, pp. 97-105, June 1996.

[173] D. J. Schell et al., "A Technical and Economic Analysis of Acid-Catalyzed Steam Explosion and Dilute Sulfuric Acid Pretreatment Using Wheat Straw or Aspen Wood Chips," *Applied Biochemistsry and Biotechnology*, vol. 28-29, no. 1, pp. 87-97, 1992.

[174] Charlotte Schubert, "Can Biofuels Finally Take Center Stage?," *Nature Biotechnology*, vol. 24, no. 7, pp. 777-784, 2006.

[175] L. R. Van Loon and M. A. Glaus, "Review of the Kinetics of Alkaline Degradation of Cellulose in View of Its Relevance for Safety Assessment of Radioactive Waste Repositories," *Journal of Environmental Polymer Degrdation*, vol. 5, no. 2, pp. 97-109, April 1997.

[176] C. E. Wyman et al., "Comparative Sugar Recovery Data From Laboratory Scale Application of Leading Pretreatment Technologies to Corn Stover," *Bioresources Technology*, vol. 96, no. 18, pp. 2026-2032, December 2005.

[177] Z. Zhou, F. Jin, H. Enomoto, T. Moriya, and H. Higashigima, "A Continuous Flow Reaction System For Producing Acetic Acid By Wet Oxidation Of Biomass Waste," *Journal of Materials Science*, vol. 41, no. 5, pp. 1501-1507, 2006.

[178] H. Zhu and H. Qiao, "Kinetics Research of Wheat Straw Atmospheric Pressure Pulping with Microwave Radiation," *Advanced Materials Research*, vol. 610-613, pp. 1726-1730, Decemeber 2012.

[179] M. N. Satheesh Kumar, A.K. Mohanty, L. Erickson, and M. Misra, "Lignin and Its Applications with Polymers," *Journal of Biobased Materials and Bioenergy*, vol. 3, no. 1, pp. 1-24, March 2009.

[180] S. Sokhansanj, S. Mani, M. Stumborg, R. Samson, and J. Fenton, "Production and Distribution of Cereal Straw on the Canadian Prairies," *Canadian biosystems Engineering*, vol. 48, pp. 3.39-3.46, 2006.

[181] (2009) Stolza News. [Online]. http://www.stolzsa.com/en/news/bio-ethanol-plant-babilafuente-full-capacity-september-2009

Appendix A

Calculation of the volume of 4% H_2SO_4 w/w concentration

Density of 72% H_2SO_4 = 1.6338 g/ml

Density of H_2O = 1.00 g/ml

Density of 4% H_2SO_4 = 1.025 g/ml

Weight of 3.00 ml 72% H_2SO_4

3.00 ml x 1.6338 g/ml = 4.90 g 72% H_2SO_4

Compostion of 3 ml of 72% H_2SO_4

4.90 g 72% H_2SO_4 x 72% = 3.53 g acid

2.90 g 72% H_2SO_4 x 28% = 1.37 g water

Concentration of H_2SO_4 after dilution

3.53 g acid / (84.00 g H_2O + 4.90 g 72% H_2SO_4) = 3.97 % H2SO4 (w/w)

Total volume of solution present after dilution

(4.90 g H_2SO_4 + 84.00 g H_2O) x (1/(1.025 g/ml)) = 86.73 ml

Sample calculation for lignin solubilization

Pretreatment condition 4% substrate loading, 90°C, 5% caustic loading

Lignin before pretreatment = 20g x 0.161 g lignin/g substrate = 3.22 g

Lignin after pretreatment = 20g x 0.766 g recovered x 0.126 g lignin/g substrate = 1.93 g

Lignin solubilized = (3.22 – 1.93)/3.22 = 39.8%

Sample calculation of annualized capital cost for oxygen delignification reactor

Assumption

10 years loan

i = 8% interest rate

For 10% substrate loading, 2 minutes residence time

Total direct cost of reactor: 6.46E05

$$\text{Annualized capital cost} = \ 6.46E05 \ \times \frac{(0.08(1+0.08)^{10})}{(1+0.08)^{10}-1} = 9.63E04$$

Sample calculation of oxygen feed cost

Based on Wilcox's assumption [**152**]

Oxygen consumption at 22 kg/dry tons (average of 20-24 kg/dry tons) [**153**]

Dry biomass flow rate fixed at 2200 tons/day

At pressure 610-800 kPa

$$\frac{22 \text{ kg } O_2}{\text{dry tons biomass}} \times \frac{2200 \text{ dry tons biomass}}{\text{day}} \times \frac{\text{tonne}}{907.185 \text{ kg}} = \frac{55.35 \text{ tonne } O_2}{\text{day}}$$

Capital cost was calculated based on a 27 million plant that has the capacity to produce 1000 tons of O_2 per day with 0.6 as the economy of scale.

$$\text{Capital cost required} = 27 \text{ million} \times \left(\frac{53.53}{1000}\right)^{0.6} = \$ \ 4.65 \text{ million}$$

Using reference the annual facility fee as 2.75% per month of the capital cost

$$\text{Facility fee} = 2.75\% \times 4.65 \text{ million} \times \frac{12 \text{ months}}{\text{yr}} = \frac{\$ \ 1.54 \text{ million}}{\text{yr}}$$

Using reference cost of electricity of 15 kWh/1000 ft^3 (15kWh/ 28.32 m^3) of O_2, the annualized electricity cost can be calculated:

$$\text{Elec cost} = \frac{48400 \text{ kg } O_2}{\text{day}} \times \frac{\text{m3}}{1.331 \text{ kg } O_2} \times \frac{15 \text{ kwh}}{28.32 \text{ m}^3} \times \frac{\$0.04}{\text{kWh}} \times \frac{365 \text{ day}}{\text{yr}} = \frac{\$ \ 0.28 \text{ million}}{\text{yr}}$$

The total annual cost for O_2 is:

$$1.54 + 0.28 = \frac{\$ \ 1.82 \text{ million}}{\text{yr}}$$

Cost of O_2 per kg:

$$\left(\frac{22\ \text{kg}\ O_2}{\text{dry tons biomass}} \times \frac{2200\ \text{dry tons biomass}}{\text{day}}\right)^{-1} \times \frac{\$\ 1.82\ \text{million}}{\text{yr}} \times \frac{\text{yr}}{365\ \text{day}} = \frac{\$\ 0.103}{\text{kg}}$$

Sample calculation for the enzyme cost

From Novozymes [**106**]:

Enzyme cost = $ 0.5/ gallon of ethanol

From Aden et al. (2002):

Enzyme loading = 12 FPU/ g cellulose

Ethanol production = 8244.1 (gallon/ h)

Cellulose flow rate to hydrolysis = 28432 (kg/h)

$$\frac{28432\ \text{kg cellulose}}{\text{h}} \times \frac{1000\ \text{g}}{\text{kg}} \times \frac{12\ \text{FPU}}{\text{g cellulose}} \times \frac{1\text{h}}{8244.1\ \text{gallon ethanol}} \times \frac{1\ \text{gallon ethanol}}{\$0.5}$$

$$= \frac{8.28\text{e}05\ \text{FPU}}{\$} = \frac{\$\ 12.08}{\text{million FPU}}$$

Sample calculations for lignin credit:

Electricity = $0.040/kWh

Electrical efficiency = 28% [**154**]

$$\frac{25.4\ \text{MJ}}{\text{kg}} \times \frac{\$0.040}{\text{kWh}} \times 28\% \times \frac{1\ \text{h}}{3600\ \text{s}} \times \frac{1000\ \text{g}}{\text{kg}} = \frac{\$0.079}{\text{kg}}$$

Sample calculation for sensitivity of biomass price:

Pretreatment cost of 0.5 $/gallon ethanol, 420 $/ton NaOH and 20 $/biomass = 23.98 ¢/lb

Pretreatment cost of 0.5 $/gallon ethanol, 420 $/ton NaOH and 40 $/biomass = 26.75 ¢/lb

Sensitivity of biomass = (26.75-23.98)/(40-20) = 0.138

Appendix B

Table B-1: Caustic loading and corresponding substrate loading initial values for solving the single ODE, improved single ODE and system of ODEs model

Initial Conditions		
	2% Substrate loading	4% substrate loading
Lignin (g/l)	3.285	6.707
Caustic loading 5% (g/l)	0.434	0.886
Caustic loading 10% (g/l)	0.867	1.770
Caustic loading 15% (g/l)	1.301	2.656

Table B 2: EASY-FIT model parameter specifications

Integration method	Implicit
Final accuracy (absolute)	1E-10
Final accuracy (relative)	1E-10
Initial stepsize	1E-07
Bandwidth of Jacobian	0
Number of iterations	100
Order of numerical differentiation tolerance	0
Termination tolerance	1E-10
Final residual estimate	1E-10
Confidence level (%)	5

Table B-3: Sensitivity analysis for pretreatment condition at 90°C, 5% caustic loading and 60 minutes of residence time

Biomass Cost ($/ton)	NaOH Cost ($/ton)	Enzyme Cost ($/gallon)	Pretreatment Cost (¢/lb)
20	420	0.1	9.76
40	420	0.1	12.53
60	420	0.1	15.29
20	635	0.1	11.25
40	635	0.1	14.02
60	635	0.1	16.78
20	850	0.1	12.74
40	850	0.1	15.51
60	850	0.1	18.27
20	420	0.5	23.98
40	420	0.5	26.75
60	420	0.5	29.51
20	635	0.5	25.45
40	635	0.5	28.24
60	635	0.5	31.00
20	850	0.5	26.96
40	850	0.5	29.72
60	850	0.5	32.48
20	420	1.47	58.46
40	420	1.47	61.22
60	420	1.47	63.98
20	635	1.47	59.94
40	635	1.47	62.71
60	635	1.47	65.47
20	850	1.47	61.43
40	850	1.47	64.20
60	850	1.47	66.96

Appendix C

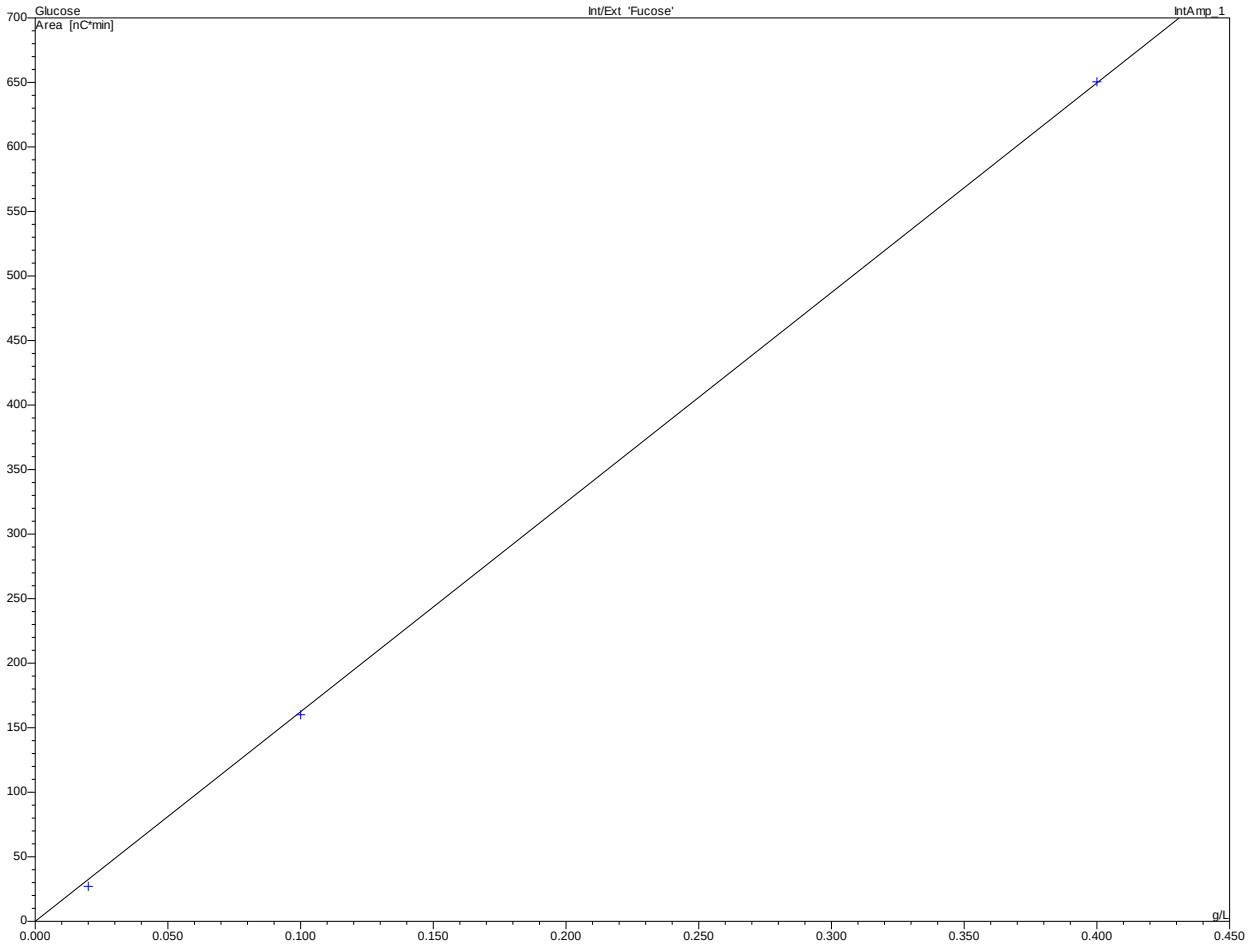

Table C-1: Example of a glucose HPLC calibration curve

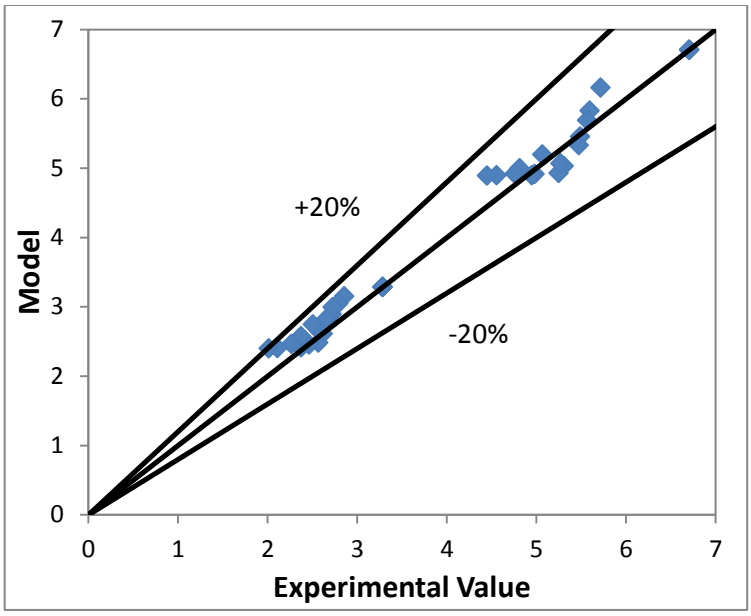

Table C-2: Improved single ODE approach parity plot for 5% caustic loading (±20% error) with full factorial dataset

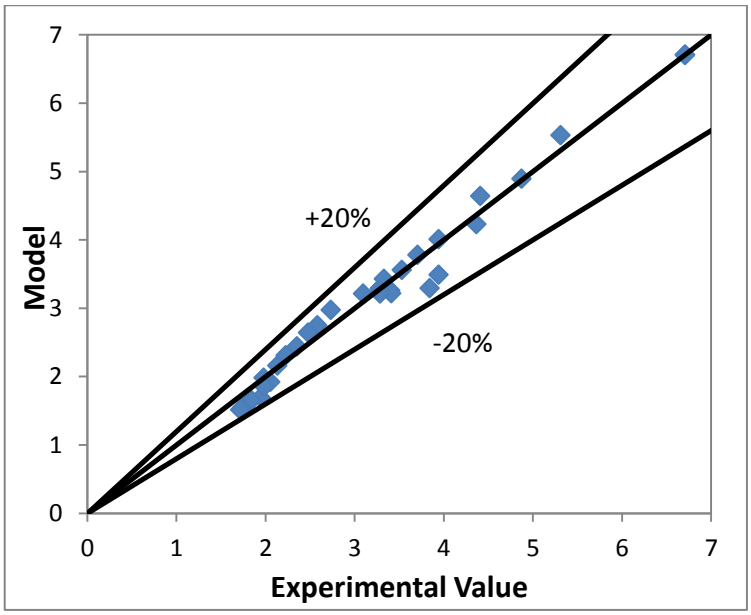

Table C-3: Improved single ODE approach parity plot for 10% caustic loading (±20% error) with full factorial dataset

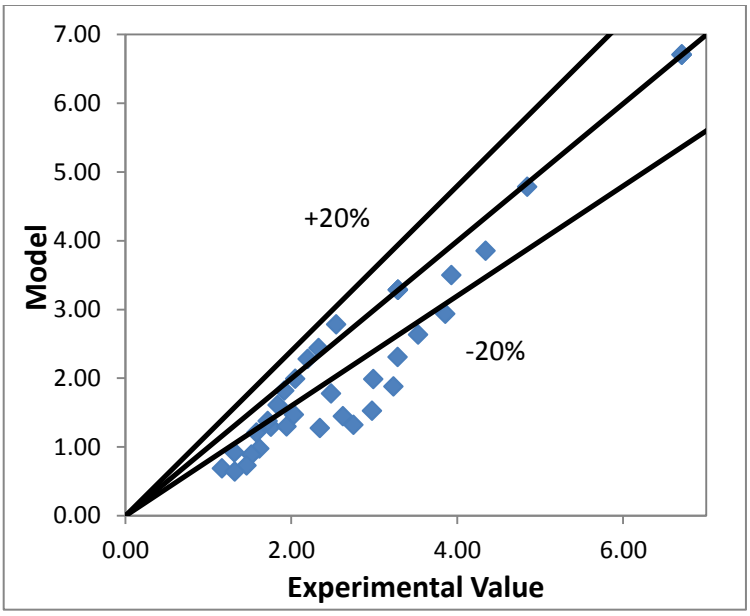

Table C-4: Improved single ODE approach parity plot for 15% caustic loading (±20% error) with full factorial dataset